Reducing Emissions of Volatile Organic Compounds (VOCs) From Agricultural Soil Fumigation: Comparing Emission Estimates Using Simplified Methodology

FINAL REPORT

California Air Resources Board, Contract No. 07-332
USDA-ARS, Project 5310-12130-009-00D

Prepared by:

Principal Investigator:
Dr. Scott R. Yates

Co-Investigators:
Dr. Daniel Ashworth
Dr. Lifang Luo

Contaminant Fate and Transport Research Unit
USDA-ARS, U.S. Salinity Laboratory
450 W. Big Springs Rd.
Riverside, CA 92507
(951) 369-4803

January 25, 2012

Prepared for the California Air Resource Board and the California Environmental Protection Agency, State of California Air Resources Board Research Division, PO Box 2815, Sacramento CA 95812

Preface

This report describes work carried out at the USDA-ARS, U.S. Salinity Laboratory, Riverside under funding from the California Air Resources Board (CARB) through contract number 07-332 and the USDA-ARS CRIS Project 5310-12130-009-00D. The CARB contract and USDA-ARS CRIS project funded most of the experimental work described in this report.

Disclaimer

The statements and conclusions in this report are those of the contractors and not necessarily those of the California Air Resources Board. The mention of commercial products, their source, or their use in connection with material reported herein is not to be construed as actual or implied endorsement of such products.

Acknowledgments

The authors thank Q. Zhang and Y. Wang for their assistance in preparing and conducting the experiments. This Report was submitted in fulfillment of ARB Contract 07-332, Reducing Emissions of Volatile Organic Compounds (VOCs) From Agricultural Soil Fumigation: Comparing Emission Estimates Using Simplified Methodology, by the USDA-ARS, U.S. Salinity Laboratory Riverside, CA under the sponsorship of the California Air Resources Board. Work was completed as of June 30, 2011.

USDA Commercial Endorsement Disclaimer

The use of trade, firm, or corporation names in this document is for the information and convenience of the reader. Such use does not constitute an official endorsement or approval by the United States Department of Agriculture or the Agricultural Research Service of any product or service to the exclusion of others that may be suitable.

Nomenclature

ADM – aerodynamic method
LOM – low organic matter soil
HOM – high organic matter soil
HDPE – high density polyethylene
VIF – virtually impermeable film
ATS – ammonium thiosulfate
1,3-D – 1,3-dichloropropene
CP – chloropicrin
MeI – methyl iodide
VOC-volatile organic compound
Telone – used to signify a 50:50 mix of 1,3-D (cis) and 1,3-D (trans)
Telone (formulation) – used to signify the commercial formulation
Telone C-35– used to signify a 32.5 : 32.5 : 35 mix of 1,3-D (cis), 1,3-D (trans) and chloropicrin
Telone C-35 (formulation) – used to signify the commercial formulation

Table of Contents Page

List of Figures Page

List of Tables Page

Abstract

Laboratory experiments and mathematical simulations were conducted to measure and predict volatilization of the 1,3-dichloropropene (Telone®), chloropicrin and methyl iodide after shank or drip application into agricultural soil.

The goals of this study were to (a) evaluate the effectiveness of several emission-reduction methods, including: sprinkler irrigation, organic amendment, deep injection, agricultural films, and fertilizer amendment on the volatilization of 1,3-dichloropropene, chloropicrin, and methyl iodide into the atmosphere; (b) determine if simplified data collection methods (i.e., laboratory systems and modeling) could be used to obtain total emission estimates that adequately represent large-scale systems.

Comparisons were made using existing measurement of fumigant volatilization rates and total emission losses from field scale experiments, new laboratory measurements involving cylindrical and/or rectangular columns, and mathematical models of a range of complexity (i.e., analytical solutions and multidimensional numerical models). This data were compared in terms of correspondence of peak emissions and total emissions.

For 1,3-dichloropropene, intermittent irrigation reduced total emissions by approximately 50 % and conducting experiments in soil with high levels of organic material (composted municipal green waste) reduced total emissions by 80–85 % compared to conventional fumigant applications. Use of a virtually impermeable film (VIF) reduced total emissions to less than 5 % of the applied material. Applying ammonium thiosulfate (ATS) to the soil surface as a low water-volume spray reduced emissions in laboratory experiments by 26 % and when applied in irrigation water reduced emissions by 43 %. In general, the laboratory and modeling results compare well to recent large-scale field studies.

Significant reductions in total emission of chloropicrin were possible when a virtually impermeable film (<0.1 % of applied) or a high-density polyethylene (HDPE) film (<2 % of applied) was used as an emission barrier at the soil surface. For chloropicrin, deep injection reduced emissions by 23 % relative to the control; applying ammonium thiosulfate to the soil surface as a low volume spray reduced emissions by 42 % and applying ammonium thiosulfate in irrigation water reduced emissions by nearly 88 %.

In laboratory experiments and modeling studies (computer programs: Hydrus 1D and Solute 1D), repeated surface irrigations and use of high organic matter soils were largely ineffective in reducing emissions of methyl iodide (MeI), with total emissions exceeding 60 %. However, covering the soil surface with a virtually impermeable film reduced emissions from >60 % to less than 1 %, if the film is removed after 14 days.

Executive Summary

Background

Ozone is formed from the photochemical oxidation of nitrogen oxides and volatile organic compounds (VOCs), such as pesticides and fumigants. This is leading to increased regulation of agricultural VOC sources. It has been estimated that 5 % of the total VOC in the San Joaquin and Sacramento Valleys are from pesticides. This has led California Department of Pesticide Regulation to require reductions in pesticide-related VOC emissions from 1990 levels. Future regulations may require additional reductions to meet 1-hour and 8-hour State Implementation Plan requirements.

Research was conducted to test the hypothesis that accurate estimates of the cumulative emission rate could be obtained using laboratory experimentation and mathematical simulation for a variety of fumigation practices. The research involved studies of several emission-reduction strategies: (*i*) intermittent irrigation water seal, (*ii*) addition of an organic surface amendment, (*iii*) deep injection, (*iv*) addition of a fertilizer amendment (i.e., ammonium thiosulfate) applied as a spray (i.e., limited water) and in irrigation water, and (*v*) the use of standard and low permeability agricultural films (i.e., high-density polyethylene and virtually impermeable film).

Methods

This research was accomplished by conducting a series of field, laboratory and modeling studies. Laboratory experiments were conducted in a controlled temperature room using cylindrical and rectangular soil chambers. In each experiment, two side-by-side emission experiments were conducted. The experiments were simulated using one, or more, computer programs, which included Hydrus 1D (Šimunek et al., 2008), Hydrus 2D (Šimunek et al., 2008), Solute 1D (Yates, 2006), and an algebraic analytical solution (Yates, 2009).

Field emission data were obtained from Yates and Gan (2010). This report documents several studies conducted at a field site near Buttonwillow, CA (near 35.442,-119.457) during 2005 and 2007. During each experiment, fumigant emissions were determined using two independent data sources. One set of emission estimates were obtained using aerodynamic (ADM), integrated horizontal flux (IHF) and theoretical profile shape (TPS) methods. These micrometeorological approaches require on-field measurement of the atmospheric fumigant concentration at one or more heights above the soil surface, wind speed measurements, and temperature measurements. Another set of emission estimates were obtained using the so-called back calculation methods, where observed ambient concentrations in the atmosphere surrounding a fumigated field are used with the Industrial Source Complex Short Term (ISCST3) or the CalPuff (v.6) dispersion models to back-calculate the field-scale emission rates. These approaches utilize atmospheric fumigant concentration collected at a single height above the soil surface at numerous locations surrounding the field, along with weather data collected from a 10-m mast placed in the vicinity.

For the purposes of the research described herein, the aerodynamic method and CalPuff emission estimates were used for comparison to the laboratory and mathematical simulations.

Laboratory soil columns were used to simulate shank-injection of fumigants. The system uses a point-source of fumigant applied at a particular depth and allows for determination of surface emissions and vertical (one dimensional, 1D) gas transport within the column. Soil was packed into the stainless steel columns as per the field depth increments and field-measured bulk density and moisture content of the soil were maintained.

Laboratory soil chambers were used to simulate the drip application of fumigants to raised beds. The system enabled determination of surface emissions and both vertical and horizontal (2-dimensional, 2D) gas distribution within the chamber. The experiments were performed using aluminum soil chambers that allowed construction of an actual size (non-scaled) half-bed and half-furrow.

For the laboratory column and chamber experiments, soil was collected from each of the fields treatments (irrigation and organic matter addition treatments in 2005; control, deep injection and ammonium thiosulfate application treatments in 2007). Due to their close proximity, the collected soils were texturally very similar to one another and were classed as sandy loam (60 % sand, 30 % silt, 10 % clay); a thermic Typic Haplargids from the Milham series. The only notable difference in the soils was the organically amended soil from the 2005 study which was determined to have an organic matter content of 3.2 %, compared to 2.1 % for the unamended soils.

Soil bed experiments were intended to serve as a bridge between smaller scale laboratory and larger scale field experiments. These experiments were conducted at University of California Agricultural Experiment Station, Riverside, CA and involved drip-applied fumigant in a furrow-bed configuration. The plots were 3 m long and included 4 treatments: bare soil; beds covered with high-density polyethylene; beds covered with virtually impermeable film; and beds covered with thermic film. Emissions of 1,3-dichloropropene and chloropicrin (i.e., Telone® C-35 formulation) were collected using flux chambers.

Simulation of fumigant fate and transport in a variably-saturated soils and soils experiencing changes in temperature involved solving three governing processes: water flow (i.e. Richard's equation), heat transport, and solute fate (convection dispersion). For fumigant transport, the convection dispersion equation included phase partition between liquid, gas and solid phase, dispersion (convection and diffusion), and degradation processes. Degradation was described using a first-order decay, and the degradation rate in each phase (liquid, vapor, and solid) could be specified. To simulate interaction between fumigant and ammonium thiosulfate fertilizers, a finite difference program that includes a 2^{nd}-order reaction process was used (Solute 1D).

The results from these experiments and simulations include: (a) short-term, period-averaged or daily emission rates, (b) total emissions, and (c) comparisons between several methods for obtaining total emission estimates, including field, laboratory and model simulations.

Results

Comparison with the 2007 Buttonwillow field campaign: These studies provided mathematical and experimental simulation of the 2007 Buttonwillow field campaign (Yates and Gan, 2010) and studied the influence of deep injection and ammonium thiosulfate application on emission of Telone C-35 after shank injection. A bare soil treatment with injection at 46 cm depth served as a control, a bare soil treatment with injection at 60 cm depth served as a deep injection scenario, and a surface spray application of ammonium thiosulfate and a 46 cm injection depth was the ammonium thiosulfate treatment.

Based on the aerodynamic and CalPuff methods used for the 2007 Buttonwillow field experiments, the total Telone C-35 (formulation) emissions for the control, deep and ammonium thiosulfate treatments, respectively, were 18.8–24.6 %, 17.1–17.2 %, and 16.6–17.5 %. For the laboratory column experiments, total Telone C-35 emissions for the control, deep and ammonium thiosulfate treatments, respectively, were 32.1 ± 0.2 %, 21.8 ± 1.4 %, and 23.7 ± 1.7 %. For the numerical simulations, total Telone C-35 emissions for the control, deep and ammonium thiosulfate treatments, respectively, were 18.8–18.9 %, 10.4–10.6 %, and 17.8 %. Using an analytical solution produced total emissions for the control and deep injection treatments, respectively, of 26.3 % and 18.0 %.

While the similarity of the laboratory, field and predicted emission rates at specific times after injection were variable, the predicted total emission estimates were found to closely match the field measurements (i.e., differences ranged from -3–1 % of applied material). The laboratory emission rates exceeded the field measurements by 5–10 % (of applied material), which suggests they were less accurate than the predictions (i.e., Hydrus). The total emission estimates obtained from the analytical solution were 1–5 % higher than the field values.

Comparing the results for the column experiments, numerical and analytical simulations, the average total emissions estimates are about 0–4 % higher than the field values. Since field measurements of scalar fluxes are considered to be accurate within ±20–50 % (Businger, 1986; Wilson and Shum, 1992; Majewski, 1997; Liu and Foken, 2001), these simplified methods for obtaining total emissions fall well within the experimental uncertainty for the large field experiments.

Comparison with the 2005 Buttonwillow field campaign: These studies provided experimental and mathematical simulation of the 2005 Buttonwillow field campaign (Yates and Gan, 2010) and examine the influence of a repeated surface water seal and high organic matter soil (HOM) on emissions of Telone II after shank injection. The studies included the use of laboratory column experiments and numerical simulation. Laboratory column experiments were conducted with a non-irrigated bare soil treatment with injection at 46 cm depth serving as a control. Three other treatments were considered: (a) an irrigated bare soil treatment with injection at 46 cm depth, (b) a non-irrigated bare soil treatment in high organic matter soil, and (c) an irrigated bare soil treatment in high organic matter soil served establish the effect of irrigation on emission is soil with normal levels of organic matter vs. soil with higher levels of organic matter.

One objective of this research was to obtain comparisons to the field measurements. Based on the results of the aerodynamic and CalPuff methods for estimating emissions for the 2005

Buttonwillow field experiments, the total Telone II (formulation) emissions for the irrigation and high organic matter treatments, respectively, were 10.0–15.3 %, and 3.8–8.1 %. For the laboratory column experiments, total Telone II emissions for the irrigation and high organic matter treatments, respectively, were 14.4 %, and 4.5 %. For the numerical simulations, total Telone II emissions for the irrigation and high organic matter treatments, respectively, were 11.1–12.4 %, and 2.8–3.6 %.

The total emission estimates obtained in the laboratory column experiments were within the total emission range based on the two field measurements. The numerical simulations produced total emission values that were within the range of the field measurements for the irrigation treatment, but were 0.2–5.3 % below the field measurements for the high organic matter treatment. Even so, for both treatments, the absolute difference was less than approximately 5 % (of applied material).

Another objective of this research was to compare emissions from laboratory experiments and numerical simulation for conditions where field measurements were unavailable, which included non-irrigated low organic matter soil and irrigated high organic matter soil. For the non-irrigated low organic matter soil, the measured and simulated total emissions, respectively, were 29.1 % and 32.4 % (3.3 % difference). For the irrigated high organic matter soil treatment, the measured and simulated total emissions, respectively, were 2.0 % and 3.9 % (1.9 % difference).

Comparing the total emissions from the irrigation and non-irrigation treatments leads to the conclusion that adopting a repeated surface water seal will reduce Telone II emissions by approximately 50 % for the tested soils and conditions.

Extending Results to other Emission Reduction Strategies: laboratory soil column experiments and numerical simulations were conducted to estimate the emissions of Telone C-35 after shank injection. The soil and environmental conditions for the experiments were similar to the 2007 Buttonwillow field study (Yates and Gan, 2010). Several emission reduction strategies were assessed and compared to a bare soil control treatment, these included: (a) deeper injection, (b) high-density polyethylene sealed over the soil surface, (c) virtually impermeable film sealed over the soil surface, (d) ammonium thiosulfate surface spray, and (e) ammonium thiosulfate applied to the soil surface with irrigation water. With the exception of the deeper injection (46 cm), the fumigants were applied at 30 cm depth.

A main objective of this research was to compare emissions from laboratory experiments and numerical simulations for conditions where field estimates were unavailable, but after testing that the approach provides reasonable field-scale total emission rates. A comparison between laboratory measurements and mathematical simulations for peak and total emissions are summarized in Figure 1.1.1. With the exception of the control and the ammonium thiosulfate spray, the total emission estimates for Telone C-35 are within ±5 % of the group average. For the control, either experimental artifacts or incorrect simulation parameters may have led to larger differences in total emissions. For the ammonium thiosulfate spray treatment, it was unclear if the 2nd order reaction coefficient was suitable for the experimental conditions. Additional research is needed to test and improve methods for simulating ammonium thiosulfate-fumigant reactions.

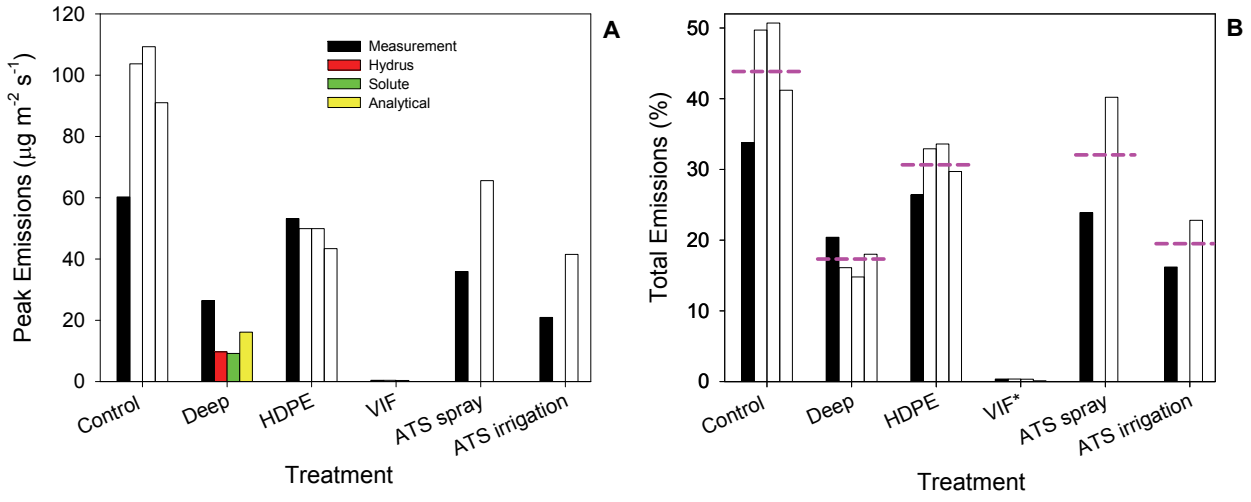

Figure 1.1.1. Comparison of different approaches to obtain peak and total emissions of Telone C-35 for several fumigation management treatments In B, horizontal dashed lines indicate the mean total emissions calculated using the four bars (or two bars for ammonium thiosulfate treatments) shown for each treatment. HDPE: high density polyethylene, VIF: virtually impermeable film; ATS: ammonium thiosulfate.

Extending Results to Methyl Iodide. Laboratory soil column experiments and numerical simulations were performed to simulate shank injection of methyl iodide in soil and to explore the potential for methyl iodide emissions to enter the atmosphere. The experiments included a bare soil control, high organic matter conditions, repeated surface water seals and use of a virtually impermeable film to seal the soil surface. For all experiments, methyl iodide was applied at 30 cm depth. The results from these experiments and simulations are reported in Table 1.1.1.

Table 1.1.1. Measured and simulated total emission losses of methyl iodide from laboratory soil columns for several fumigation management treatments.

Total emissions (%)	control	HOM*	VIF*	Irrigated
Measured	83.3	63.2	0.04	81.6
Hydrus 1D	85.6	71.7	0.7	76.9
Solute 1D	87.0	73.5	0.8	79.1
Average	85.3	69.5	0.51	79.2
Standard Deviation	1.9	5.5	0.41	2.4

*HOM: high organic matter; VIF: virtually impermeable film

With the exception of the high organic matter soil treatment, the results shown in Table 1.1.1 and presented in Section 3.4.3 suggest that simulations provide reasonably accurate emissions of methyl iodide that are based on laboratory experimentation (i.e., standard deviations < 5 %). The larger difference for the high organic matter soil treatment may be due to incorrectly specifying the soil degradation rate. Further study is needed to determine if these estimates of total emission correspond to field conditions.

Emissions after drip application: Rectangular laboratory soil chambers were used to study the effect of drip application of Telone C-35 to soil beds (Table 1.1.2). A control (bare soil) experiment was performed, along with high-density polyethylene and virtually impermeable film covered treatments. Total 1,3-dichloropropene emissions for the bare soil, high-density polyethylene, and virtually impermeable film treatments, respectively, were 36 %, 26 %, and 10 %. For chloropicrin, respectively, the total emissions were 39 %, 14 %, and 2.7 %.

The surface treatment had a significant effect on the fraction of fumigant emitted from the bed, sidewall or furrow surface. For a bare soil and high-density polyethylene treatments, over 90 % of the escaped fumigant was lost from the bed and sidewall. For the virtually impermeable film treatment, more than 95 % of the escaped fumigant was lost from the furrow. To improve the reduction in fumigant emissions when virtually impermeable films are used, efforts should concentrate on reducing emissions from the furrow.

Table 1.1.2. Fraction of total emissions (%) of 1,3-dichloropropene and chloropicrin escaping from bed, sidewall and furrow for several fumigation management treatments.

Treatment	Location	1,3-D*	CP*
Bare Soil	Bed	73 %	91 %
	Sidewall	22 %	8 %
	Furrow	6 %	2 %
	Total Emissions (% of applied)	**36**	**39**
HDPE**	Bed	89 %	97 %
	Sidewall	11 %	3 %
	Furrow	0 %	0 %
	Total Emissions (% of applied)	**26**	**14**
VIF**	Bed	5 %	1 %
	Sidewall	3 %	3 %
	Furrow	96 %	96 %
	Total Emissions (% of applied)	**10**	**2.7**

* 1,3-D: 1,3-dichloropropene; CP: chloropicrin

** HDPE: high-density polyethylene; VIF: virtually impermeable film

For both 1,3-dichloropropene and chloropicrin, the predicted peak and total emissions for the virtually impermeable film treatment were very similar to the experimental values. The predicted peak 1,3-dichloropropene emission rate was about 2.5 $\mu g\ m^{-2}\ s^{-1}$ and the measured peak rate was about 2.0 $\mu g\ m^{-2}\ s^{-1}$. For the Bare soil and high-density polyethylene treatments, the model predicted high emission rates which were not observed in the experiment and the fraction of emissions from the bed and sidewall were substantial. This could be due to the close proximity of the drip injection point to the soil surface, which led to rapid fumigant transport occurring during and shortly after injection. It appears that either (a) the simulation was unable to correctly predict transport or emissions for this physical system, or (b) experimental artifacts were encountered but not identified. Further research in this area is warranted to find a satisfactory explanation for this observation.

A Raised-Bed Field Study was carried out at Field 2B University of California – Riverside during 2009 to obtain emission estimates after drip fumigation with Telone C-35 (formulation). The drip line was placed at 10 cm depth at the center of raised beds. Two application rates (equivalent to 100 and 70 % of typical field application rates) were considered. The 100 % rate was used for bare soil (control) and high-density polyethylene-covered beds, while the 70 % rate was used for high-density polyethylene-, virtually impermeable film- and thermic film-covered beds. Emissions of 1,3-dichloropropene and chloropicrin were obtained using dynamic flux chambers placed on the bed surface. Figure 1.1.2 gives a summary of the total emissions.

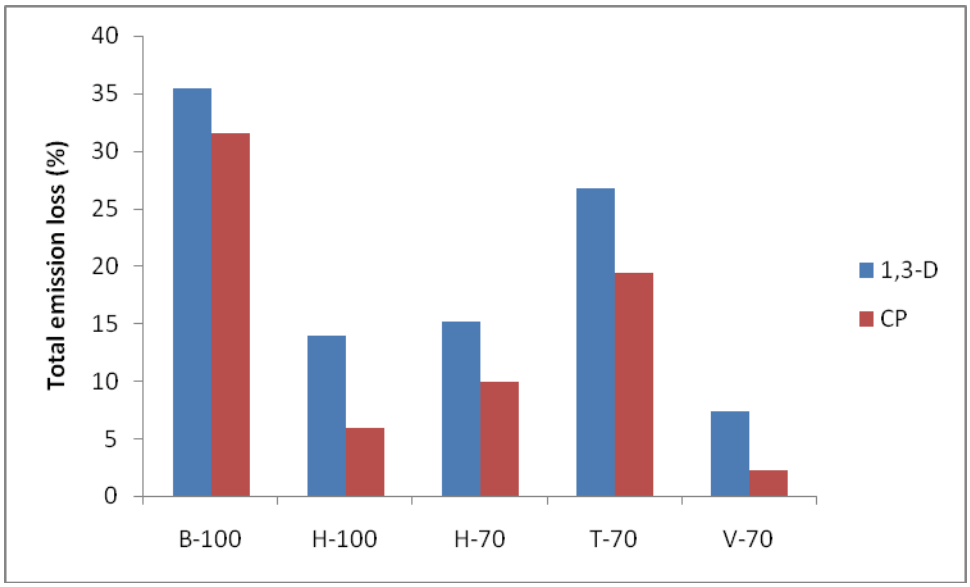

Figure 1.1.2. Total percentage emission loss of 1,3-dichloropropene and chloropicrin from "B" bare soil, "H" – high-density polyethylene, "T"-thermic film, and "V"-virtually impermeable film treatment and full rate (i.e., 100 %) or reduced rate (70 %) application. The experiment was conducted in Field 2B soil.

Based on high-density polyethylene-100 and high-density polyethylene-70, total emissions were not strongly effected by application rate. The lowest emissions were observed from the virtually impermeable film treatment, followed by the high-density polyethylene, thermic film and bare soil treatments. Also, the total emissions from the Field 2B study are comparable to the laboratory column experiments (see Table 1.1.2).

Conclusions

All the approaches used in this research project to manage soil fumigations reduced emissions of 1,3-dichloropropene and chloropicrin compared to standard fumigation practices. Emissions were reduced the most by using virtually impermeable films, followed by high organic matter soils, repeated irrigations and deep injection. Applying composted municipal green waste to the upper 15 cm of the soil reduced 1,3-dichloropropene emissions by approximately 80 %; but

further research is needed to determine the practicality of this method and the potential for plant pest control to be compromised by a reduction in fumigant concentrations at the soil surface.

Surface Water Seals. Repeated surface irrigation appears to be a simple, relatively low cost, and effective method to reduce fumigant emissions (approximately 50 % 1,3-dichloropropene emission reduction). The current research shows that most of the 1,3-dichloropropene had either been emitted or degraded after 4–5 days, suggesting that further application of water would not offer any greater benefit to emission reduction. Incorporating this emission-reduction strategy into existing production systems should relatively easy and straightforward. Recent laboratory and field research has also demonstrated similar results providing additional support for this methodology.

Fertilizer Amendments. Application of fertilizer amendments as a low-volume water spray reduced emissions by approximately 20–30 % across a range of large-scale field measurements and laboratory measurements. However, simulated emissions for a low-water spray of ammonium thiosulfate showed only modest reduction in emissions (i.e., < 2 %). If the experimental results hold for typical agronomic conditions, this methodology would represents a relatively simple approach to reduce emissions and could be readily incorporated into typical production systems. Simulation models need to be modified to incorporate the inhibiting effect of ammonium thiosulfate on fumigant emissions.

Both experiments and simulations demonstrate that additional reductions in emissions are possible if the fertilizer amendment ammonium thiosulfate is applied with 1 cm or more of irrigation water. However, research is needed to quantify the relationship between amounts of water added relative to applied thiosulfate. Previous research has shown that increasing the total applied water also increases the effectiveness of this emission reduction strategy.

Virtually Impermeable Films. Simulated emission rate for virtually impermeable film treatments (i.e., 1,3-dichloropropene, chloropicrin and methyl iodide) correctly predicted the order of magnitude of the measured emission rates and accuracy improved when the virtually impermeable film permeability was adjusted for the effects of relative humidity. Due to a scarcity of data, additional research is warranted to better describe the relationship between film permeability and relative humidity. For all experiments and simulations, emission flux rates and total emission percentages were very low.

Drip Applied Fumigants. For drip-applied 1,3-dichloropropene and chloropicrin in a bed-furrow system with the bed and sidewall covered with virtually impermeable film, the predicted peak and total emissions for the virtually impermeable film treatment were very similar to the experimental values. The predicted peak 1,3-dichloropropene emission rate was about 2.5 $\mu g\ m^{-2}\ s^{-1}$ and the measured peak rate was about 2.0 $\mu g\ m^{-2}\ s^{-1}$. The total emissions from the simulation and experiment, respectively, were 12.4 % and 11.9 %. For chloropicrin the predicted and measured total emissions, respectively, were 2.7 % and 4.2 % and the peak emission rate for both were less than 0.8 $\mu g\ m^{-2}\ s^{-1}$. The similarity between results implies that the mathematical model is suitable for predicting fumigant fate and transport when travel distances to through soil are relatively large (i.e., from drip application site to furrow surface). For this scenario, the virtually impermeable film would limit emissions from the bed and

sidewall so the modeling results would not be affected by bed or sidewall surface boundary conditions.

The model proved less accurate in predicting fumigant emissions for bare and high-density polyethylene covered soil. It is unclear why the model fails to accurately predict fumigant behavior over the relatively short transport distances from the injection point to the bed surface and additional research is needed to address this discrepancy.

Predicting Field Scale Emissions. Overall, mathematical simulation predicted the large scale field emission experiments with reasonable accuracy. While, the period emission rate deviated, the total emissions were generally within about 5 % of total emissions and within the range of uncertainty for field-scale emission estimates (i.e., aerodynamic method and Calpuff). For the 2007 field experiment, comparing aerodynamic, Calpuff, Hydrus and Solute simulations gave percent mass loss estimates for the control, deep injection and ammonium thiosulfate spray treatments, respectively, of 28.9±4.6, 22.3±5.1, and 25.5±1.1 % (see Table 3.1.4). Based on the increased accuracy of the 1-D modeling approach, it appears that the fumigations can be predicted sufficiently well that incorporating the additional complexity of a shank fracture may be unwarranted.

For the 2005 Buttonwillow field experiment, comparing aerodynamic, Calpuff, Hydrus and Solute simulations for the Irrigation and high organic matter soil treatments, respectively, gives 12.2±2.3 and 4.6 ± 2.4 % total emissions. The deviation between methods for estimating total emissions is well within the difference between field measurement methods (i.e., 5 %).

Using the average total emission values for Telone C-35 shown in Figure 1.1.1, the following order of total emission becomes evident: bare soil > ammonium thiosulfate spray > high-density polyethylene > ammonium thiosulfate irrigation > deep injection > virtually impermeable film. This data leads to average total emission percentages and standard deviation for this sequence of fumigation practices, respectively, of 43.9±7.9 %, 34.3±9.1 %, 30.7±3.3 %, 19.5±4.7 %, 17.3±2.4 % and 0.28±0.12 %. With the exception of the bare soil and ammonium thiosulfate spray treatments, the deviation between estimation approaches is below 5 %.

In addition the specific conclusions listed above, this research project also provided a wealth of information that can be used to determine if proposed methods to control VOC emissions will be adequate to achieve necessary reductions. The information obtained from this research provides ample evidence that simple and relatively low cost methods for estimating total emissions are sufficiently accurate to be used as surrogates for large-scale flux studies.

1. Introduction

1.1. Problem Description

Ground-level ozone is a primary ingredient of smog, which remains a severe pollution problem in California. Ozone is formed in the atmosphere by the reaction of VOCs and NO_x in the presence of sunlight and the reaction rate increases with temperature. Therefore, hot, dry weather is favorable to the formation of ozone. The highest concentration levels are typically found in suburban areas due to the transport of precursor emissions from the urban center. Local topographic effects can exacerbate ozone levels.

From 1975 to 2003, summer emissions of nitrogen oxides (NO_x) decreased 35 % from 900,000 to 600,000 tons statewide. In 2003, the principal sources of NO_x emissions were found to be on-road vehicles (46 %), fuel combustion from industries (26 %), and off-road sources (24 %) (i.e., engines, aircraft, marine vessels, and railroads). VOC emissions decreased significantly from over 1.2 million tons in 1975 to less than 500,000 tons in 2003.

Ground level ozone is a public and environmental health concern. Ozone is a main component of smog and exposure to ozone for several hours has been identified as a potential factor in that may reduce lung function and increase respiratory inflammation. This has led to concern for active children who spend considerable time outdoors during summer months. For example in Fresno, the rate of childhood asthma is 16.4 %, more than three times the national rate and may be partly due to high ozone levels. Ozone may also contribute to higher rates of premature death, lost school days, increased health-care costs, and may lead to economic loss by damaging crops and reducing productivity, although further research is needed to substantiate these claims.

Current non-fumigant pesticide VOC inventories are based on an estimated 100 % loss of the VOC portion of the pesticide even though most pesticides are affected to some degree by irreversible sorption, and abiotic and biotic degradation. Since information is available on many types of field-scale emissions for fumigant applications, the VOC inventories should be based on the median emission from the particular fumigation method (i.e., <100 % loss), which is based on information available from recent field-scale experimentation. This provides more accurate VOC inventories for fumigant use, but requires a large and extensive data set for different fumigation practices.

In California, for example, pesticide VOC emissions are believed to be less than a few percent of the total VOC emissions statewide. In urban regions, pesticide VOC emissions are probably insignificant compared to the more common industrial and automotive sources of VOCs. However, in some agricultural areas such as the San Joaquin and Sacramento Valleys, pesticide emissions may be a significant fraction of the VOC emissions inventory. In these areas, pesticide use may have a significant effect on VOC levels in the atmosphere.

Recently, U.S. EPA has established a new federal 8-hour ozone standard that requires regulators to develop and submit State Implantation Plans (SIPs) to meet the 2007 deadline. Initial data from California Air Resources Board (ARB) and the California Department of Pesticide

Regulation (DPR) indicate the need for reductions from many sources, including pesticides. Both agencies are working with stakeholders to determine the impact of pesticide emissions on ozone formation and the possible methods to reduce emissions.

As new stricter rules governing ambient ozone levels are implemented, regulations will be placed on activities that produce ozone. In regions with significant agricultural production, emissions of VOC from soil fumigation will likely be considered in an effort to be in compliance with regulation. Therefore, research is needed to find methods to accurately determine VOC emissions from fumigation and to develop methods to reduce emissions to low levels. Failure to do so may cause agricultural producers to face potentially restrictive control strategies.

The traditional approach to measure fumigant emissions from soil, field experiments are carried out where meteorological measurements are coupled with air concentrations above a fumigated field. However, such studies are complex, time-consuming and expensive. In addition, they are not easily replicated and are difficult to control in terms of environmental conditions (soil type, weather etc). These problems can potentially be overcome by performing the experiments in laboratory soil columns. In this way, several of the important environmental conditions can be easily controlled and replication can be carried out. Using established, previously reported, soil column approaches, coupled with modeling simulation, there exists a potential to move away from the requirement for field experiments towards simpler, more cost-effective, methods for determining fumigant emissions. This report describes laboratory and modeling approaches which aimed to simulate field studies performed in 2005 and 2007 at Buttonwillow, CA (described in previous ARB final report; Yates and Gan, 2010). The 2005 field study considered the effects of irrigation and organic matter addition on emissions of shank-injected 1,3-dichloropropene (1,3-D), i.e. Telone® II (formulation). The 2007 study considered the effects of deeper injection and ammonium thiosulfate (ATS) sprayed on the soil surface on the emissions of shank injected 1,3-D and chloropicrin (CP), i.e. Telone® C-35 (formulation). Comparisons between the laboratory and model results with those from the field studies are presented. The range of emission reduction strategies for 1,3-D and CP is extended using the laboratory and modeling approaches. In addition, the influence of drip application of 1,3-D and CP is also considered, together with the use of methyl iodide (MeI).

1.2. Project Objectives

a) Using soil from a single site where a range of emission reduction strategies for 1,3-D and CP have recently been assessed in the field, undertake laboratory soil column and model simulations to obtain cumulative and period emission rates for 1,3-D and CP under shank application.

b) Determine the extent to which the laboratory and model approaches are able to accurately reflect each other, and the emissions data derived from the field studies.

c) Extend, beyond those previously studied in the field, the range of fumigants under investigation (to include MeI), and the range of emission reduction strategies assessed. Obtain cumulative and period emission rates in each case.

d) Assess the influence of drip application of 1,3-D and CP on their emissions potential using a locally performed field study (UC Riverside), and compare with results obtained from laboratory and modeling studies using the Buttonwillow soil.

2. Methodology

2.1. Materials

Field Location. During the 2005 and 2007 field studies at the Buttonwillow field site (near 35.442,-119.457), soil was collected from each of the treatment fields (irrigation and organic matter addition treatments in 2005; control, deep injection and ammonium thiosulfate (ATS) application treatments in 2007). Due to their close proximity, the soils collected were texturally very similar to one another and were classed as sandy loam (60 % sand, 30 % silt, 10 % clay); a thermic Typic Haplargids from the Milham series. The only notable difference in the soils was the organically amended soil from the 2005 study which was determined to have an organic matter content of 3.2 %, compared to 2.1 % for the unamended soils.

Soil Properties (Buttonwillow 2005). The two soils collected in 2005 are referred to as low organic matter (LOM) and high organic matter (HOM) based on content, respectively. All soils were collected in depth increments of 0-15, 15-30, 30-45, 45-60 and >60 cm into clean plastic buckets and sealed to prevent moisture loss. The soil bulk density and moisture content within the field soil profile were also determined and average values calculated for use when packing the soil into experimental columns. For the 2005 soil, bulk density values of 1.0 g cm^{-3} (0-15 cm depth), 1.2 g cm^{-3} (15 to 25 cm depth) and 1.5 g cm^{-3} (25 to 150 cm depth), and moisture content, values of 5 % (0 to 2 cm depth), 12 % (2 to 4 cm depth), 17 % (4 to 25 cm depth), and 12 % (> 25 cm depth), were used for packing soil columns.

Soil Properties (Buttonwillow 2007). For the 2007 soil, a bulk density of 1.5 g cm^{-3} was used throughout the soil column (determined throughout the field profile as 1.5 (± 0.09) g cm^{-3}). Target moisture contents were: 13 % (0-15 cm depth), 17 % (15-30 cm depth), and 19 % (> 30 cm depth).

Soil Degradation. Fumigant degradation rates in the soils were determined (25 °C) in preliminary experiments using the method described by Ashworth and Yates (2007). For the 2005 soils, the soil from the irrigation treatment (i.e., LOM) field gave degradation half-lives of 5.3 and 10.9 days for 1,3-D and MeI, respectively. For the organically amended (HOM) soil, the values were 1.2 and 2.9 days, respectively. For a composite sample of the 2007 soils (mixing was considered acceptable due to the similar nature of the soils from the three fields), half-lives were measured as 3.8 and 0.12 days for 1,3-D and CP, respectively.

Chemicals. Standard solutions of Telone II (98.9 % purity; 50:50 *cis* 1,3-D : *trans* 1,3-D ratio) and chloropicrin (99.9 % purity) were donated by Dow Agrosciences (Indianpolis, IN). Methyl iodide standard (>99 % purity) was obtained from Sigma Chemical Co. (St Louis, MO). Ammonium thiosulfate was obtained from Sigma Aldrich (Milwaukee, WI), hexane (GC-MS/HPLC grade) and acetone (HPLC grade) from Fisher Scientific (Fairlawn, NJ), and XAD-4 (2 section 400/200 mg) and Anasorb CSC charcoal (2 section 400/200 mg) sorbent tubes from SKC Inc (Eighty Four, PA). The flame-sealed ends of the sorbent tubes were cut and ground flat using a mechanical grinder immediately prior to deployment. Deionized water was used for making up solutions.

Plastic Films. A 1 mil, clear HDPE tarp was supplied by Dow Chemical Company (Midland, MI), a 1.5 mil, clear VIF (Hytibar) was supplied by Klerk's Plastics (Hoogstraten, Belgium), and a 1 mil, clear 'thermic' tarp was supplied by Pliant Corporation (Washington, GA). Diffusion resistance (R values) of the tarps were determined in preliminary experiments using the approach previously described (Papiernik et al., 2011). For the HDPE, R values of 0.29, 0.19, 1.1 and 1.0 cm h^{-1} (25°C) were used for 1,3-D (cis) 1,3-D (trans), CP and MeI, respectively. These are summarized in Table 2.1.1. For the VIF, R values of 1075, 525, 3000 and 1000 cm h^{-1} were determined for 1,3-D (cis), 1,3-D (trans), CP and MeI, respectively.

Table 2.1.1 Film materials and properties used in experiments and simulations.

Material	Mass Transfer* Coefficient h (cm/h)	Resistance Factor R (h/cm)	Equivalent** Boundary Layer Thickness, b_{ref} (cm)	Arrhenius Equation Activation Energy, E_a, for b
Bare soil surface	–	–	0.5	–
High density polyethylene				
1,3-D (cis)	3.4	0.2–0.4	90.0	-13.6 kJ mol^{-1}
1,3-D (trans)	5.4	0.1–0.2	56.0	-14.6 kJ mol^{-1}
chloropicrin	0.9	0.2–1.5	330	-31.7 kJ mol^{-1}
methyl iodide	1.0	0.8–1.2	–	–
Virtually impermeable film				
1,3-D (cis)	9.3 10^{-4}	670–1480	324,970	-102 kJ mol^{-1}
1,3-D (trans)	1.9 10^{-3}	230–800	159,070	-100 kJ mol^{-1}
chloropicrin	<3 10^{-4}	>2800	998,060	-104 kJ mol^{-1}
methyl iodide	1.0 10^{-3}	650–1260	370,531	-102 kJ mol^{-1}

* reported h value is the midpoint of the R range. ** b_{ref} (20°C) was used in simulations

2.2. Laboratory Studies

2.2.1. Soil Column Design

Laboratory soil columns (Figure 2.1.1; Plate 2.2.1) were used to simulate shank-injection of fumigants. The system uses a point-source of fumigant applied at a particular depth and allows for determination of surface emissions and vertical (one dimensional, 1D) gas distribution within the column. General details of the approach are given in this section, with greater detail given in the relevant experiment-specific discussion later in the report. Soil was packed into cylindrical (12 × 150 cm) stainless steel columns as per the field depth increments (see Section 2.1). Field-measured bulk density and moisture content of the soil was maintained in the columns.

A stainless steel emissions chamber placed on the surface of the soil column was swept with clean air to channel emitted fumigant through sorbent tubes. As the primary sorbent tube, either XAD-4 (for studies involving CP) or charcoal (for studies involving only 1,3-D or MeI) were used. In each case, a backup charcoal tube (connected in series) was employed to check for breakthrough of 1,3-D.

To simulate the shank injection, liquid fumigant was injected into the soil column using a glass syringe fitted with a side-port needle. Injection was carried out on day 0 at the relevant soil depth (typically 30, 46 or 60 cm) and to the center of the soil body. The application port was immediately sealed. Application reflected typical agricultural application rates (experiment-specific details are given in relevant sections below).

Near-surface soil temperatures were manipulated by programming the ambient temperature of the room in which the column experiments were conducted. Figure 2.2.2 shows the diurnal temperature regime that resulted in soil temperatures typical of those observed during the field studies. Below 30 cm depth, the columns were insulated with 1 cm thick foam to reduce temperature fluctuations at depth.

Immediately following fumigant application, the sweeping of headspace air through the sorbent tubes was initiated at a nominal rate of 140 mL min^{-1}. Sample times for each tube were based on the field studies (experiment-specific details given in relevant sections below), and switching between tubes was controlled by a system of solenoid valves activated by data logger. Typically short sample times (e.g., 2–4 h) at the start of the experiment were extended to longer periods (e.g. 6 h) at later times when fumigant emissions were expected to be significantly lower. Details of the various treatments studies using the soil column approach are given in the experiment-specific sections below.

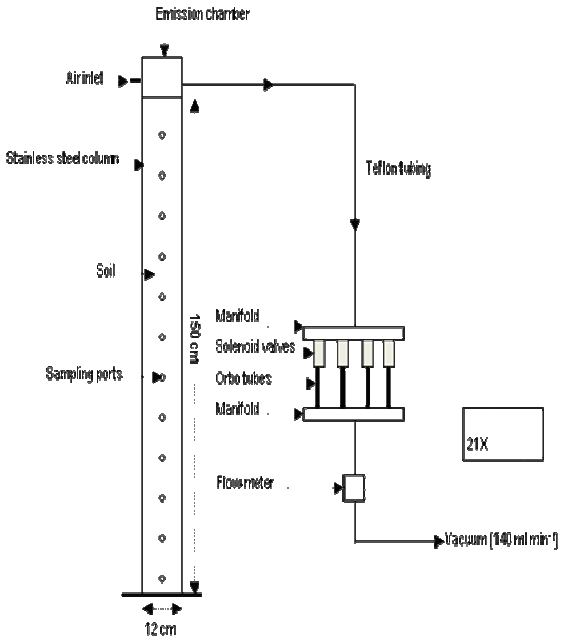

Figure 2.2.1. General design of laboratory soil columns (Ashworth and Yates, 2007).

Plate 2.2.1. Photograph of soil columns used for shank injection studies.

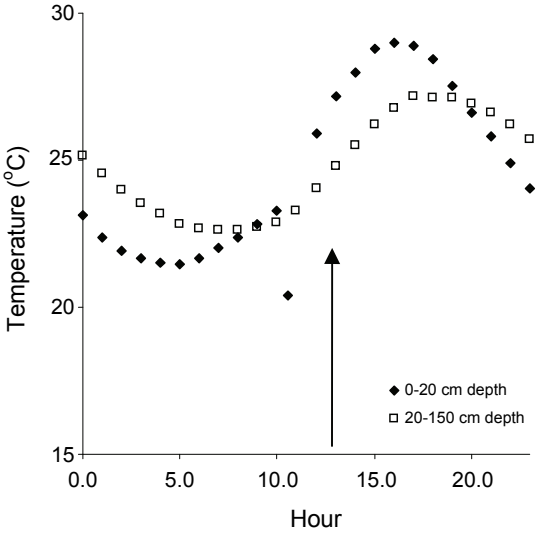

Figure 2.2.2. Diurnal temperature regime for soil columns. Arrow represents typical time of fumigant application.

2.2.2. Soil Chamber Design

Laboratory soil chambers (Figure 2.2.3; Plate 2.2.2) were used to simulate the drip application of fumigants to raised beds. The system allows for determination of surface emissions and both vertical and horizontal (2D) gas distribution within the chamber. The experiment was performed using purpose-built aluminum soil chambers that allowed for an actual size (non-scaled) construction of half-a-bed and half-a-furrow.

Rectangular soil chambers (120 cm high × 80 cm wide × 10 cm deep) were packed with the Buttonwillow soil in such a way as to form half a bed (50 cm wide) and half a furrow (30 cm deep, 30 cm wide at its top and 25 cm wide at its base) across the width of the chamber. Field-measured bulk density and moisture content of the soil was maintained in the columns. An aluminum volatilization chamber was placed atop. Within the volatilization chamber, it was possible to seal and isolate the headspace above the bed, sidewall and furrow compartments and thus determine the contribution of each compartment to the overall emissions loss. Each compartment was swept with clean air at a rate of 1 L min^{-1}, from which a sub-sample (50 mL min^{-1}) was directed through sorbent tubes for collection of fumigant vapors. Because these chambers were only used for studies involving both 1,3-D and CP combined, XAD-4 sorbent tubes were used as the primary tube. A backup charcoal tube was used to check for breakthrough of 1,3-D.

The fumigants were applied at a depth of 5 cm below the bed surface at two-thirds distance from the bed shoulder (Figure 2.2.3), which represents Day 0. Application equated to field application rates of approximately 160 kg ha^{-1} 1,3-D and 84 kg ha^{-1} CP (based on bed surface area). These rates closely matched the ratio of 1,3-D to CP in the commercial drip application product 'Inline', (although in contrast to the commercial product, no surfactant was added to our system). Immediately following injection of the fumigants via a sealable port in the face of the chamber, 1L water was applied through the same port at a rate of 8 mL min^{-1}. Thus, the application took place over a period of around 2 hours. The relatively high solubility of both fumigants ensured the downward and lateral movement with the flow of irrigation water from the point of application. This procedure was used as a surrogate for a typical 2 hour field drip-application of 1,3-D and CP using standard 0.67 gallon min^{-1} 100 ft^{-1} drip tape.

Near-surface soil temperatures were manipulated by programming the ambient temperature of the room in which the column experiments were conducted. As shown in Figure 2.2.4, diurnal temperature regime that resulted in soil temperatures typical of those observed during the field studies was employed (ranging from 23 to 32 °C at 5 cm depth). Below 30 cm depth, the columns were insulated with 1 cm thick foam to reduce temperature fluctuations at depth.

Immediately following fumigant application, the sweeping of headspace air through the sorbent tubes was initiated. In all these laboratory drip-application experiments, tubes were initially sampled for 2 hours during the day (7 am to 7 pm) and 12 hours at night. The day-time sampling period was increased later in the experiment when emissions were expected to be lower. Details of the various treatments studies using the soil chamber approach are given in the experiment-specific sections below.

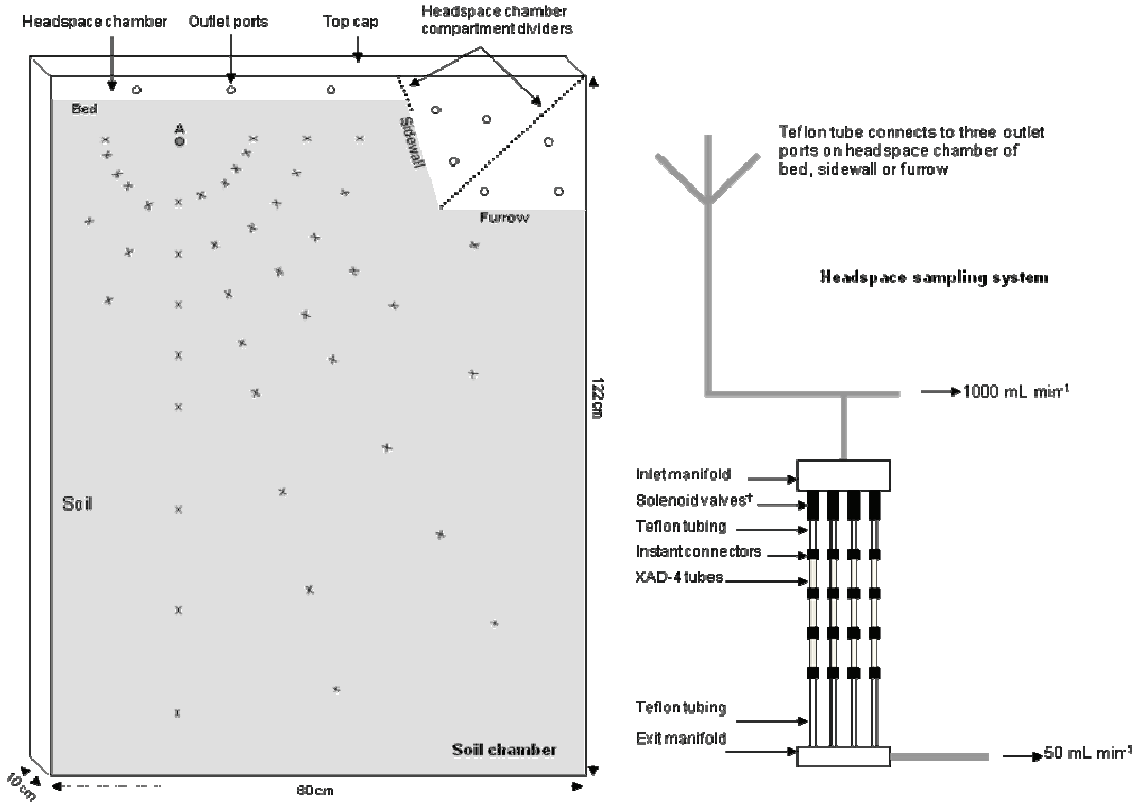

Figure 2.2.3. General design of laboratory soil chambers (Ashworth et al., 2008).

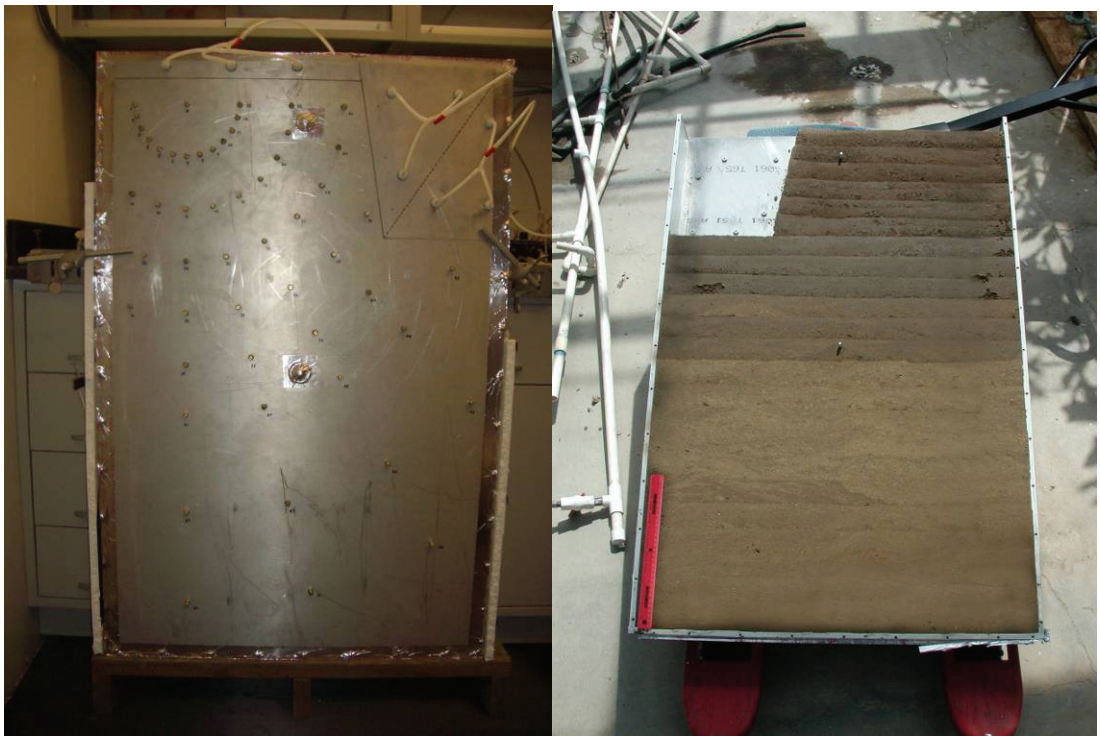

Plate 2.2.2. Photographs of aluminum soil chamber (left) and opened chamber showing soil profile after drip application experiment (right).

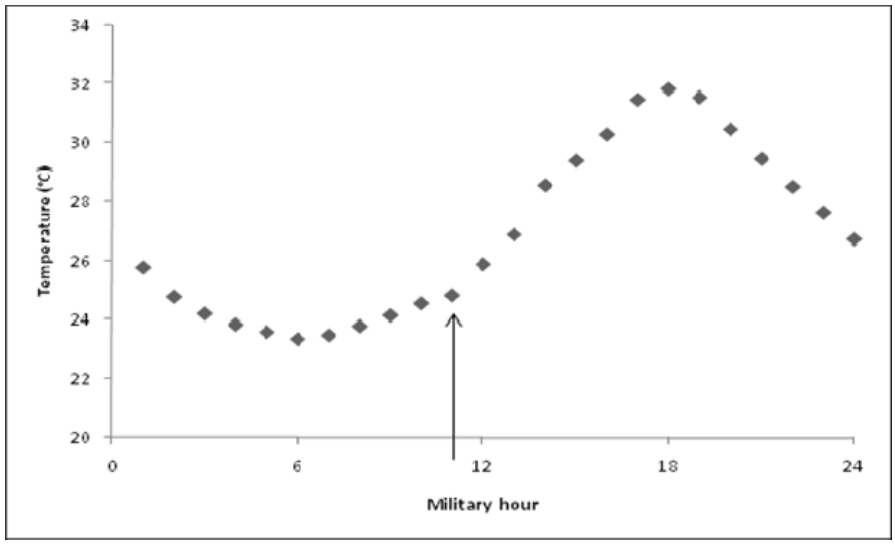

Figure 2.2.4. Diurnal temperature pattern in the soil chambers, measured at 5 cm depth. Arrow represents typical time of fumigant application.

2.3. Field Plot Study Methods (Field 2B, 2009)

A raised-bed field fumigation experiment was carried out from September 22, 2009 to October 06, 2009 at the University of California Agricultural Experiment Station, Riverside, CA. The soil is an Arlington sandy loam (coarse loamy, mixed, thermic, Haplic Durixeralf) with a particle size distribution of 75 % sand, 18 % silt, and 7 % clay, and an organic carbon content 0.9 % (organic matter content of 1.6 %; assuming 58 % carbon content of organic matter).

Prior to formation of the raised beds, the soil was wetted daily by sprinkler irrigation for several weeks. This ensured favorable conditions for the formation of raised beds, that is, moist soil to a depth of around 1m. The soil was then plowed and a bed shaper pulled through the soil by tractor to form the beds. The dimensions of the bed/furrow system are shown in Figure 2.3.1. At the same time, drip tape (Ro-Drip, 20 cm dripper spacing, flow rate of 250 L h^{-1} 100 m^{-1}) was mechanically installed along the center of each bed at a target depth of 10 cm.

Beds were sectioned into plots (each around 4.5 m long) for the differing fumigation treatments. A 3 m long buffer between the plots was also formed. Plots were arranged according to a triplicate randomized block design. Treatments were: bare soil; covered with HDPE; covered with VIF; and covered with thermic film. Each treatment plot had a plastic barrel placed at one end (in the buffer zone) which acted as a reservoir for the fumigant solution to be applied to that plot. An outlet from each barrel was connected to the dripline running through the relevant plot. Into each barrel, running from a central manifold, was a pressure source capable of maintaining around 8-11 psi within each barrel. Thus, application of the fumigants could be controlled, off-site, using an air compressor.

Onto each bed, a dynamic flux chamber was placed as shown in Figure 2.3.1. A schematic diagram of the flux chamber design is shown in Figure 2.3.2. The inlet to each chamber was connected to a pipe running to a point approximately 30 m upwind of the fumigated area. Mass flow rate of the clean air through the chamber was maintained at 17.5 L min^{-1}. To achieve this, the outlet from each chamber was connected to a central manifold attached to an industrial vacuum pump. The mass flow rate at each flux chamber was checked periodically throughout the study and adjusted as required to maintain the target rate. For determination of fumigant concentrations within the air flow, the mass flow was sub-sampled at the chamber outlet at a target rate of 80 mL min^{-1} and directed through an XAD-4 sorbent tube. A charcoal tube was used as a backup tube to check for breakthrough of 1,3-D. Sorbent tubes were housed within an insulated wooden box together with the sub-sample pump and a system of solenoid valves that allowed for the sequential sampling of up to four consecutive sorbent tubes per chamber. Using a sampling time of 3 hours per tube, a maximum of 12 hours (e.g. overnight) could therefore pass between tube-collection events. The solenoid valves were controlled using datalogger. Hourly average sub-sample flow rates were also recorded by the datalogger.

At the time of fumigation, 38 L of tap water were added to each barrel followed by a known mass of Telone C-35, either 71.0 or 49.7 g. Based on surface area of the raised bed (top and sidewalls), this equated to application rates of 192 and 134 kg ha^{-1}, respectively (i.e., 100 or 70 % of typical agricultural application rates). By applying the Telone C-35 as drip irrigation, it was expected to be comparable to the application of 'Inline'; the commercially available form of Telone C-35 used for drip irrigation. The 100 % rate was applied to bare soil and HDPE plots.

The 70 % rate was applied to HDPE, VIF and thermic film plots. Immediately following addition of the fumigant, the barrels were sealed and shaken to aid mixing. Fumigation was initiated at 11:30 am on September 22, 2009 (Day 0) by starting the air compressor.

Sorbent tube sampling was initiated at 7 am on Day 0. Therefore, the first tubes (7 am to 10 am) from each chamber were sampled prior to fumigation and served as blanks. Collection of tubes occurred daily at both at 7 am and 7 pm. On Day 5, the sampling time was increased to four hours, and on Day 9, to six hours. The experiment was terminated on Day 14 (October 6, 2009).

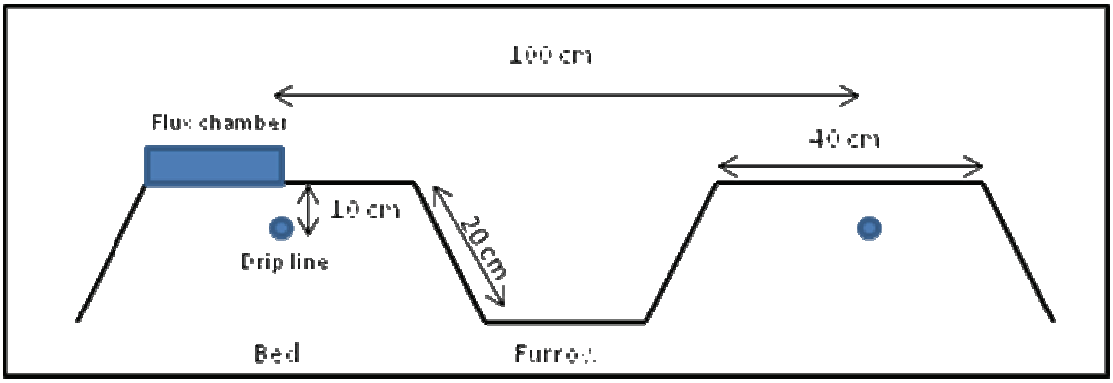

Figure 2.3.1. Schematic diagram of raised bed cross section.

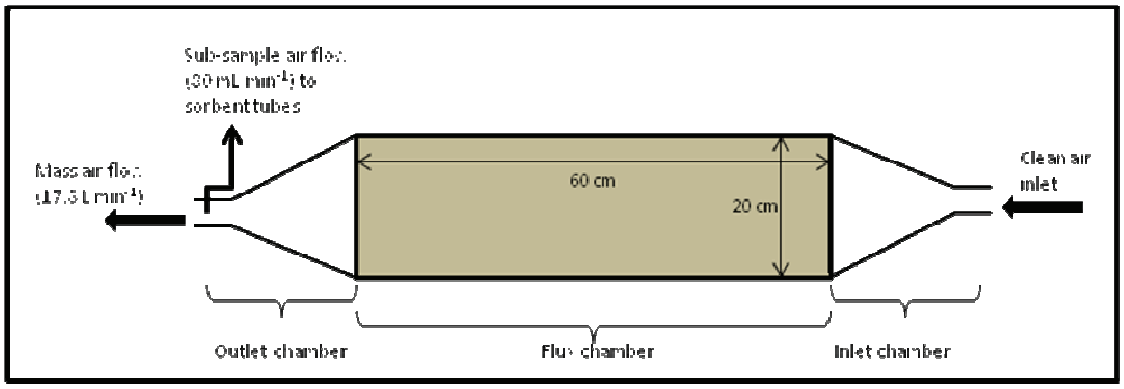

Figure 2.3.2. Schematic diagram of dynamic flux chamber system. Underside of shaded area (flux chamber) is open to soil surface. Mesh screens across width of inlet chamber aid the disturbance of incoming air to effectively sweep the entire width of the flux chamber. Mesh screen between the outlet and flux chambers aids mixing of swept air prior to sampling.

2.4. Sample Handling

2.4.1. Sample Storage

XAD-4 and charcoal sorbent tubes removed during the experiments were capped at both ends, placed into plastic bags. The bags of tubes were then placed in a freezer (-19 °C) prior to extraction and analysis.

2.4.2. Sample Extraction

Sorbent tubes were extracted by separating the A and B bed sections of the sorbent material, placing a section into a 20 mL glass vial, adding 4 mL Hexane (for XAD-4 tubes) or Acetone (for charcoal tubes), shaking for 30 mins. Following shaking, for samples containing CP and/or 1,3-D, the vials were opened and 1.5 mL of supernatant was poured to an amber GC vial. The extraction efficiency of this procedure has previously been determined as around 85 %. Due to its high vapor pressure, samples containing MeI were not opened for transfer to the amber GC vial. Instead, sub-sampling of the supernatant acetone was performed using a gas-tight syringe inserted through the septum. The efficiency of this procedure was determined to be about 70 %. All vials were stored at -19 °C prior to analysis.

2.4.3. Sample Analysis

All samples were returned to room temperature prior to analysis. For samples containing only 1,3-D, concentrations were determined using a Hewlett Packard HP7890 gas chromatograph equipped with a microelectron capture detector (μECD). The column was a 30.0 m × 0.25 mm × 1.4 μm capillary column (Agilent Technologies) running at a flow rate of 1.6 mL min^{-1} and using He as the carrier gas. The oven temperature was fixed at 90 °C. The inlet temperature was 240 °C and the detector temperature 280 °C. 1,3-D standards encompassing the range of concentrations observed in the samples were prepared in acetone.
For samples containing 1,3-D and CP, analysis was carried out as above except for the GC oven temperature program. Here, the oven temperature was maintained at 45 °C for 1 min after sample injection, increasing to 75 °C at a rate of 2.5 °C min^{-1}, and then to 140 °C at a rate of 35 °C min^{-1} before being held at this temperature for 3 min. Combined 1,3-D and CP standards encompassing the range of concentrations of the samples were prepared in either hexane (XAD-4 tubes), or acetone (charcoal tubes).

For samples containing MeI, analysis was carried out using the equipment described above. Conditions of the analysis were the same except that the helium flow rate was 1.0 mL min^{-1}, and oven temperature was fixed at 60 °C. Standards for the charcoal extract analysis were prepared by injecting differing amounts of MeI (encompassing the range of sample amounts) onto clean charcoal tubes under vacuum (150 mL min^{-1}), prior to acetone extraction using the same procedure as for the samples.

In all analyses, concentrations of total 1,3-D were calculated from the *cis* and *trans* isomer data, and Telone C-35 were calculated by total of 1,3-D and chloropicrin.

2.5. Modeling Methods

2.5.1. Transport Equations

Besides the laboratory and field experimental tests, simulation models were also used to determine the effect of each emission reduction strategy. To simulate fumigant fate and transport with consideration of variably-saturated soils and variable soil temperature, three governing processes: water flow, heat transport, and solute fate and transport were included. For fumigant transport, the governing equation describes the phase partition between liquid, gas and solid phase, dispersion (convection and diffusion), and degradation processes. Degradation was described using a first-order decay reaction, and included the ability to specify the degradation rate in each phase (liquid, vapor, and solid). The governing transport equations were written as follows (Šimunek and van Genuchten 1994):

$$\text{Water Transport: } \frac{\partial \theta}{\partial t} = \frac{\partial}{\partial x}[K_x(h)\frac{\partial h}{\partial x}] + \frac{\partial}{\partial z}[K_z(h)\frac{\partial h}{\partial z} + K_z(h)] - S \quad (1)$$

where θ is the volumetric water content ($cm^3\ cm^{-3}$), h is the pressure head (cm), K is hydraulic conductivity tensor ($cm\ s^{-1}$), and S is a sink term (s^{-1}); t is time(s), x and z is distance (cm).

$$\text{Heat Transport: } C_h(\theta)\frac{\partial T}{\partial t} = \frac{\partial}{\partial x}[\lambda_x(h)\frac{\partial T}{\partial x}] + \frac{\partial}{\partial z}[\lambda_z(h)\frac{\partial T}{\partial z}] - C_w q\frac{\partial T}{\partial z} \quad (2)$$

where T is soil temperature (K), C_h and C_w are the volumetric heat capacity for the porous media ($J\ m^{-3}\ K^{-1}$) and liquid, respectively, and λ is the apparent thermal conductivity ($W\ m^{-1}\ K^{-1}$).

Solute transport:

$$\eta\frac{\partial C_g}{\partial t} + \theta\frac{\partial C_l}{\partial t} + \rho_b\frac{\partial C_s}{\partial t} = \frac{\partial}{\partial x}[D_g\frac{\partial C_g}{\partial x} + D_l\frac{\partial C_l}{\partial x} - q_x C_l] + \frac{\partial}{\partial z}[D_g\frac{\partial C_g}{\partial z} + D_l\frac{\partial C_l}{\partial z} - q_z C_l] - \eta\mu_g C_g - \theta\mu_l C_l - \rho_b\mu_s C_s \quad (3)$$

where C_g, C_l, and C_s are gas-, liquid-, and solid-phase concentrations (μg cm^{-3}), respectively; D_g and D_l are liquid- and gas-phase diffusion coefficients ($cm^2\ s^{-1}$), respectively; μ is a first-order degradation coefficient (s^{-1}); θ, ρ_b, and η, respectively, are water content ($cm^3\ cm^{-3}$), bulk density ($g\ cm^{-3}$), and air content ($cm^3\ cm^{-3}$); q is the Darcian flux density; and the subscripts: l, s, and g indicate liquid-, solid-, and gas- phases, respectively.

The partitioning between liquid- and gas-phase was assumed to obey Henry's Law and the partitioning between liquid- and solid-phase was assumed to be equilibrium adsorption:

$$C_g = K_h C_l \quad (4)$$

$$C_s = K_d C_l; \quad \text{and} \quad K_d \approx f_{oc} K_{oc} \tag{5}$$

where K_h is the Henry's law constant (dimensionless), K_d is the linear equilibrium sorption coefficient (cm^3 g^{-1}), f_{oc} is the fraction organic matter and K_{oc} is the soil organic carbon sorption coefficient.

A volatile surface boundary condition was used to simulate the volatilization process.

$$(D_e \frac{\partial C_l}{\partial z} - qC_l) = h(C_g - C_{air}) \tag{6}$$

where C_{air} is gas concentration in the atmosphere (μg cm^{-3}), and $D_e = D_l + K_h D_g$ is effective dispersion coefficient (cm^2 s^{-1}) and h is a mass transfer coefficient (cm s^{-1}) defined as

$$h = \frac{D_g^{air}}{b} \tag{7}$$

where D_g^{air} is the binary gas diffusion coefficient in the air and b is the thickness of a stagnant boundary layer at the soil surface (Jury et al., 1983). For an impermeable boundary condition, Equation 6 is used with h, q and D_e all equal to zero.

Temperature Dependence. The degradation rate, Henry's Law constant, vapor diffusion coefficient, and film permeability are temperature-dependent. To account for temperature, the Arrhenius equation is used in model simulation to calculate a value for these parameters at a specific temperature and time:

$$\beta_T = \beta_r e^{-E_a \frac{(T-T_r)}{RTT_r}} \tag{8}$$

where β_T is the temperature-dependent parameter; β_r is the reference value for the parameter at a reference temperature (293 K); E_a is the activation energy for parameter β_T (J mol^{-1}); T_r is the reference temperature (K); and R is the universal gas constant (8.314 J mol^{-1} K^{-1}).

Modeling Second-order Reaction Processes. Fumigant emissions can be reduced by enhancing degradation in soil. One approach to accomplish this is by the addition of a reacting compound, such as ammonium thiosulfate (ATS). In a several experiments (e.g., Gan et al., 1998a; Gan et al. 2000a), it was observed that many pesticides could be rapidly degraded in solutions or soils containing thiosulfate compounds. The proposed reaction mechanism was second-order, e.g.,

$$\omega_1 C_1 + \omega_2 C_2 \xrightarrow{k_{12}} \text{products} \tag{9}$$

where ω_i are stoichiometric coefficients, C_i are the concentrations of the fumigant and thiosulfate and k_{12} is the second-order reaction coefficient (cm^3 μmole^{-1} s^{-1}). To simulate this reaction

process requires adding an additional term to the right hand side of Eq. (3) (see Yates and Enfield, 1988) to describe second-order loss, that is:

$$\text{Second-order loss} = -k_{12} C_{fumigant} C_{ATS} \qquad (10)$$

This additional term describes the loss of material from the second-order reaction mechanism. The loss only occurs when both chemicals are present together in soil or solution at the same time, and hence the two concentrations are multiplied together. This creates a system of nonlinear partial differential equations.

Numerical solutions to the transport equations. Equations 1 – 10 were solved using either finite element or finite difference methods. Three computer programs were used to predict fumigant emission rates using various emission reduction strategies: a public domain Hydrus 1D (Šimunek et al., 2008) version 4.14 (downloaded from www.hydrus2d.com on 9-11-2010); the commercial Hydrus 2D/3D (Šimunek et al., 2008) version 1.11x08, and Solute 1D version 2.1 (Yates, 2006). The Hydrus software programs were modified to include various fumigant-related processes described above, such as temperature dependent properties of the surface tarp and a removal of tarp at a specified time. These solution algorithms were used in a forward prediction mode based on the experimental parameters and fumigant properties at the time of the experiments. Unless otherwise indicated, the results given below were not obtained using inverse approaches.

Since the Hydrus programs do not formally include a 2nd-order reaction mechanism, simulations of experiments that involved the use of ATS were obtained from Solute; which is a 1-D finite difference program that solves the water flow, heat and solute transport equations listed above (Equations 1–10). Simulations from this program have been compared to Hydrus and analytical solutions and were found to be essentially equivalent (Yates, 2009).

Analytical solution to the transport equation. When soils are relatively dry (e.g., for hot-gas and shank fumigation) and water movement and chemical carried by water can be ignored. Gas-phase transport is the dominant process. For such cases, a simple analytical solution can be used to estimate the fumigant volatilization rate to air (Yates, 2009).

The analytical solution describes fumigant transport in a 1–D (vertical). For simulations using the analytical solution, it was assumed that (a) the soil water content was very low so that water movement over relatively short time periods could be neglected; (b) the soil diffusion coefficient and surface mass transfer coefficient at the soil-atmosphere interface are appropriate constants that represent the average temperature conditions during fumigation; (c) isothermal conditions exist; (d) the fumigant moves via liquid and vapor diffusion and (e) the fumigant degrades following a first-order process in all three phases (i.e., soil, water and gas phase).

For these conditions, the total fumigant emissions for a shank injection assuming a point source is

$$\textit{Total Volatilization} = \frac{C_o H_E e^{\frac{-z_o\sqrt{\mu}}{\sqrt{D_E}}}}{H_E + \sqrt{D_E}\sqrt{\mu}} \qquad (11)$$

where $H_e = h/R_G$ is the effective mass transfer coefficient (cm s^{-1}), $D_E = (D_L/R_L + D_G/R_G)$ is the effective dispersion coefficient with $D_L = (\theta^{(10/3)}/\theta_s^2)D_{water}$, $D_G = (\eta^{(10/3)}/\theta_s^2)\, D_{air}$, $R_L = (\theta + \rho_b\, K_d + \eta K_H)$ is the liquid-phase retardation coefficient, K_H is the Henry's Law constant, $R_G = R_L/K_H$, μ is the first-order decay rate, z_o is the injection depth (cm) and C_o is the mass applied (μg cm^{-1})

An equation for total fumigant emissions that would be appropriate if the shank creates a soil fracture that can be represented as a line source initial condition

$$Total\ Volatilization = \frac{C_o H_E \sqrt{D_E}\left(e^{\frac{-z_d\sqrt{\mu}}{\sqrt{D_E}}} - e^{\frac{-z_o\sqrt{\mu}}{\sqrt{D_E}}} \right)}{\left(z_o - z_d\right)\left(H_E + \sqrt{D_E}\sqrt{\mu}\right)\sqrt{\mu}} \qquad (12)$$

where z_d is the depth at the top of the fracture (e.g., if soil was disced immediately after fumigation, z_d would be the depth of discing operation)

2.5.2. Parameterization

Simulation parameters included the properties of soil, solute and film (if applicable) and initial and boundary conditions. The parameters were obtained from either a direct experimental measurement or from the literature, when a measured value was not available. Default soil hydraulic properties and heat transport properties for the sandy loam soil in Hydrus were used for all simulations and the values used for specific parameter are listed in Table 2.5.1 or are given in the relevant results sections below.

1,3-dichloropropene (1,3-D). The first-order degradation rate constant at 25ºC was 0.0054 h^{-1} for the untreated soil based on previous experimental measurement (Ashworth and Yates, 2007). The activation energy of the first-order degradation rate constant was estimated from the data reported by Dungan et al., (2001). Henry's constant, K_H, was 0.074 for 1,3-D (cis) and 0.043 for 1,3-D (trans) at 25ºC according to reported values (Dow Agrosciences, personal communication). The activation energy of Henry's constant was estimated from the data reported by Leistra (1970).

Chloropicrin. The first-order degradation rate constant at 25ºC was very high, 0.2390 h^{-1} for the untreated soil based on previous experimental measurements (Ashworth and Yates, 2007). However, based on this rate, CP would be degraded very rapidly and little would be volatilized after injection (i.e., according to a simulation, the total emissions would be < 0.5 %). Other measured chloropicrin degradation half-life for similar soil types range from 5–100 h (Wilhelm et al., 1996; Gan et al., 2000b; Zheng et al., 2003) and a half live of 24 h is suggested by Wauchope et al. (1992). An alternative approach for estimating the degradation coefficient is obtained from an inverse procedure using Hydrus 1D. This procedure adjusts the degradation rate until the differences between measured and estimated concentrations are minimized. This

leads to first-order degradation rates of 0.0036 h^{-1} for 1,3-D and 0.0169 h^{-1} for chloropicrin. These lower rates were used to predict the emission rate for other treatments. Henry's constant, K_H, was 0.096 (Ashworth et al, 2009). The activation energy of the first-order degradation rate constant was not available so the value for 1,3-D was used for CP due to their similarity in physicochemical properties. The E_a for K_H was estimated using the SPARC online calculator® to obtain estimates of K_H for several temperatures and fitting the Arrhenius equation to the results.

Methyl iodide. The first-order degradation rate constant was 0.0026 h^{-1} for the untreated soil based on the experimental measurement (Ashworth et al, 2010). The activation energy of the first-order degradation rate constant was estimated from the data reported by Zheng et al. (2004). Henry's constant was 0.23 at 25ºC (Gan et al. 1996). The activation energy of Henry's constant was not reported in the literature. Instead, the value of MeBr was used (Yates et al., 2003) because the similarity between MeI and MeBr.

Table 2.5.1. Default soil and chemical properties used in simulations. The cross-sectional area of the column was 113.1 cm^2 and depth of injection was 46 or 60 cm. See **Table 2.1.1** for film and bare soil surface properties.

Data type	Properties	Value (1,3-D / CP)*	Units
Soil properties	Bulk density	1.5	cm g^{-1}
	Porosity	0.434	
	Residual water content	0.04	cm^3 cm^{-3}
Pesticide properties at 25°C	Henry's law constant	0.059** / 0.096	
	Binary Gas diffusion coefficient	302 / 296.4	cm^2 h^{-1}
	Binary water diffusion coefficient	0.0416 / 0.096	cm^2 h^{-1}
	Degradation rate	0.0036 / 0.0169	h^{-1}
	Organic carbon partition coeff.	5.4 / 10	cm^3 g^{-1}
	Sorption coefficient	0.05 / 0.1	cm^3 g^{-1}
Activation energies	Binary Gas diffusion coefficient	4403	J mol^{-1}
	Henry's law constant	43200/26150	J mol^{-1}
	Degradation rate constant	58893	J mol^{-1}
Heat transport	Initial soil temperature	25-22	°C
	Temperature range	19-32	°C
	Thermal properties	Default properties for sandy soil	
Initial application	Initial mass in column	182.0 / 99.0	mg
ATS- spray, 46 cm injection.	Applied mass	0.565	g
	Water applied	1.6	mL
	The second-order reaction constant	0.2 / 0.2	mL μmole^{-1} h^{-1}
	1st-order degradation coefficient	0.046	h^{-1}
	Target molar ratio ATS : fumigant	1.7 : 1.00	

* - when two values are shown, the first is for 1,3-D and the second for chloropicrin

** - value is weighted average of 0.074 for 1,3-D (cis) and 0.043 for 1,3-D (trans)

Gas diffusion. The binary gas diffusion coefficient, D_{ab}, and its activation energy was estimated using Fuller correlation (Reid et al., 1987). Tortuoisty of the porous space was calculated using the Moldrup method as implemented in Hydrus 1D/2D and Solute 1D.

Boundary layer thicknesses. For a volatile boundary condition, stagnant boundary layer theory with a boundary layer thickness (b) of 0.5 cm was used to calculate the mass transfer coefficient (h) for the non-tarped treatments (Jury et al., 1983). For HDPE, the mass transfer coefficient and stagnant boundary layer thickness, and activation energy were determined from Papiernik et al. (2002). For VIF, the mass transfer coefficient and stagnant boundary layer thickness, and activation energy were determined from Papiernik et al. (2011). The atmosphere boundary for water and heat transport was used for the soil surface and non-flow boundary was used for the bottom end of the soil column.

3. Shank Injection Studies

3.1. Laboratory Experiments Simulating the 2007 Buttonwillow Field Experiment: Influence of deep injection and ammonium thiosulfate application on shank injected Telone C-35 emissions.

3.1.1. Experiment Information

Duplicated laboratory soil column experiments with simulated shank injection of Telone C-35 were performed using the general description given in Section 2.2.1, and mimicked the three treatments studied in the 2007 Buttonwillow field study. A bare soil treatment with injection at 46 cm depth, a bare soil treatment with injection at 60 cm depth, and a surface spray application of ammonium thiosulfate treatment with injection at 46 cm depth were completed (Ashworth et al., 2009). The ATS was applied to the surface of the soil columns 0.5 h prior to fumigant injection and was approximately equivalent to the field application rate of 500 kg ha^{-1} (565 mg ATS in 1.6 mL). The molar ratio of thiosulfate ion to Telone C-35 was 1.7:1. Model simulations of the column experiments were carried out using Hydrus 1D and Solute 1D (Sections 2.5.1 – 2.5.2).

3.1.2. Results and Discussion

Peak emission rates (μg m^2 s^{-1}) and total emissions (as a percentage of the amount added to the system) are shown in Table 3.1.1 for 1,3-D, CP and Telone C-35 (i.e. combined 1,3-D and CP). These experiments demonstrate that deeper injection and ATS treatment can be effective in reducing total emissions of 1,3-D compared to the control treatment (i.e., Bare 46 cm).

For CP, the emission fluxes were at times higher than the control treatment, but overall the total emission loss from each of the three treatments was similar. This suggests that deeper injection and ATS treatment may not be effective as emission reduction strategies for chloropicrin. The reason for the difference in behavior between 1,3-D and CP is thought to be due to their physical and chemical differences. CP possesses a greater Henry's constant (K_H) value than 1,3-D (Table 2.5.1), which would enhance its potential to volatilize from the soil and thus may limit the effectiveness of the emission reduction strategies. Considering the 1,3-D and CP together, as Telone C-35, it is evident that emission reduction was observed for both the deeper injection and ATS treatments, which is primarily due to the differences in 1,3-D.

For the 46 cm, 60 cm and ATS treatments, respectively, the measured temporal Telone C-35 emissions are shown as circles in Figures 3.1.1 to 3.1.3. In general, fluxes followed a pattern of rapidly reaching an early peak value, which is followed by an extensive tailing over the remainder of the experiment. The initial peak was reached after around 30 h which relates to late afternoon on the day following application. Following the maximum peak value, several smaller peaks in emission were observed during the tailing of the flux curve. These were associated with late afternoon periods on each day, as the higher soil temperatures enhanced fumigant diffusion and volatilization. Within each treatment (graphs not shown, see Table 3.1.1), 1,3-D fluxes were higher than CP (due primarily to the higher application rate of 1,3-D and greater degradation of CP) and were measureable over a longer period of time. Generally, by 150 h, the CP emissions

were no longer detectable, while 1,3-D was detected up to the end of the experiment. This reflects the degradation half-life values. For example, degradation half-lives of 5.3 days (1,3-D) and 1.2 days (chloropicrin) were previously measured (Ashworth et al., 2007) for this soil.

Table 3.1.1. Peak emission rates (μg m^{-2} s^{-1}) and total measured emission losses as a percent of applied fumigant for three treatments.

		Peak Emissions, μg m^2 s^{-1}			Total Emission Loss, %		
	k_{12}*	1,3-D	CP	C-35	1,3-D	CP	C-35
Laboratory Measured							
Bare 46 cm	–	31.1	7.7	38.8	40.8 (±0.1)	16.0 (± 0.6)	32.1 (± 0.2)
Bare 60 cm (deep)	–	17.3	9.1	26.4	26.3 (±1.6)	13.3 (± 1.0)	21.8 (± 1.4)
ATS 46cm	–	20.2	11.2	31.5	27.1 (±1.5)	17.3 (± 2.0)	23.7 (± 1.7)
Simulated (Hydrus)							
Bare 46 cm	–	17.9	6.5	24.1	27.7	2.5	18.9
Bare 60 cm	–	7.9	1.9	9.7	15.5	1.7	10.6
ATS 46cm	Yes	–	–	–	–	–	–
ATS 46cm	No	15.2	5.5	20.4	25.8	5.2	18.6
Simulated (Solute)							
Bare 46 cm	–	19.9	6.7	26.3	27.7	2.4	18.8
Bare 60 cm	–	7.6	1.7	9.2	15.3	1.6	10.4
ATS 46cm	Yes	15.7	5.4	21.0	24.9	4.8	17.8
ATS 46cm	No	16.2	5.5	21.6	25.9	4.9	18.5
Simulated (Analytical)							
Bare 46 cm	–	23.6	9.3	32.8	32.5	14.0	26.3
Bare 60 cm	–	12.3	4.0	16.1	23.2	7.7	18.0

* k_{12} – "Yes": indicates 2nd order reaction process between fumigant and ATS was simulated, "No": identical simulation but k_{12} was set to zero, and "–" indicates does not apply to this case.

Comparing the emission rates for the three treatments shows that total and peak Telone C-35 fluxes were reduced compared to the Bare 46 cm (i.e. control) level by both deeper injection (i.e. 60 cm) and ATS spray applied to the soil surface. Interestingly, the 60 cm injection and ATS treatment produced very similar emission patterns over time.

Due to the increased path length between the point of injection and the soil surface, deep injection potentially reduces and delays fumigant emissions. The increased contact time between the fumigant and degrading soil surfaces (e.g. organic materials) has the potential to further reduce emissions under this management strategy.

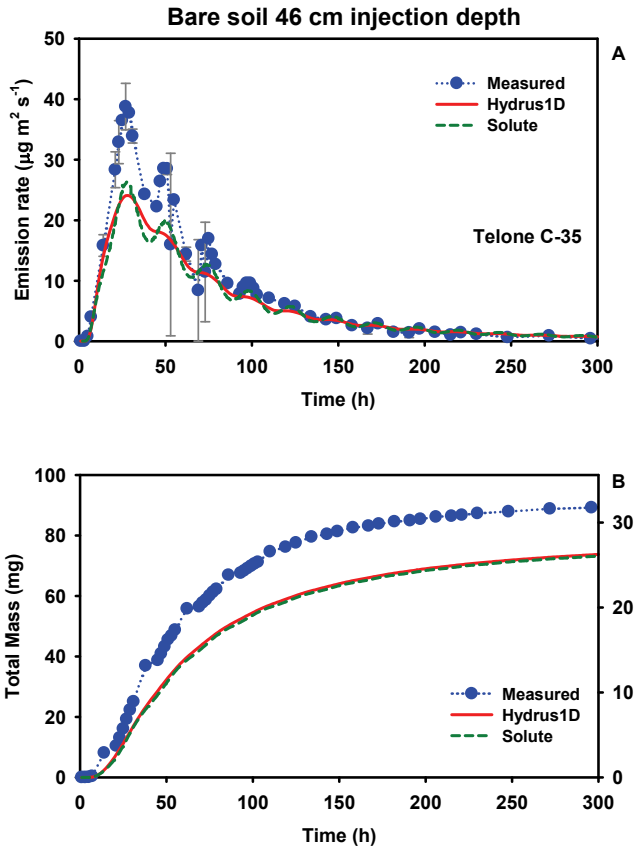

Figure 3.1.1. Measured and simulated Telone C-35 flux density for bare soil 46 cm injection depth (A), and total volatilization mass and percent lost (B).

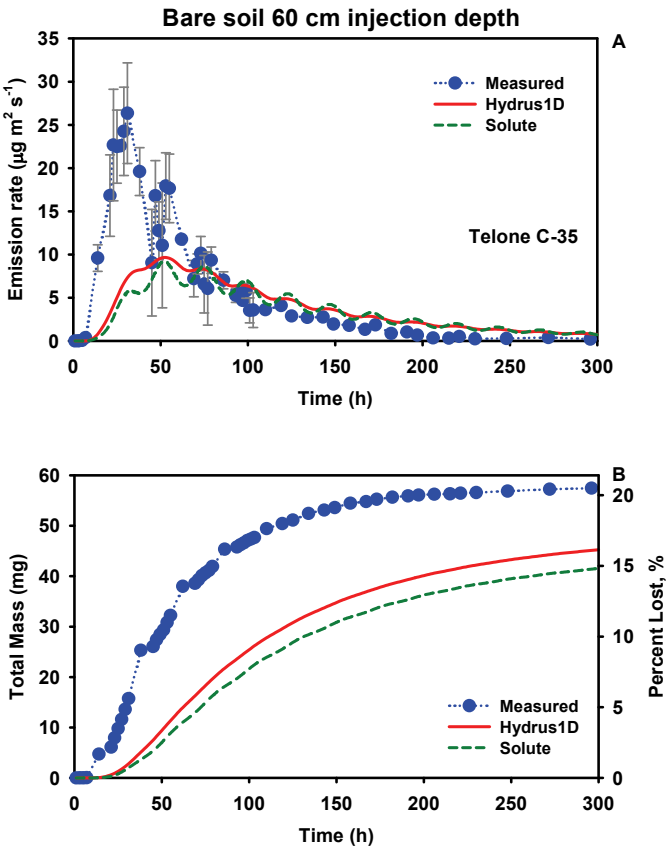

Figure 3.1.2. Measured and simulated Telone C-35 flux density for bare soil 60 cm injection depth (A), and total volatilization mass and percent lost (B).

The application of ATS to the soil surface prior to fumigation has the potential to reduce fumigant emissions by stimulating the thiosulfate-induced dehalogenation of the fumigants via nucleophilic substitution (Gan et al., 1998). Gan et al. (2000) found that when ATS is added to soil in irrigation water, the amount of water applied affected the emission rate, and that increasing applied water decreased 1,3-D emissions. The results here show a 35 % reduction in 1,3-D emissions and a 19 % reduction in Telone C-35 emissions when the ATS is applied with 1.6 mL of water (see Table 3.1.1).

In contrast to 1,3-D, neither deeper injection or the ATS treatment led to a reduction in emission of CP fluxes (see Table 3.1.1). In both cases, the peak emissions were slightly greater than the Bare 46 cm control. Nevertheless, emissions in the control increased later in the experiment, and fluxes were generally greater than in the 60 cm injection and ATS treatments (which showed similar flux patterns during this later stage).

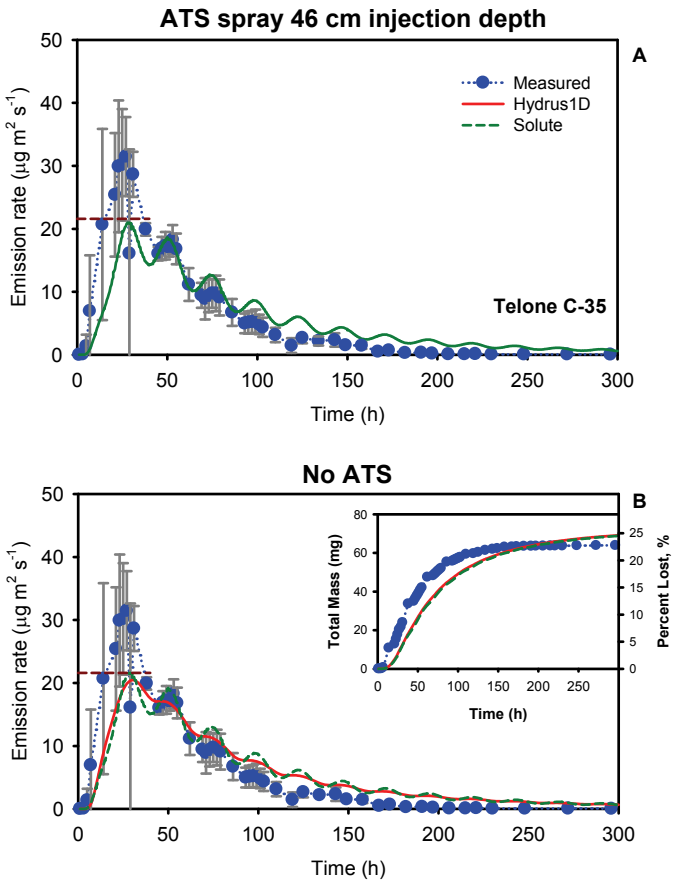

Figure 3.1.3. Measured Telone C-35 flux density for bare soil 46 cm injection depth after spraying surface with ATS. Simulations with ATS (A) and no ATS (B) are shown. The horizontal dashed line illustrates the reduction in the peak emission rate when second-order reaction is included.

3.1.3. Comparison of Soil Column Experimental Data and Model Simulations

The parameters of the experimental conditions and Hydrus 1D and Solute 1D model simulations are listed in Table 2.5.1 and Table 3.1.2. For 1-D simulations of the shank column experiments a uniform grid spacing (Δz = 0.5 cm) was used for Hydrus 1D. For Solute 1D simulations a finer grid spacing was needed near the soil surface to accommodate the ATS and fumigant interaction. For Solute 1D, the grid spacing near the surface was Δz = 0.025, 0.025, 0.05, 0.1, 0.3, and 0.5 thereafter. For both Hydrus 1D and Solute 1D simulations, the initial mass applied to the column was distributed to a single node at the injection depth with Δz = 0.5 cm.

Table 2.5.1 and Table 3.1.2 provide the soil and chemical parameters that were used in simulating 1,3-D (cis), 1,3-D (trans) and chloropicrin fate and transport in the laboratory columns. Results for 1,3-D were derived by combining the 1,3-D (cis) with 1,3-D (trans) simulations. Results for Telone C-35 were derived by combining the 1,3-D (cis + trans) and chloropicrin simulations.

Table 3.1.2. Parameters used for Hydrus 1D and Solute 1D simulations of Bare Soil 46 cm Injection, Bare Soil 60 cm Injection, and ATS Spray 46 cm Injection, treatments for 1,3-D and chloropicrin.

Treatment	Data type	Properties	Value	Units
Bare soil, 46 cm injection	**Soil properties**	Initial water content		
		0–15 cm deep,	12.9	$cm^3\ cm^{-3}$
		15–30 cm deep,	15.1	$cm^3\ cm^{-3}$
		30–45 cm deep,	16.4	$cm^3\ cm^{-3}$
		45–60 cm deep,	14.5	$cm^3\ cm^{-3}$
		>60 cm deep,	10.5	$cm^3\ cm^{-3}$
		Organic matter content	2.7	%
Bare soil, 60 cm injection	**Soil properties**	Initial water content		
		0–15 cm deep,	12.6	$cm^3\ cm^{-3}$
		15–30 cm deep,	16.6	$cm^3\ cm^{-3}$
		30–45 cm deep,	18.9	$cm^3\ cm^{-3}$
		45–60 cm deep,	19.5	$cm^3\ cm^{-3}$
		>60 cm deep,	19.0	$cm^3\ cm^{-3}$
		Organic matter content	2.7	%
ATS- spray, 46 cm injection.	**Soil properties**	Initial water content		
		0–15 cm deep,	12.6	$cm^3\ cm^{-3}$
		15–30 cm deep,	16.6	$cm^3\ cm^{-3}$
		30–45 cm deep,	18.9	$cm^3\ cm^{-3}$
		45–60 cm deep,	19.5	$cm^3\ cm^{-3}$
		>60 cm deep,	19.0	$cm^3\ cm^{-3}$
		Organic matter content	2.7	%

Final simulations for the Bare 46 cm, Bare 60 cm and ATS spray 46 cm injections are shown with the measured values in Figures 3.1.1–3.1.3 for Telone C-35. Overall, the simulations follow the shape and trend of the measured values with peak flux rates occurring at approximately the same time as measured peak flux rates. However, the simulated flux rates underestimate the measured flux values at early times and, in particular, for the Bare 60 cm treatment. For the most part, the simulations follow the day/night pattern in the measured emission fluxes but the daily peak values are underestimated. At later times, the simulated flux values exceed the measurements, which may be a consequence of inaccurate degradation rates.

Compared to the measured values shown in Table 3.1.1, the simulated peak emission fluxes were lower. For 1,3-D, chloropicrin, and Telone C-35, respectively, the simulated peak fluxes for the Bare 46 cm injection were from 24–42 %, 16–21 % and 16–38 % lower than measured values. For Bare 60 cm injection depths, the peak fluxes were from 29 % (1,3-D) to 81 % (chloropicrin) lower than measurements. For the ATS spray 46 cm treatments, the peak fluxes were about 22 % lower than measurements for 1,3-D but approximately 51 % for chloropicrin.

For 1,3-D, simulated total emission losses were 28–32 %, 16–23 % and about 25 %, respectively, for the Bare 46 cm, Bare 60 cm and ATS spray 46 cm treatments. For CP, the total emission losses were, respectively, 2–14 %, 2–8 % and about 5 % for the three treatments. The analytical solution produced the most comparable total emission values, even though the model describes the fewest fate and transport processes.

The horizontal dashed line Figure 3.1.3 can be used to show the effect of spraying ATS to the soil surface on the peak flux value. Due to the small volume of water, the ATS spray was confined to the upper 0.025 cm of the soil surface. Since the 2^{nd} order reaction process only operates when the ATS and fumigant are in contact, a shallow application of ATS appears to limit the effectiveness in reducing the predicted peak emission rate (i.e., in both cases, the simulated emission curve touches, or nearly touches the dashed line). Over the course of the simulation (see Table 3.1.1), the 2^{nd} order reaction process reduced total Telone C-35 emissions by about 1 % of total applied. This compares to a recent field study (Yates and Gan, 2010), where a spray treatment of ATS reduced Telone C-35 emissions from 17 ± 6 % to about 13 ± 4 %.

There are many factors that could lead to simulations that under predict the laboratory measurements. For example, it is possible that the degradation rates of both 1,3-D and CP differed between the surface and sub-surface soils. Because soils were packed into the columns according to field depth intervals, a single degradation rate may not be accurate. For the simulations, the soil degradation rate was based on measurements from the 0–15 cm soil region. However, potential differences in the quantity and quality of organic materials may have led to a lower rate of degradation for the deeper soil during the experiments compared to the surface layer. This could have led to underestimated simulated values due to overestimating degradation in the deeper soil layers. Improved simulations might be possible by using more detailed degradation rates for the entire soil profile; however, this type of information is rarely available. Furthermore, conducting simulations based on hypothesized vertical distributions for soil degradation are not justified when the study goals involve testing model performance in a predictive approach; i.e. when extensive experimental information are unavailable.

Experimental uncertainty is another factor that can lead to differences between measurements and predictions. Figure 3.1.4 shows a comparison of the relationship between total emission and injection depth. The circles are the results from the laboratory experiments and the dashed green line is the theoretical behavior based on an analytical solution (Yates, 2009) and the solid red line is the predicted behavior based on the Hydrus 1D simulations. This figure suggests that soil diffusion and volatilization process in the experimental columns did not behave in a strictly theoretical manner with respect to depth of injection, and further research is warranted.

The departure from theory could be due to many factors, some of which include: analytical and/or experimental uncertainty, pressure effects in the column system, experimental artifacts, to name a few. It is also clear that using a simplified analytical model or a comprehensive numerical model both provide a clear indication of departure. The large error bars for the 30 cm injection depth experiments suggest that these columns contribute significantly to the deviations with predictions.

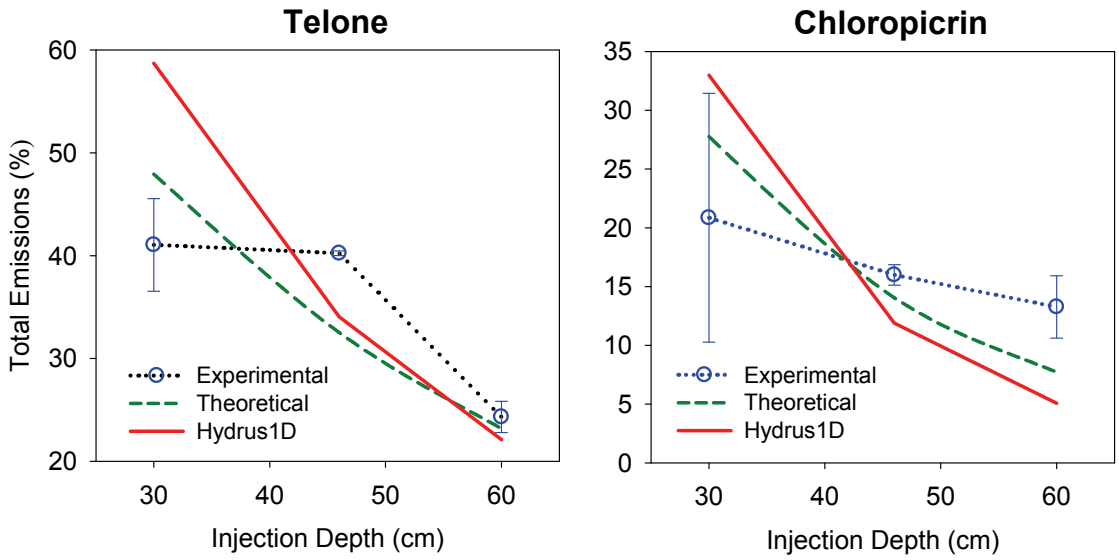

Figure 3.1.4. Measured (circles) and theoretical (red line) total emissions of 1,3-D and chloropicrin as related to injection depth. Error bars are ±standard deviations.

3.1.4. Comparing Simulations to the 2007 Buttonwillow Field Study Emission Data

During the 2007 Buttonwillow field study emissions of 1,3-D and CP from control (Bare 46 cm injection), deep injection (Bare 60 cm injection) and ATS spray (46 cm injection) treatments were obtained. The experiment and data are described by Yates and Gan (2010) in a previous California Air Resources Board report.

In calculating the field emission fluxes, the aerodynamic method (ADM) was one of several approaches that were used. Because this method uses an array of meteorological measurements, it is often considered a good approach for determining fumigant emissions. Another approach often used in a regulatory environment involves the use of an atmospheric dispersion model and measured air concentrations surrounding a treated field. The process involves fitting the dispersion model to the air concentration measurements by adjusting the field-scale fumigant emission rate (i.e., a back-calculation approach using CalPuff v6.112, Earth Tech, Inc.). For comparative purposes, the measured ADM and CalPuff emission rates are used here to compare with the experimental and simulated data sets.

In the 2007 field study, total emissions of CP were found to be very low (less than 1-2 % of the amount added). Although emissions for CP were also lower than for 1,3-D in the laboratory experiments (Section 3.1.2), the field data clearly do not compare well to the values obtained from the laboratory experiments where total emissions ranged from 13-17 %. It is not clear why emissions of CP were so low in the field study, since such emissions are generally found to be more similar to those obtained from the laboratory study (e.g. 15-20 %). The difficulty in elucidating the reasons for low emissions in the field may demonstrate an advantage of the laboratory approach in measuring fumigant emissions since the experimental conditions can be

more closely controlled and monitored. Chloropicrin fluxes from the Buttonwillow 2007 field experiments were not simulated due to very low measured values (see Yates and Gan, 2010).

The three fumigation treatments were simulated using Hydrus 2D and with Solute 1D; the latter program required an additional assumption that the fumigant was injection as a "point source" (i.e., in the simulation, all of the fumigant was assigned to a single node at the injection depth). For a field study where the fumigant is injected in a manner that can be represented as a planar source at depth z_o, a 1-D model and with a point source is appropriate. The parameters of the experimental conditions and model simulations are shown in Table 2.5.1 and Table 3.1.3.

Table 3.1.3. Parameters used for numerical simulations of control, deep injection and ATS spray treatments for 1,3-D and CP in 2007 Buttonwillow field experiment (see Table 2.5.1 for fumigant properties).

Treatment	**Properties**	**Value**	**Units**	**Note**
Control	Injection depth	46	cm	
	Bulk density			Field values
	0-18cm	1.25	g cm $^{-3}$	
	18-25	1.5	g cm $^{-3}$	
	25-55	1.44	g cm $^{-3}$	
	>55	1.55	g cm $^{-3}$	
	Initial water content			Field values
	Initial mass (1,3-D)	163.9	kg/ha	Treated field area was 2.89 ha
	Initial mass (chloropicrin)	76.8	kg/ha	
	Temperature			Field values (see Figure 3.1.6)
	Evaporation			Field values (see Figure 3.1.6)
Deep injection	Injection depth	61	cm	
	Initial mass (1,3-D)	153.3	kg/ha	Treated field area was 2.80 ha
	Initial mass (chloropicrin)	86.3	kg/ha	
ATS	Molar ratio (ATS/Telone)	1.8/1		
	Initial mass (1,3-D)	163.6	kg/ha	Treated field area was 2.87 ha
	Initial mass (chloropicrin)	86.8	kg/ha	

See Yates and Gan (2010).

As noted in the 2007 field study report (Yates and Gan, 2010), the equipment used to inject the fumigants led to shank fractures within the soil profile. The fractures were particularly prominent for the Deep Injection treatment. Since fractures could have had a marked impact on the diffusion of the fumigants through the soil and volatilization into the atmosphere, a Hydrus 2D model was constructed that included a fracture-like opening into the simulation design (Figure 3.1.5). Because the soil surface was disked following fumigant application, fractures were present only from around 30 cm depth to the point of injection. The field data (experimental and model simulations) were then compared with the experimental and modeling data determined for the laboratory column studies.

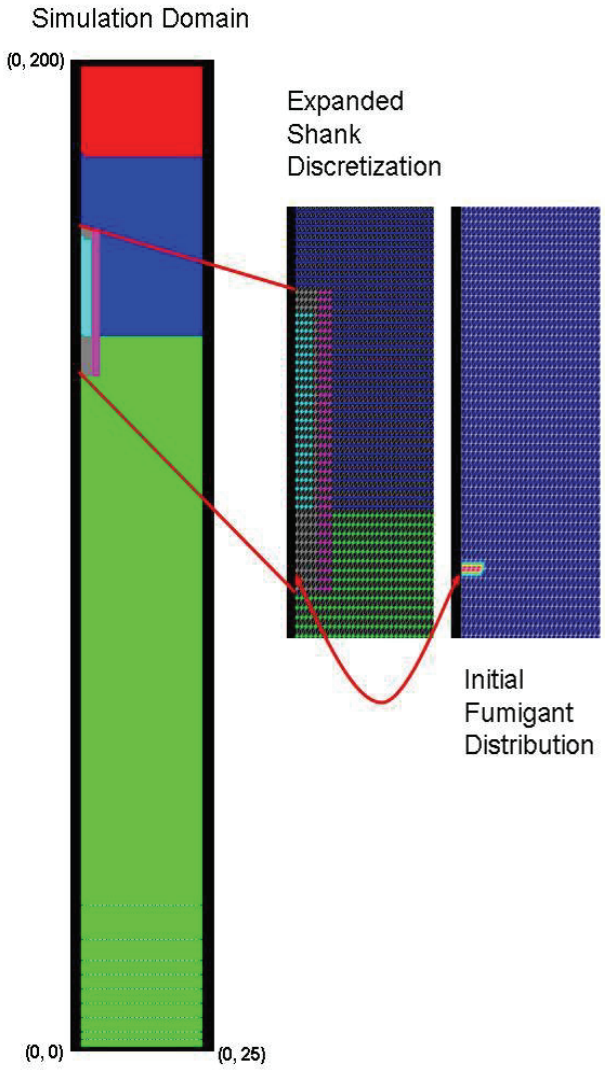

Figure 3.1.5. Finite element grid for Hydrus 2D simulations.

For the Control plot, a fracture (5cm wide, 32–46cm deep, with a density of 1.25 g cm^{-3}) was used.

For Deep Injection, a fracture (5cm wide, 32–55cm deep, with a bulk density of 1 g cm^{-3}) was used.

For ATS plot, Hydrus 2D/3D is unable to simulate the ATS-fumigant degradation via a second-order process shown in Equations 9–10 therefore a 1–D simulation was conducted using Solute 1D. For verification purposes, a Hydrus 1D simulation was conducted that used the same input parameters used in Solute 1D for the Control Plot.

The soil surface temperature and potential evaporation rate for the three treatments were nearly identical and Figure 3.1.6 shows the data from the Control Plot. The surface temperature and potential evaporation shown in Figure 3.1.6 were used to characterize the surface boundary condition of the Control Plot in both Hydrus 2D and Solute 1D simulations. Furthermore, the actual field measurements for the Deep injection and ATS treatments were used in each of these simulations.

Figure 3.1.7–Figure 3.1.10, respectively, show measured and simulated 1,3-D emission fluxes for the Control, Deep Injection and ATS spray field treatments. Simulation of the control, deep injection and ATS treatments are in general agreement with the experimental measurements in terms of both the pattern over time and the magnitude of the emission fluxes. However, it is evident from the simulations that the start of emissions is delayed somewhat compared to the field observations. This is particularly the case with the deeper injection. Theoretically, a deeper injection should lead to a delay in emissions, but the measured emission flux on Day 0 was found to be similar for all treatments. This may indicate some preferential pathway for fumigant transport from the injection depth to the soil surface. The model's inability to match early time behavior could also be due, in part, to the length of fumigation injection process, which occurred

over several hours. For the model, the fumigation injection was simulated as an instantaneous process, which may lead to an apparent delay in emissions.

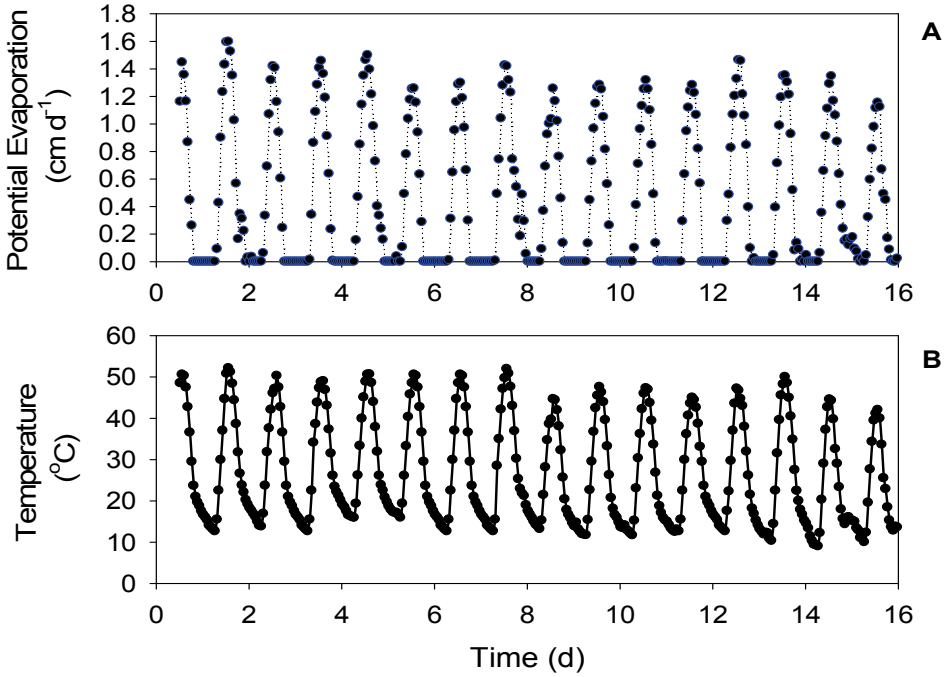

Figure 3.1.6. Potential evaporation rate and surface temperature (°C) for the Control Plot. Evaporation and surface temperature for the three treatments were nearly identical, so only this figure is shown.

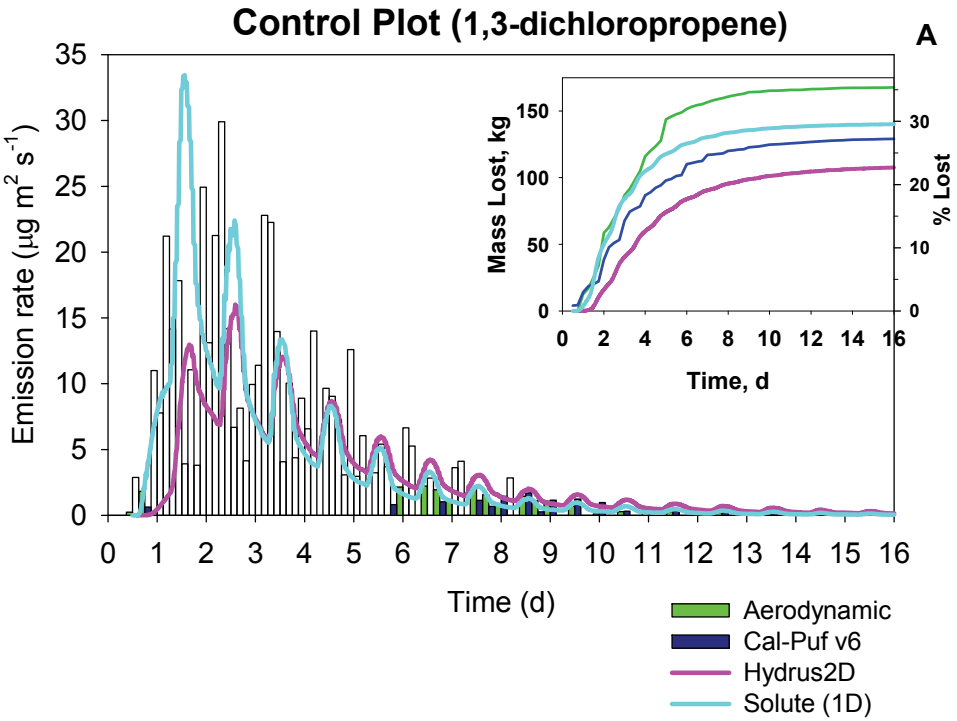

Figure 3.1.7. Measured (using ADM and CalPuff back calculation methods) and simulated (Hydrus 2D and Solute 1D) emissions of 1,3-D from the 2007 Buttonwillow field study Control plot (Bare soil, 46 cm injection).

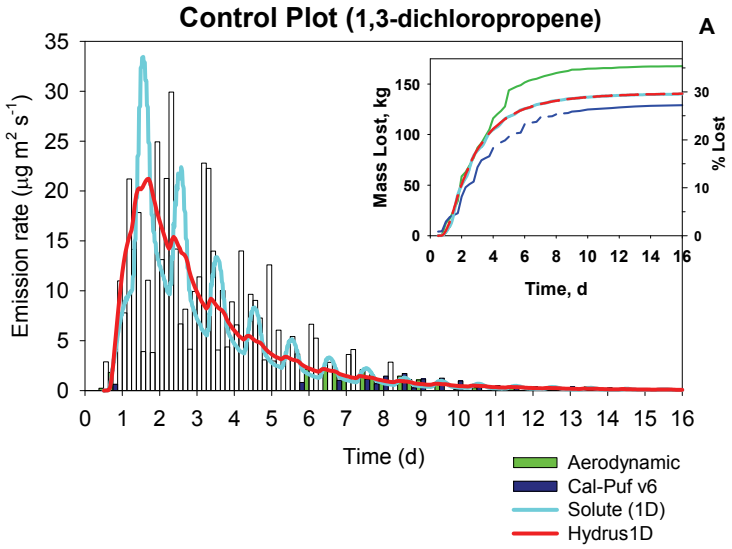

Figure 3.1.8. Comparison of measured and predicted 1,3-D emission from the 2007 Buttonwillow field study Control plot (Bare soil, 46 cm injection). The red line is for a Hydrus 1D simulation, the blue line is the Solute 1D simulation.

The simulated flux rates based on a 2-D analysis that included a shank fracture differs from a 1-D "point source" scenario (Table 3.1.4). For the Control treatment (Figure 3.1.7), the Solute 1D simulation predicted a peak flux of 33.4 µg m^{-2} s^{-1}, which was 12 % larger than the measured peak emission rate (29.9 µg m^{-2} s^{-1}, CalPuff). The Hydrus 2D simulation predicted a peak flux rate of 12.9 µg m^{-2} s^{-1}, which was about 56 % less than the measured rate. The total emission rate from the Hydrus 2D simulation was 23 %, and therefore, was below both the ADM (35 %) and CalPuff (27 %) measurements. The total emissions from the Solute 1D simulation were 30 % and nearly the same as the average of the two field measurements (31 %).

For comparative purposes, a Hydrus 1D simulation was conducted using the same model configuration as the Solute 1D simulation (Figure 3.1.8). For the 1-D analysis, both models produce the same total emission rate (30 %) and the Hydrus 1D simulation follows the same time course as the Solute 1D simulation, albeit with damped fluctuations in the emission rate. This was probably due to differences in how each computer algorithm models the effect of temperature on the emission process, especially the volatilization boundary condition. It is interesting to note that the Hydrus 2D and Solute 1D simulations shown in Figure 3.1.7 have similar fluctuations in the emission, especially at later times, but these are damped in Hydrus 1D. During the first few days, the fluctuations in the emission rates predicted by Solute 1D are larger, which probably reflects differences in problem configuration (1-D vs. 2-D) and that the Hydrus 2D simulation included a shank fracture.

Both the Hydrus 2D and Solute 1D simulations under predicted the emission rate for the Deep injection treatment (Figure 3.1.9). Much of the discrepancy is due to a very large measured emission rate occurring during the 3rd day, which alone accounts for roughly 2 % total emissions. With the exception of this event, the Solute 1D simulation predicts this scenario fairly well. Based on Figure 3.1.9, it appears that the Deep injection treatment can be predicted well using a 1-D model configuration and, for this case, incorporating the additional complexity of a shank fracture may be unwarranted.

The predicted total emissions based on the Hydrus 2D simulation were 16 % for the Deep injection treatment, which was below both the ADM (27 %) and CalPuff (26 %) measurements. The total emissions from the Solute 1D simulation were 21 %, also below the measurements.

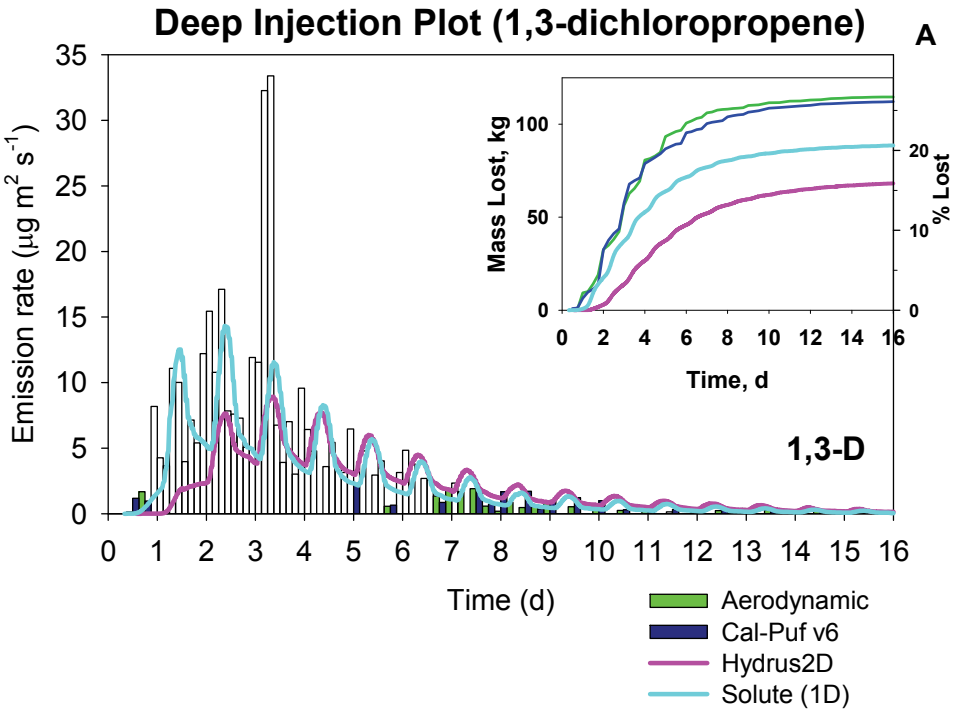

Figure 3.1.9. Measured (using ADM and CalPuff back calculation methods) and simulated (Hydrus 2D and Solute 1D) emissions of 1,3-D from the 2007 Buttonwillow field study Deep Injection plot (Bare soil, 61 cm injection).

Shown in Figure 3.1.10 are the measured and predicted emission rates and total emissions for the ATS treatment. For this field experiment there was a more prolonged period of relatively high emission rates compared to the Control site. The simulated values are nearly the same as the Control treatment since the effect of the 2nd order reaction process between ATS and 1,3-D was limited. However, the measured peak emission rates were less compared to the Control plot. The simulated emission rate had a peak flux of 32.9 µg m^{-2} s^{-1}, which was 67 % larger than the measured peak emission rate (19.7 µg m^{-2} s^{-1}, CalPuff) and the simulated emission rate was consistently less than the measurements at later times, unlike the Control Plot. The total emission rate from the simulation was 25 %, which was approximately the same as the ADM (25 %) and CalPuff (27 %) measurements.

The horizontal dashed line in Figure 3.1.10 compares the peak emission rates for (A) a simulation that includes 2nd-order reaction between ATS and 1,3-D and (B) when there is no 2nd-order reaction. The simulation that includes a 2nd-order reaction process leads to a reduction in the peak emission rate from 33.7 to 32.9 µg m^{-2} s^{-1} and reduces total emissions by 2 %. This compares to the field values where the spray treatment of ATS reduced Telone C-35 emissions from 17 ± 6 % to about 13 ± 4 % (Yates and Gan, 2010).

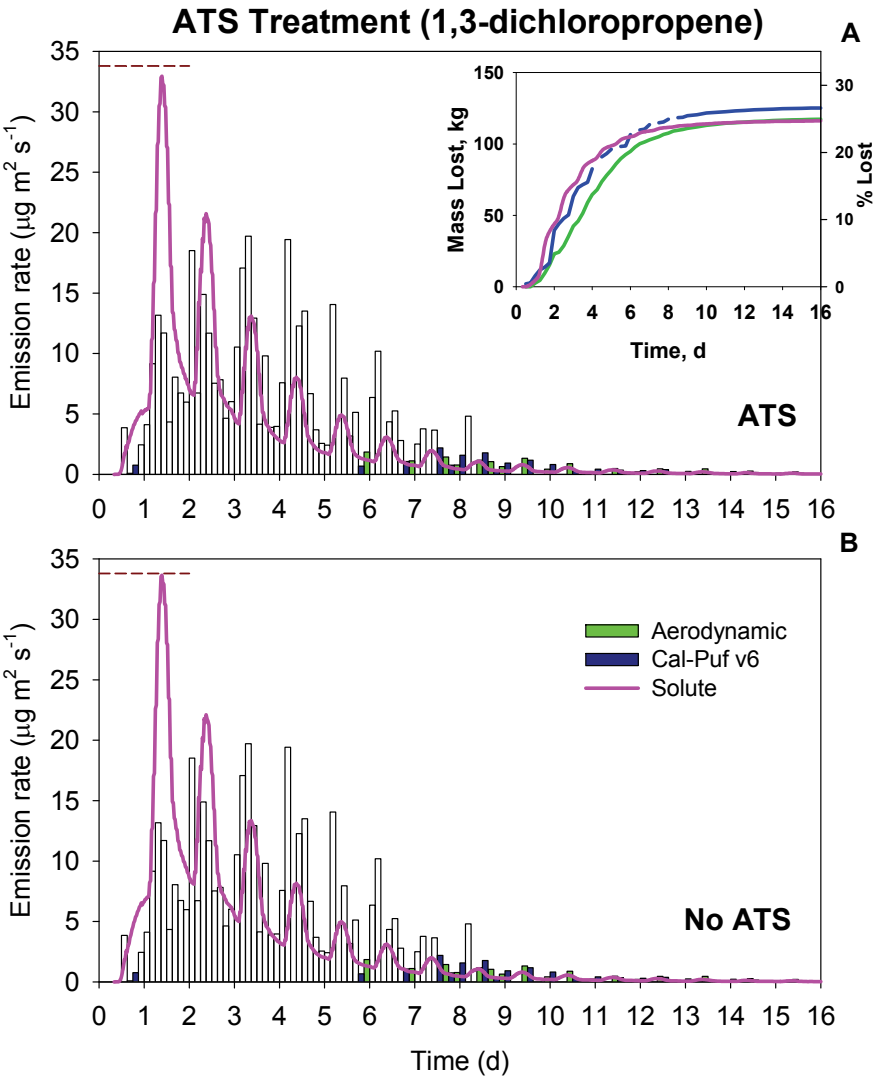

Figure 3.1.10. Measured (using ADM and CalPuff back calculation methods) and simulated (Solute 1D) emissions of 1,3-D from the 2007 Buttonwillow field study ATS spray plot (Bare soil, 46 cm injection).

The total emissions of 1,3-D determined by the ADM method for the field study were 35.4, 26.7 and 25.0 % for the Bare 46 cm, Bare 60 cm and ATS 46 cm, respectively (Table 3.1.4). The total emissions of 1,3-D determined by the CalPuff method were 27.2, 26.1 and 26.7 % for the Bare 46 cm, Bare 60 cm and ATS 46 cm, respectively. Comparing these to the values in Table 3.1.1, it is clear that the laboratory experiments were relatively successful in estimating the field emissions; with differences ranging from 0.4 to 5.4 % for the ADM method and 0.2–13.6 % for the CalPuff method. The CalPuff method was within 1 % of the total emissions measured in the field study Deep and ATS treatments.

Table 3.1.4. Summary of total 1,3-D mass lost from emissions and percent of the applied fumigant lost for the 2007 Buttonwillow field experiments. The values from the aerodynamic (ADM), CalPuff, Hydrus 2D and Solute 1D methods are compared.

Method	Peak Emissions ($\mu g\ m^{-2}\ s^{-1}$)	Total Mass Loss from Emissions, kg	Percent of Applied Mass Lost, %
Control Plot			
ADM Mass	24.9	167.7	35.4
CalPuff Mass	29.9	129.1	27.2
Hydrus 2D	16.0	107.8	22.7
Hydrus 1D	21.2	140.5	29.6
Solute 1D	33.4	140.1	29.5
Avg (±std)			28.9±4.6
Deep Injection Treatment			
ADM Mass	32.3	114.7	26.7
CalPuff Mass	33.4	112.1	26.1
Hydrus 2D	8.9	68.2	15.9
Solute 1D	14.3	88.6	20.6
Avg (±std)			22.3±5.1
ATS Spray Treatment			
ADM Mass	19.4	117.4	25.0
CalPuff Mass	19.7	125.2	26.7
Hydrus 2D	–	–	–
Solute 1D	32.9	116.1	24.7
Avg (±std)			25.5±1.1

Shown in Figure 3.1.11 is a comparison of the average daily fluxes of 1,3-D from each treatment for the laboratory soil columns and the ADM-derived values for the 2007 field study (CP values not shown due to low flux rates in field. Overall, the comparison for 1,3-D shows relatively good agreement in terms of the time-wise trend and in absolute values. Largest differences were observed for the ATS 46 cm treatment. In general, the laboratory soil columns followed a simpler trend of increasing to a peak on Day 1 followed by a subsequent tailing of the fluxes over time. In the field, often Days 1-3 (Bare 60 cm and ATS 46 cm) or 2-4 (Bare 46 cm) exhibited similar daily values. Essentially, this suggests that the peak in emissions under field conditions was broader than in the laboratory. Model simulations of such systems (see Figure 3.1.1 and Figure 3.1.2) usually produce a flux curve more similar in shape to the laboratory situation. This suggests that the differing trend in the field is a result of the more complex environmental conditions that occur under outdoor conditions.

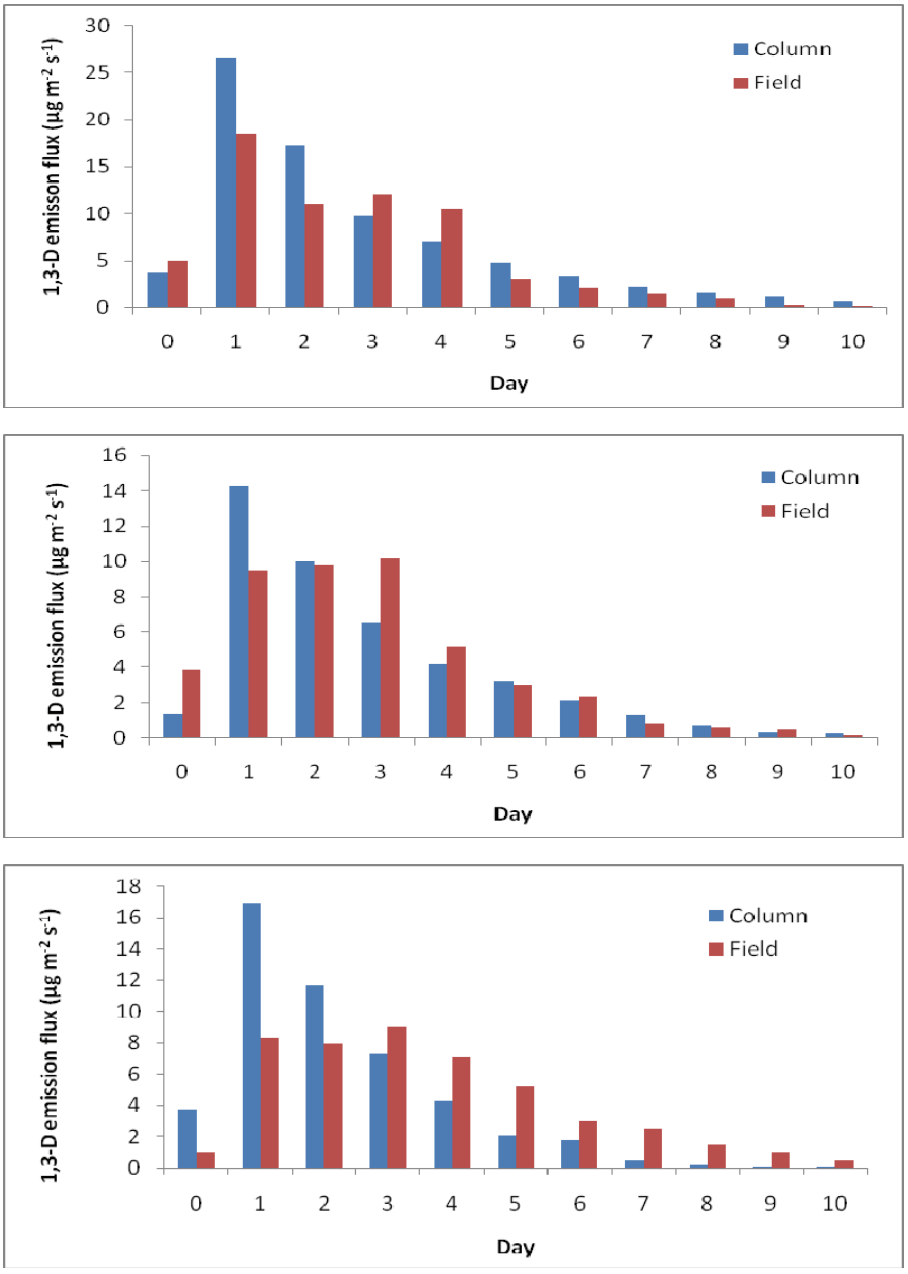

Figure 3.1.11. Comparison of average daily fluxes of 1,3-D for the Bare 46 cm (upper), Bare 60 cm (middle) and ATS 46 cm (lower) treatments in the laboratory and field (ADM) experiments.

3.2. Laboratory Experiments Simulating the 2005 Buttonwillow Field Experiment: Influence of irrigation and organic matter addition on shank-injected Telone II emissions.

3.2.1. Experimental Information

Duplicated laboratory soil column experiments with simulated shank injection of Telone II (1,3-D) were performed using the general description given in Section 2.2.1. The data have been reported previously (Ashworth and Yates, 2007). The experiments mimicked the treatments studied in the 2005 Buttonwillow field study, in which the effect of irrigation and organic matter addition on the emissions of 1,3-D (Telone® II formulation) were assessed. Although no true 'control' was included in the field study, appropriate controls were included for the soil column studies. Injection of the Telone II was made at 46 cm depth. For each of the two soils, the control (or low organic matter, LOM soil) and the high organic matter (HOM) soil, non-irrigated and irrigated treatments were imposed. Irrigation was performed by inserting a pronged irrigation device into the volatilization chamber and evenly distributing 1 cm of water (113 mL) onto the soil surface. This was performed three hours after application of Telone II and was repeated daily for the first five days; simulating the irrigation regime used in field study. Model simulations of the column experiments were carried out using HYDRUS 1D (Section 2.5.1 – 2.5.2).

3.2.2. Results and Discussion

Emission fluxes of 1,3-D over the course of the experiment for the LOM and HOM soils are shown in Figure 3.2.1. The principal peak in emissions occurred at around 25 hours in the LOM soil, and at around 50 hours in the HOM soil. The measured peak was around six times greater in the LOM soil than in the HOM soil, for the same treatment. Several smaller peaks were consistently observed at subsequent times. Detectable emissions in both soils occurred over approximately the first 150 hours of the experiment. In both soils during this time period, irrigation markedly reduced flux rates. The total emissions (percentage of that amount added) of 1,3-D over the entire experiment were, in the LOM soil, 29 and 14 % for the non-irrigated and irrigated treatments, respectively and, in the HOM soil, 4.5 and 2.0 % for the non-irrigated and irrigated treatments, respectively (see Table 3.2.1). The measurements in Table 3.2.1 also show that irrigation reduced total emissions by approximately 50 %. Comparing soils, emissions from the HOM soil were around 6-7 times lower than the emissions from the LOM soil for each treatment.

Degradation of 1,3-D in the two soils was markedly different due to the influence of the additional organic matter (composted municipal green waste). The degradation half-time (25 °C) was previously measured to be 5.3 days in the LOM soil, and 1.2 days in the HOM soil (Ashworth and Yates, 2007). In both treatments, the enhanced degradation of the 1,3-D in the HOM soil led to smaller amounts of the fumigant being available for emission from the soil surface. Hence, dramatically reduced flux rates were observed in the HOM soil (for both non-irrigated and irrigated treatments). Clearly, the organic matter treatment had a much more marked effect on reducing emissions than the irrigation treatment. In addition, the primary 1,3-D emission peak from the HOM soil occurred later than in the LOM soil, suggesting that the higher level of organic matter also delayed the emission release of the 1,3-D. Again, the role of the organic matter in the enhanced degradation of the 1,3-D is likely to be important here, but, also,

since organic matter is known to chemically complex, a possible explanation for this delayed emission may be a slower movement of the 1,3-D from the point of injection towards the soil surface, i.e. a greater degree of interaction with the soil solids.

In both soils, total emissions of 1,3-D from the column surfaces were substantially reduced (halved) due to irrigation treatment. This was likely a result of much slower diffusion of the gas through the wet surface soil; which in turn gave the 1,3-D a longer contact time with the soil and a greater potential to degrade rather than be emitted. Reductions in emission due to irrigation were much greater than those recently reported by Gao and Trout (2006) who, using soil columns, found values of 41–46 % emission (as a percentage of the total added) for irrigated treatments, compared to 51 % for the control. Their greatest irrigation-induced emission reduction was found at the highest level of water addition (a total of 13.2 mm over the first 24 h).

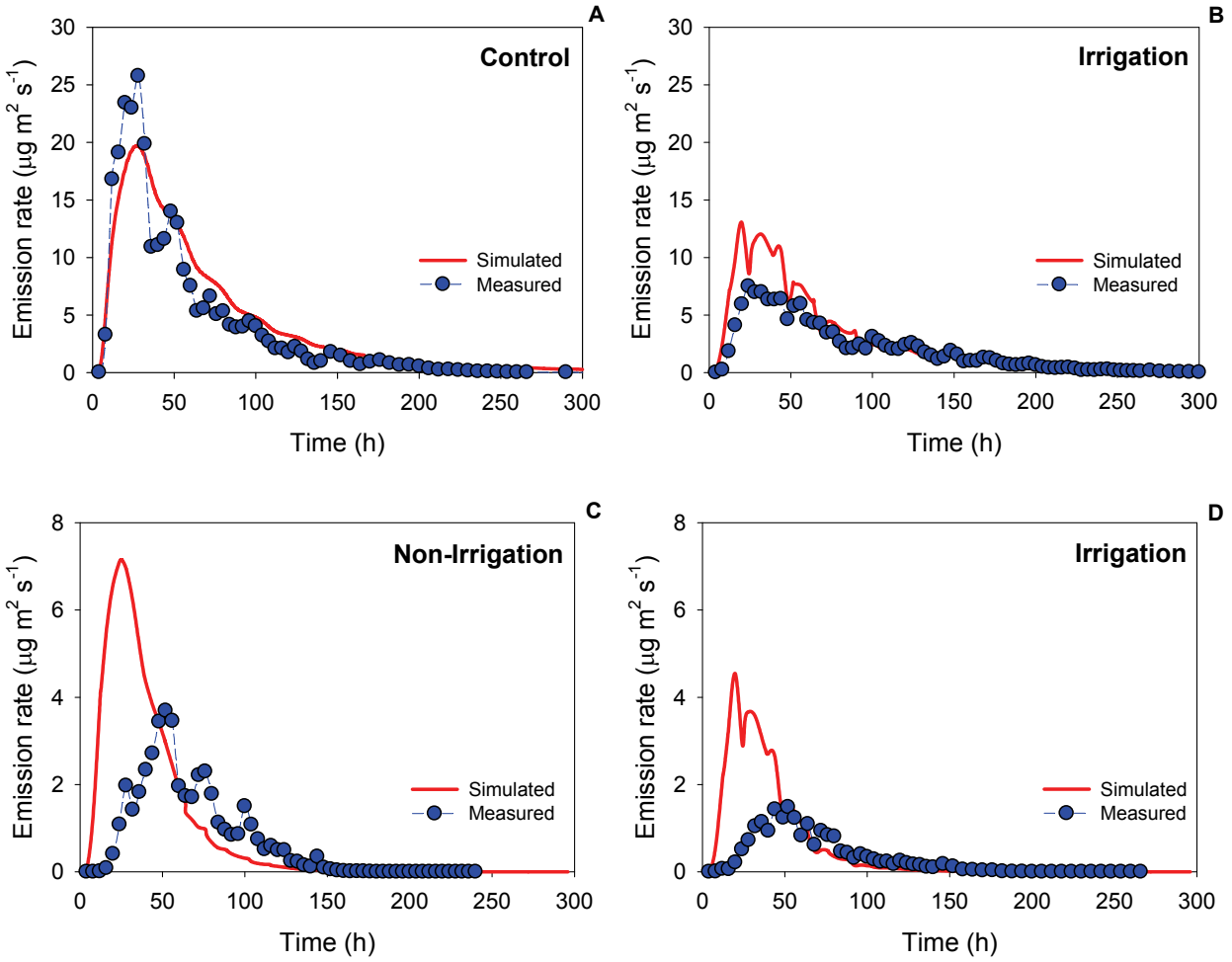

Figure 3.2.1. Comparison of measured and simulated (Hydrus 1D) 1,3-D emission fluxes from the (A) low organic matter (LOM) non-irrigated (control), (B) LOM irrigated, (C) high organic matter (HOM) non-irrigated and (D) HOM irrigated treatments.

They concluded that 'frequent' addition of water would be required to substantially reduce emissions. Here, application for each of the first 5 days appears to have achieved this, presumably because this is the period over which the vast majority of the added 1,3-D is emitted. The fact that by 5 days most of the 1,3-D had either been emitted or degraded, suggests that further application of water would not offer any greater benefit to emission reduction. It is considered that application of irrigation water during the first 5 days following fumigation is a practicable emission-reduction strategy for a grower to employ. The reductions in 1,3-D emissions were not as marked as have been noted for other emission reduction approaches. For example, thiourea and thiosulfate amendments were reported to produce emission reductions of 80-90 % (Gan et al., 2000; Zheng et al., 2006).

Table 3.2.1. Summary of peak emissions (μg m^{-2} s^{-1}), total emissions (mg) and total mass lost as a percentage of applied fumigant (%) for the laboratory column experiments simulating the 2005 Buttonwillow field experiment.

	LOM		HOM	
	Non-Irrigated	Irrigated	Non-Irrigated	Irrigated
Emission Summary				
Peak Emissions (μg m^2 s^{-1})	25.8	7.50	3.69	1.48
Total Emissions (mg)	47.7	23.7	7.28	3.23
Mass Lost (%)	29 %	14 %	4.5 %	2.0 %
Reduction Due To Irrigation				
Peak Emissions		71 %		60 %
Total Emissions		50 %		56 %
Reduction Due To HOM Soil				
Peak Emissions			86 %	80 %
Total Emissions			85 %	86 %

Several other field-plot and laboratory studies have been reported that found addition of organic material to surface soil reduces emissions of 1,3-D. Dungan et al. (2005) conducted a field plot experiment on raised beds (5 m x 1 m x 0.15 m) and found that steer manure or chicken manure, respectively, incorporated into the top 5 cm of the bed would result in emissions of 1,3-D that were 48 and 28 % less than the unamended control plot. They also found that the measured reduction in emissions did not change after increasing the rate at which organic material was applied from 5 % to 10 %. Gan et al. (1998b) found that total emissions of 1,3-D were reduced from 30 % to 16 % by the addition of 5 % organic matter to the top 5 cm of a soil column. In a laboratory column study, McDonald et al. (2008) found that the addition of 5 % organic material (steer manure) to the upper 5 cm of the soil reduced emission from 51 % to 29 %. All of the current literature investigating the effect of adding organic material to the surface prior to soil fumigation demonstrates that emissions can be reduced by 40 % or more. The type of organic material, aging and the method for incorporating organic material into soil plays a factor in how effective this methodology will be in reducing emissions.

However, the use of organic matter may not be as cost-effective nor as easily carried out as irrigation. Irrigation may therefore represent an effective compromise between reducing the environmental impact of fumigant use and practicability. In addition, the balance of rapid degradation of 1,3-D under conditions of high organic matter (and its beneficial effect in terms of emission reduction) with the time required for pesticidal efficacy must be taken into account.

3.2.3. Comparison of Soil Column Experimental Data and Model Simulations

The parameters for the experimental conditions needed to use Hydrus 1D model are listed in Table 3.2.2 and information on the finite element grid are provided in Section 3.1.3. Unless stated otherwise, parameters for the previously described simulations (e.g., Table 2.5.1) were also used for these simulations.

Table 3.2.2. Parameters used for Hydrus 1D simulations of the LOM and HOM soils, irrigated and non-irrigated for 1,3-D (1,3-D properties listed in Table 3.1.2). The cross-sectional area of the column was 113.1 cm^2 and the injection depth was 46 cm.

Treatment	Properties	Depth	Value	Units
All Treatments	Initial application, 1,3-D		140	µL
	Mass 1,3-D (cis)		90	mg
	Mass 1,3-D (trans)		74	mg
	Bulk density	0-15cm	1	g cm^{-3}
		15-25cm	1.2	g cm^{-3}
		>25cm	1.5	g cm^{-3}
	Porosity	0-15cm	0.623	%
		15-25cm	0.547	%
		>25cm	0.434	%
	Initial water content	0-2cm	5	%, cm^3 cm^{-3}
		2-4cm	12	%, cm^3 cm^{-3}
		4-25cm	17	%, cm^3 cm^{-3}
		>25	12	%, cm^3 cm^{-3}
LOM	Organic matter content		2.09	%
	Fraction of organic carbon		1.17	%
	Sorption coefficient , K_d		0.05	cm^3 g^{-1}
	Degradation rate constant		.0054	h^{-1}
HOM	Organic matter content		3.16	%
	Fraction of organic carbon		1.77	%
	Sorption coefficient , K_d		0.10	cm^3 g^{-1}
	Degradation rate constant		0.0241	h^{-1}
Irrigation	Spray 1-cm water 3 h after injection, and repeat the irrigation on days 2-5			

The most notable change from the previous simulations was the greater degradation rate constant ($0.0241 h^{-1}$) applied to the HOM soil simulation, which was based on experimental measurement. Similarly, a sorption coefficient of 0.1 cm^3 g^{-1} was used for the HOM simulation, which is twice

that of the control soil. Although not measured experimentally, this K_d value was used since the organic matter for HOM soil was nearly double the control soil, and given a specific K_{oc}, doubling the fraction of organic matter would double the K_d (see Equation 5).

Emission flux simulation results are shown in Figure 3.2.1 as solid lines. Simulation of the LOM (control) soil without irrigation showed relatively good agreement with the measured values. The peak emission rate was underestimated by 6 μg m^{-2} s^{-1}, or about 24 %; but the closeness of fit of the simulation to the measured emission rates suggests that the selected parameters were generally appropriate. When the LOM soil was irrigated, the model overestimated the emission fluxes over the first 100 hours, although the trend in emission flux was similar to the measured values. The simulated peak emission rate overestimated the peak measurement by 5.5 μg m^{-2} s^{-1}, or approximately 73 %. In both these cases, the simulated total emission loss was very close to the measured value (Table 3.2.3).

For the HOM treatments, the model overestimated the emission fluxes for the irrigated and non-irrigated treatments. This suggests that the model did not adequately represent the changes in fumigant diffusion due to the soil pores filling with irrigation water, or the enhanced degradation and sorption associated with higher level of organic matter. For these treatments, the simulated peak emission overestimated measurements by about 3.0–3.5 μg m^{-2} s^{-1} or about 2 times higher. Even though the emission flux rates overestimated the measurements, the simulated total emissions were relatively close to the measured values (Table 3.2.3) and were within 2–6 % of the total applied mass. Moreover, by further increasing the surface layer K_d value (by 10 times), in response to an expected greater level of adsorption due to a higher level of organic matter, the closeness of the simulated and measured total losses was further improved (Table 3.2.3).

Table 3.2.3. Summary of total emissions of 1,3-D (μg cm^{-2}) from 2005 1-D column experiments. Percentages are based on mass applied to column (each treatment: 1450 μg cm^{-2}).

Treatment	Measured Emissions		Simulated Emissions	
	(μg cm^{-2})	(%)	(μg cm^{-2})	(%)
LOM-non irrigation	421.5	29.1	484.0	32.4
HOM-non irrigation	64.4	4.5	103.5	6.9
(Surface Layer K_d 10x)			65.1	4.5
LOM –irrigation	209.3	14.4	301.3	20.2
HOM -irrigation	28.5	2.0	57.6	3.9
(Surface Layer K_d 10x)			28.6	1.9

3.2.4. Comparing Simulations to the 2005 Buttonwillow Field Study Emission Data

The 2005 Buttonwillow field study determined emissions of 1,3-D (Telone® II formulation) from the LOM soil with irrigation treatment, and the HOM soil (i.e. organically amended treatment). The experiment and data are described by Yates and Gan (2010). Here, these field experiment data were simulated using Hydrus 2D and Solute 1D. The parameters of the experimental conditions and model simulations are shown in Table 3.2.4. The field data (experimental and model simulations) were then compared with the experimental and modeling data determined for the laboratory column studies.

Table 3.2.4. Parameters used for Hydrus 1D and Solute 1D simulations of LOM irrigated and HOM treatments for 1,3-D in 2005 Buttonwillow field experiment (1,3-D properties listed in Table 3.1.2). Injection depth was 46 cm.

Treatment	Properties	Value	Units	Notes
HOM	Bulk density			
	0-18cm	1.25	g cm $^{-3}$	
	18-25	1.5	g cm $^{-3}$	
	25-55	1.44	g cm $^{-3}$	
	>55	1.55	g cm $^{-3}$	
	Initial water content			See Yates and Gan (2010) pg 32
	Initial mass (1,3-D)	446.7	kg	Treated Area was 3.36 ha
Irrigation	Initial water content			See Yates and Gan (2010) pg 42
	Initial mass (1,3-D)	446.7	kg	Treated Area was 3.41 ha
	Irrigation	1.88 cm immediately after application, 1.4±0.13cm each day for the following 4 days, totally 7.48cm water		

Measured and simulated 1,3-D emissions during the 2005 Buttonwillow field study for the LOM irrigated and HOM non-irrigated soils are shown in Figures 3.2.2 and 3.2.3, respectively. Two methods to analyze the field measurements and obtain emissions values are presented. The ADM, which requires gradients of wind speed, temperature and fumigant concentration are shown as green bars. The CalPuff emission measurements are shown as blue bars and were obtained by fitting an atmospheric dispersion model (i.e., CalPuff) to measured air concentrations surrounding a treated field. These methods were selected because they each utilize independent data sets for the fumigant concentration, and, the calculation methodologies are very different. This would suggest that similarities in the emission rates between the two methodologies are due to real events.

For the irrigation treatment, the simulations underestimated the emission rates at early times and overestimated them at later times. After about 5 days, the peak field measured emission rates were less than about 1.5 μg m^{-2} s^{-1}. The simulated values were as high as 3.0 μg m^{-2} s^{-1} on day 5 and continued to exceed 1.0 μg m^{-2} s^{-1} for another 5 days, while the measurements quickly approached nearly zero. The long trailing off of the simulated emissions also affects the shape of the total emission curve with a lower slope at early times. The total emission for the ADM exceeded 15 %, while the CalPuff and simulated total emissions were from 10–12.4 %.

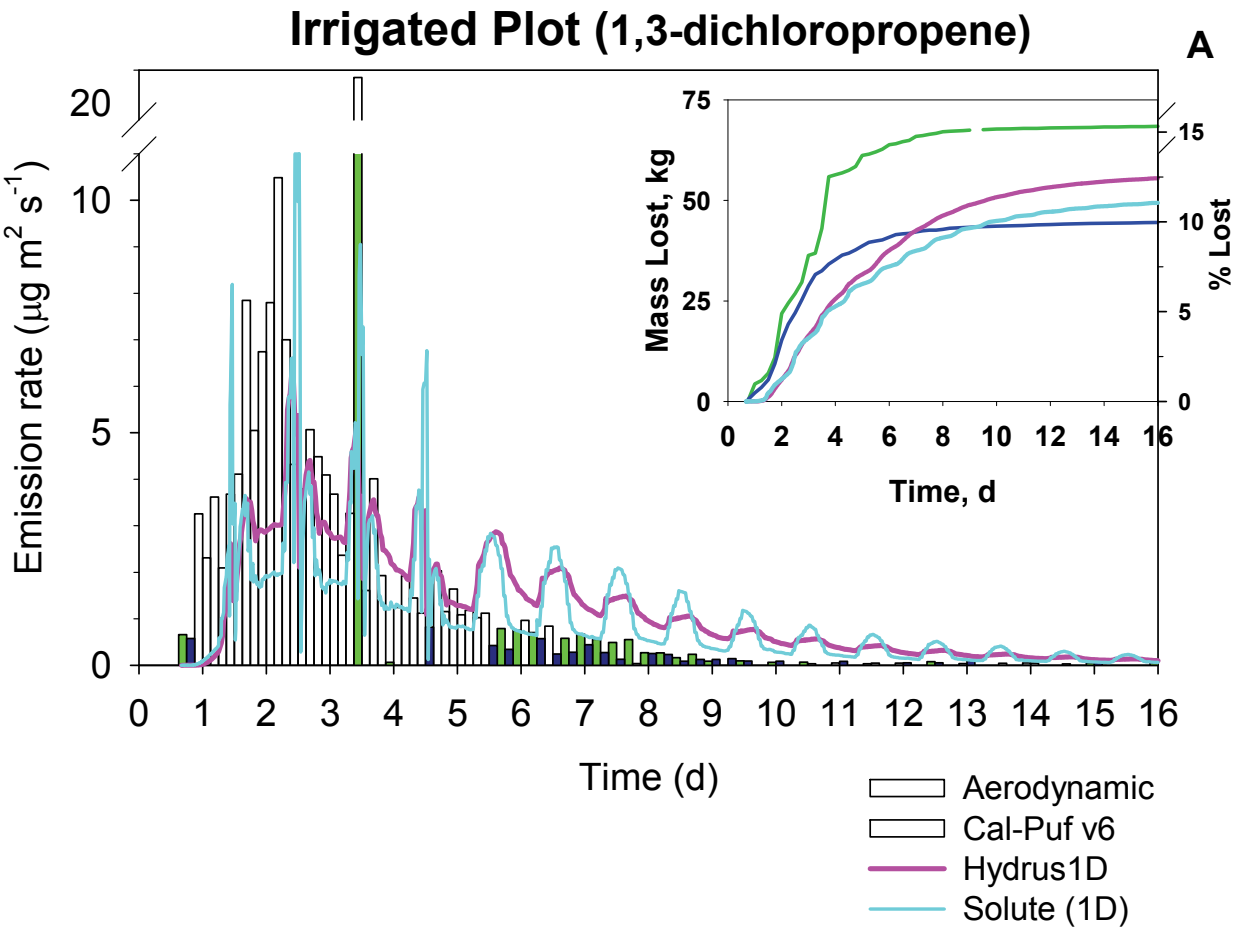

Figure 3.2.2. Measured and simulated 1,3-D emission rates from the LOM irrigated soil during the 2005 Buttonwillow field study (Yates and Gan, 2010). Inset shows the cumulative emissions as mass lost (kg) and as amount of applied fumigant lost (%).

For the HOM treatment (Figure 3.2.3), the agreement between the field-measured and simulated emission fluxes is relatively good when comparing to the CalPuff emission rates. The peak emission rate obtained from simulation appears about ⅓ – ½ day earlier than was measured. The model does not simulate the effects of soil water content on vapor adsorption; therefore, the model produces mid-day peak emission values. Clearly shown in Figure 3.2.3 are daily peak emission rates occurring shortly after midnight during the first days of the experiment. Even though the timing of the peak flux rate doesn't match, both the magnitude of the fluxes and the overall pattern in emissions over the course of the experiment were well reproduced by the model simulations. Simulated total 1,3-D emissions (Hydrus 1D and Solute 1D), respectively, were 2.8 and 3.6 % which compares to 3.8 and 8.1 %, respectively, for CalPuff and ADM.

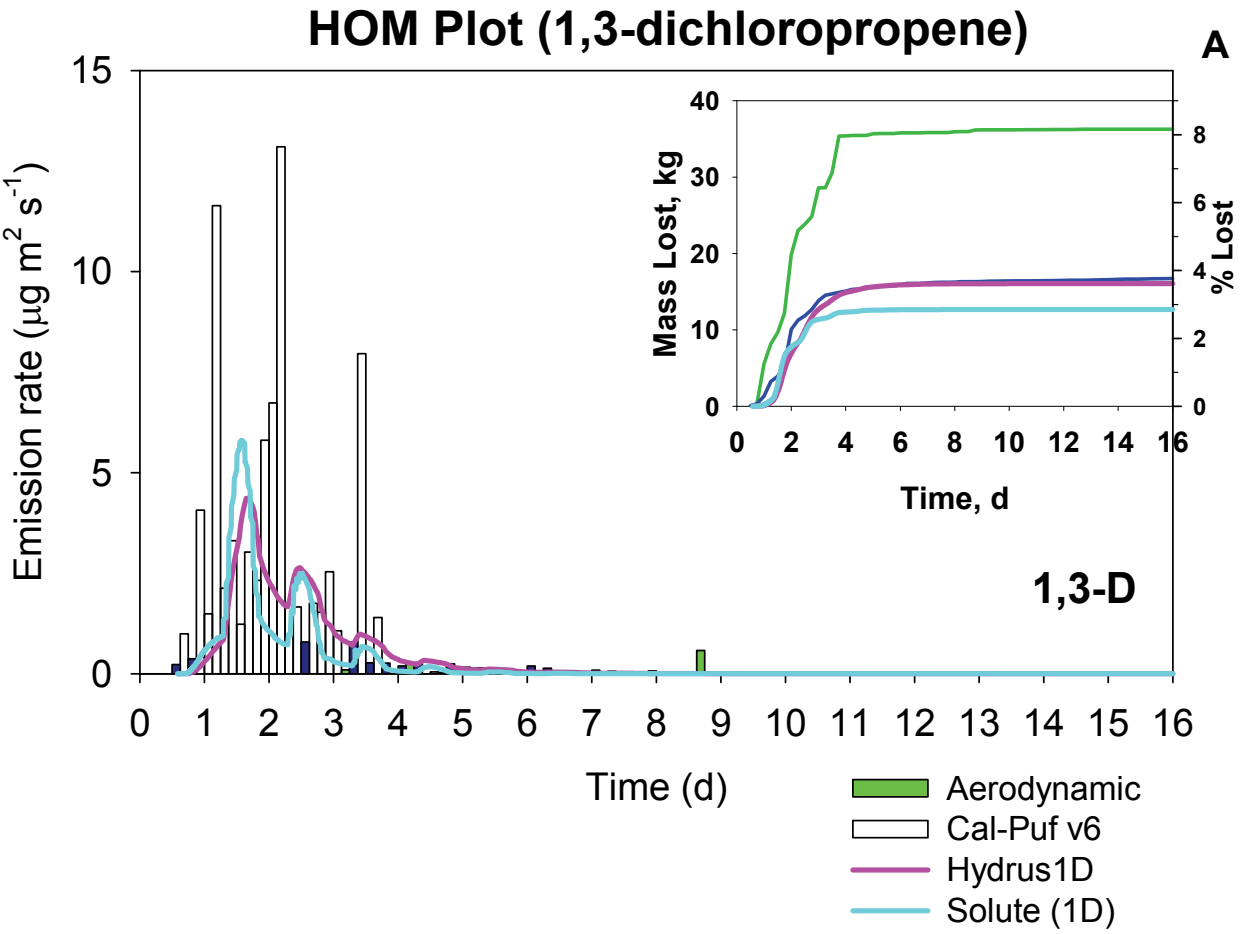

Figure 3.2.3. Measured and simulated 1,3-D emission rates from the HOM non-irrigated soil during the 2005 Buttonwillow field study (Yates and Gan, 2010). Inset shows the cumulative emissions as mass lost (kg) and as amount of applied fumigant lost (%).

The results were also similar to the two column experiments that simulated this field study (see Section 3.2.2), where the total 1,3-D emissions from the laboratory column containing LOM soil (i.e., same as irrigation treatment) were 14.4 % and for the HOM soil were 4.5 %. In both cases, the laboratory emission measurements fall between the percent lost values shown in Table 3.2.5, obtained using the ADM and CalPuff methods.

As was the case when comparing the 2007 field study data to the associated laboratory column study, the ADM and CalPuff methods gave estimates for the total 1,3-D emissions for the control LOM (irrigated) treatment that was consistent to the value obtained from the laboratory study (10.0–15.3, field vs. 14.4 %, laboratory). The field-scale numerical simulations gave total emissions of 11.1–12.4 % (Table 3.2.5) and the value from the laboratory column experiment was higher at 20.2 % (Table 3.2.3). Utilizing all of the information for the LOM (irrigated) treatment; the estimated total emissions were 13.9 ±3.7 %.

For the HOM treatment, there is close agreement between methods for estimating the percent total emissions. The field-scale measurements (ADM and CalPuff) of total emissions were

comparable to the laboratory study (3.8–8.1, field vs. 4.5 %, laboratory). Also, the field-scale simulations gave total emissions of 2.8–3.6 % and the laboratory column model simulation was higher at 6.9 %. Utilizing all of the information for the HOM treatment, the estimated total emissions were 4.95±2.1 %. Furthermore, based on the differences between values for percent mass lost, it appears that the simulated field-scale emission fluxes for this study correlate better with the CalPuff method than the ADM.

Table 3.2.5. Summary of total mass lost from emissions and percent of the applied fumigant lost for the 2005 Buttonwillow field experiments. The values from the aerodynamic (ADM), CalPuff, Hydrus 1D and Solute 1D methods are compared.

Method	**Total Mass Loss from Emissions**, kg	**Percent of Applied Mass Lost**, %
Irrigation Treatment		
ADM Mass	68.4	15.3
CalPuff Mass	44.5	10.0
Hydrus 1D	55.6	12.4
Solute 1D	49.4	11.1
Avg (±std)		12.2±2.3
High-Organic Matter Treatment		
ADM Mass HOM	36.3	8.1
CalPuff Mass HOM	16.7	3.8
Hydrus 1D	16.0	3.6
Solute 1D	12.7	2.8
Avg (±std)		4.6±2.4

3.3. Laboratory Shank Injection Studies with Telone C-35: Extension to wider range of emission reduction strategies.

3.3.1. Experimental Information

Duplicated laboratory soil column experiments with simulated shank injection of Telone C-35 were performed using the general description given in Section 2.2.1, and was used to simulate the soil and environmental conditions of the 2007 Buttonwillow field study (see Section 3.1). The data have been previously reported (Ashworth et al., 2009). A number of emission reduction strategies were assessed and compared to a control (Bare soil) treatment, *viz*: deep injection, ATS sprayed onto the soil surface (ATS spray), HDPE sealed over the soil surface, VIF sealed over the soil surface, and ATS applied with irrigation water to the soil surface (ATS irrigation). In all but one case, fumigants were applied at 30 cm depth. The exception was the 'deep injection' treatment where a depth of 46 cm was used (this was the same treatment as the 'control' in the soil column simulation of the 2007 field study, see Section 3.1). In the ATS spray treatment; approximately 565 mg of ATS in approximately 1.6 mL of water was sprayed to cover the soil surface directly prior to fumigation. In the ATS irrigation treatment, the same amount of ATS was added but in 113 mL (1 cm depth) of water. The ATS spray treatment with a 46 cm injection depth was previously described in Section 3.1.4 and can be referred to for comparison with the ATS spray 30 cm injection depth and the ATS irrigated treatment. The HDPE and VIF tarps were applied over the soil surface and sealed between the soil column and the emissions chamber using epoxy resin so as to produce a leak-free covering. Except for the ATS irrigation, each treatment was duplicated. Most treatments were run for 14 days, except for the tarped treatments which, at 15 days, had the tarps ripped using a hooked device temporarily inserted into the emissions chamber. This was done to simulate and assess the effect of tarp removal, or tarp ripping for planting purposes, on fumigant emissions over the following 2 days. Model simulations of the column experiments used HYDRUS 1D and Solute 1D (Section 2.5.1–2.5.2).

3.3.2. Results and Discussion

The emission rates of the fumigants from the soil surface are shown in Figure 3.3.1 and Figure 3.3.2 for 1,3-D and CP, respectively. Overall, the lower emission rates observed for CP were expected due to the lower application rate (approximately half that of 1,3-D), and its shorter degradation half-life (0.12–1.2 d, compared to 3.8–5.3 d for 1,3-D; Ashworth et al., 2007; 2009). In the majority of treatments, emissions of CP occurred over a period of around 100 h (to around 125 h in the deep injection treatment). In contrast, the emission rate curve for 1,3-D showed extensive tailing beyond this period. This difference was again most likely the result of the much shorter degradation half-life determined for CP compared to 1,3-D. In the control columns, the peak emission rate was reached more rapidly (after 7 and 14 h for the CP and 1,3-D, respectively) than for any of the treatments.

As observed for the previous studies, maximum emission rate for each treatment generally occurred 1 day after fumigation, indicating that each emission reduction strategy delayed the release of fumigants relative to the control. At this time, the decreasing order of the emission rate maxima was: HDPE > Control > Deep Injection > ATS spray > ATS irrigation > VIF for 1,3-D,

and: Control > ATS spray > Deep Injection > ATS irrigation > HDPE > VIF for CP. Therefore, except for 1,3-D in the HDPE treatment, the emission reduction strategies reduced emission rates relative to the control. VIF was most effective at reducing emission rates due to its high resistance (R)-value (see Section 2.1). Upon ripping of the VIF, a spike of 1,3-D was observed, indicating that the fumigant was maintained in the soil up to this time. No other tarp/fumigant combination produced this spike. Of the non-tarped treatments, deep injection and both ATS treatments were effective in reducing emission rates compared to the control. Most marked reductions were observed for the ATS irrigation treatment, particularly for CP. The effect of deep injection on the time-course trend in CP emissions is also worthy of note. Despite markedly reducing the magnitude of the emission rates (relative to the control) up to the end of day 1, the deep injection then led to a continued release of CP, characterized by relatively high emission rates over several days. Although not as pronounced relative to the other treatments, a similar trend was observed for 1,3-D.

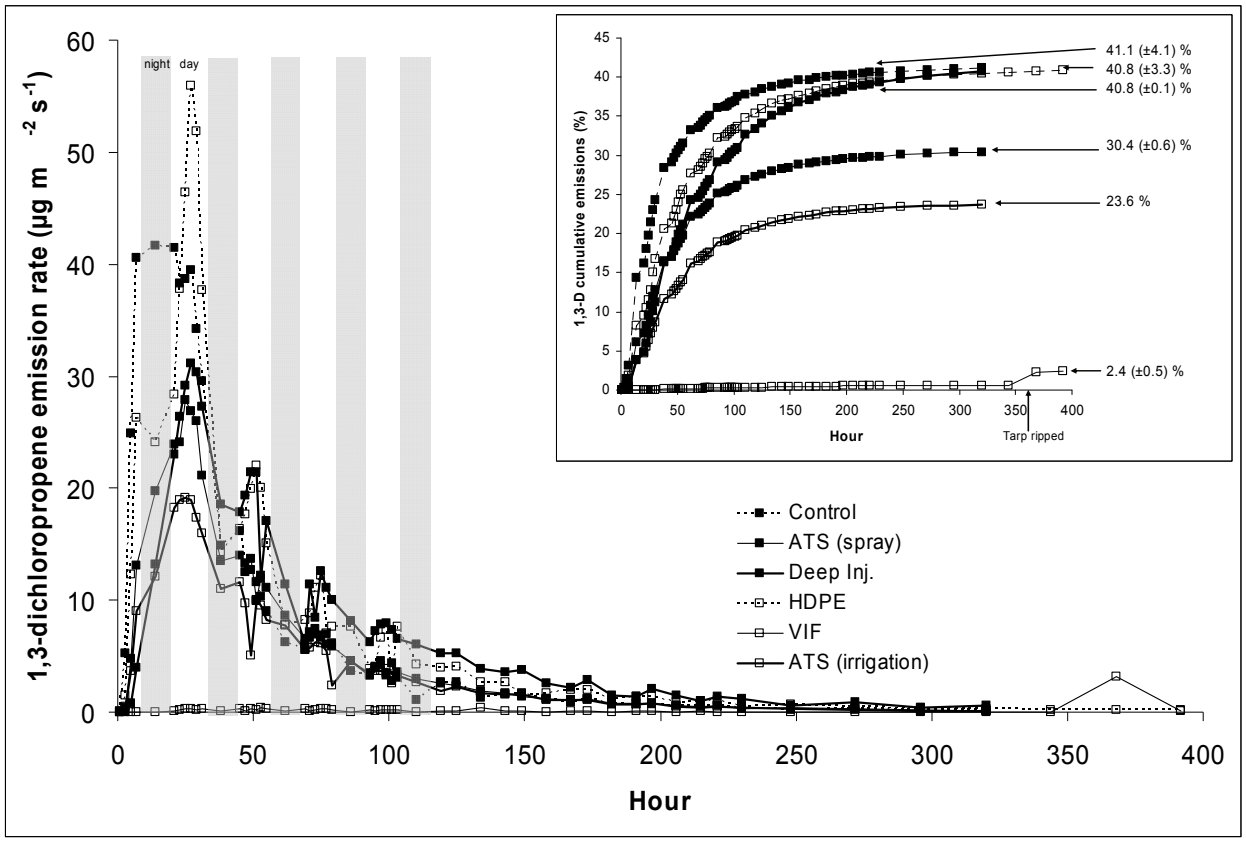

Figure 3.3.1. Measured 1,3-D emission rates for Control and emission reduction strategy treatments. All applications made at 30 cm depth except deep injection (46 cm depth) (Ashworth et al., 2009).

Figure 3.3.1 and Figure 3.3.2 also show emission rates in relation to the 'daytime' and 'nighttime' temperature regime. Peaks in emission flux during daytime were likely associated with the higher temperatures, particularly between 12:00 and 18:00 hours when soil temperature

at 5 cm depth increased from 25 to 32 °C. Since fumigant vapor pressure increases with increasing temperature, higher emissions would be expected during this time when compared to the cooler nighttime periods. Tarped soils can exhibit greater fumigant emission rates under conditions of higher temperature due to increases in tarp permeability (Wang et al., 1999; Papiernik and Yates, 2002).

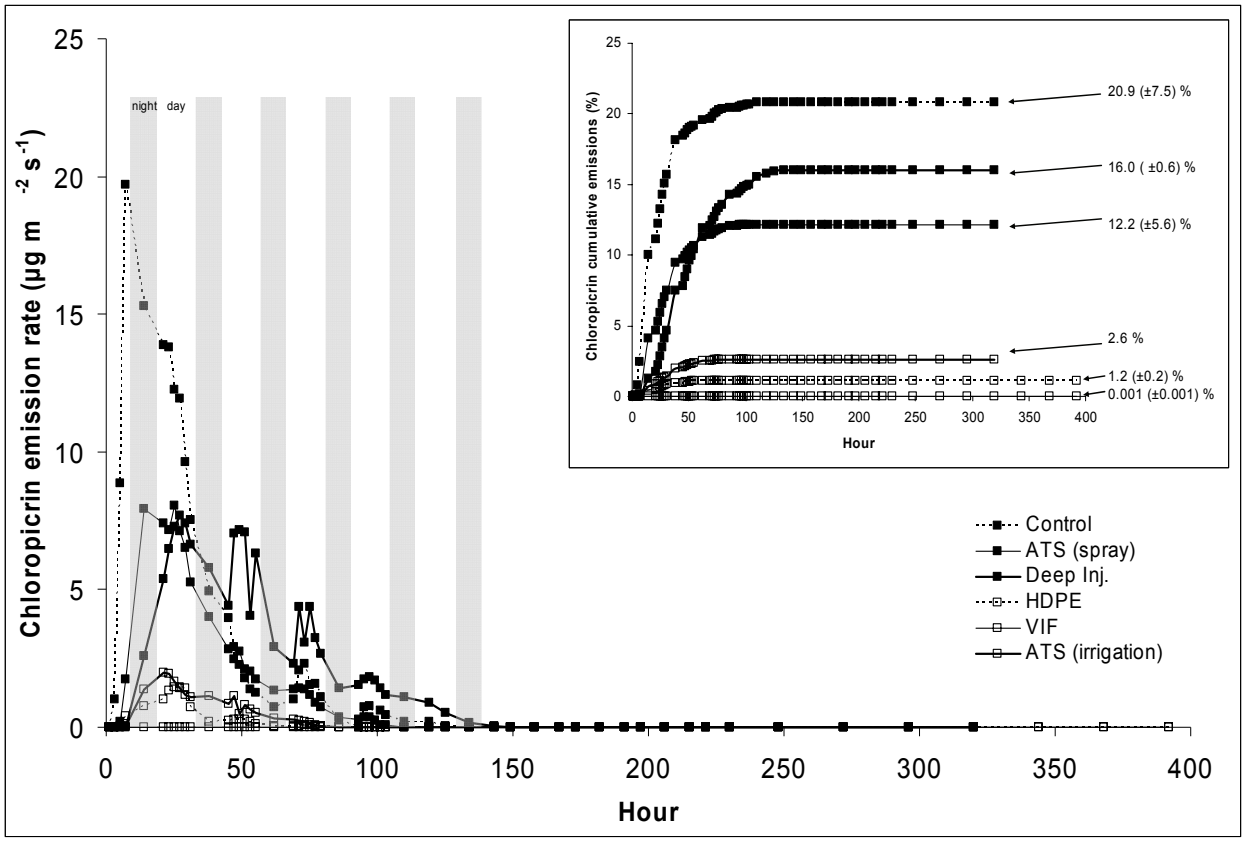

Figure 3.3.2. Measured CP emission rates for Control and emission reduction strategy treatments. All applications made at 30 cm depth except deep injection (46 cm depth) (Ashworth et al., 2009).

The cumulative fumigant emissions, expressed as a percentage of the total amount added, over the course of the experiment are shown in Figure 3.3.1 and Figure 3.3.2 (insets) for 1,3-D and CP, respectively and are summarized in Table 3.3.1. The HDPE and deep injection offered no benefit in terms of 1,3-D emission reduction when compared to the control (all yielding around 41 % total emissions). In the case of HDPE, this has been previously noted by other workers (Gao et al., 2008) and is consistent with the relatively high 1,3-D mass transfer values determined for this tarp; 3–5 cm/h as shown in Table 2.1.1. Comparing to the value of 0.9 cm/h for CP, it is not surprising that emissions of CP were reduced (in contrast to 1,3-D) in the HDPE treatment (1.2 %) when compared to the control (20.9 %). Deep injection emissions of CP (16.0 %) were also reduced from control levels. The reason for this difference in the behavior of the

two fumigants in the HDPE and deep injection treatments may be the lower vapor pressure of the CP which would likely limit its ability to diffuse as effectively from the deeper soil or through the HDPE tarp, thus leading to lower emissions. The effectiveness of HDPE in reducing emissions of CP has been reported (Gan et al., 2000b), as has the potential for fumigant emission reduction by deep injection (Yates et al., 1997; Papiernik et al., 2004).

Most marked emission reductions for both fumigants were obtained by using the VIF tarp which produced total emissions of just 0.001 % for CP; representing a ~2×10^4 times reduction from the control levels. Emission reductions of 1,3-D from the VIF tarped treatment were more moderate and were also significantly affected by the ripping of the tarp towards the end of the experiment. Immediately before ripping, total emissions were just 0.6 %, but increased to 2.4 % afterwards. In contrast, an increase in CP emissions was not observed following tarp ripping, probably due to its degradation within the soil by this time. For the same reason, ripping of the HDPE tarp did not result in an increase in CP emissions. The absence of an emissions increase for 1,3-D spike following ripping of the HDPE tarp was presumably due to the ineffectiveness of the HDPE in maintaining 1,3-D within the soil during the earlier part of the experiment.

Like previous work, the addition of ATS to the surface of the soils reduced fumigant emissions. In the case of 1,3-D, total emissions were reduced from 41 % in the control to 30 % in the ATS spray treatment and 24 % in the ATS irrigation treatment. Despite the same amount of ATS being applied in both ATS treatments in the present experiment, the greater volume of solution in the irrigated treatment apparently induced the better emission reductions, presumably due to a better distribution of the ATS throughout the upper soil layer. Thus, the likelihood of chemical interaction between the ATS and the upward-diffusing fumigants was increased. In addition to an enhanced chemical effect, the greater volume of water is also likely to reduce emissions by physically restricting gas diffusion through the soil pore space.

Table 3.3.1. Summary of total 1,3-D and chloropicrin emissions (% of the applied fumigant) from laboratory column experiments after shank injection.

Treatment	1,3-D (cis+trans) Emissions, %	Chloropicrin Emissions, %
Control	41.1 ± 4.1	20.9 ± 7.5
Deep Injection	40.8 ± 0.1	16.0 ± 0.6
HDPE	40.8 ± 3.3	1.2 ± 0.2
ATS (spray)	30.4 ± 0.6	12.2 ± 5.6
ATS (irrigation)	23.6	2.6
VIF (before ripping)	0.6	< 0.1
VIF (after ripping)	2.4 ± 0.5	< 0.1

3.3.3. Comparison of Soil Column Experimental Data and Model Simulations

The experimental parameters used in Hydrus 1D and Solute 1D model simulations are listed in Table 2.5.1 and the finite element grid established for the simulations are described in Section 3.1.3. Unless stated otherwise in Table 3.3.2, parameters for the previously described simulations (Table 3.1.2) were used. With the exception of deep injection (46 cm), all simulations had an injection depth of 30 cm. The film properties used in the simulations are shown in Table 2.1.1.

Table 3.3.2. ATS parameters used for simulation of ATS spray, ATS irrigation treatments. Additional relevant parameters and properties of fumigants given in Table 3.1.2.

Treatment	**Properties**	**Value**	**Units**
ATS	Applied at the surface with density	50	g m^{-2}
	Applied mass	0.57	g
	ATS molecular weight	148	g/mol
	ATS density	5	mmol/cm^2
	ATS first-order rate constant‡, k_{12}	0.046	h^{-1}
	ATS second-order rate constant‡, k_{12}	0.2	mL μmol^{-1} h^{-1}
ATS-spray	ATS-water solution applied	1.6	mL
	Depth of wetted soil	0.0375	cm
ATS-irrigation	ATS-water solution applied	113	mL
	Depth of wetted soil	3.25	cm

‡Wang et al. (2000) in the aqueous-phase

Shown in Figure 3.3.3–Figure 3.3.5 are the simulated Telone C-35 emission fluxes along with measured values for each treatment. For the control treatment, the simulation over predicted the measured peak flux. After about 40 h, the simulated and measured flux rates are nearly the same. The overestimate of the peak emission flux led to an overestimate of the total fumigant lost by about 15 % of applied fumigant. While it is somewhat unclear whether these differences are due to difficulties with the experiments or if the model parameters are suboptimal, given the theoretical behavior shown in Figure 3.1.4 and that the total emissions for the Control treatment (30 cm injection) and the Deep treatment (46 cm) are nearly the same, this provides some evidence that lack of agreement might be due to experimental artifacts for the Control treatment.

Comparison of the measured and simulated emissions for the deep (46 cm) injection (see Figure 3.1.1) shows the effect of injection depth on peak and total emissions. Measured peak emissions were reduced from about 60 to 40 μg m^{-2} s^{-1}. The simulated peak emissions were reduced from about 110 to 25 μg m^{-2} s^{-1}. Compared to the control, where simulated total emissions overestimated the measurements by approximately 15 %, the simulated total emissions for the deep injection treatment were about 6 % (of applied fumigant) lower than measurements.

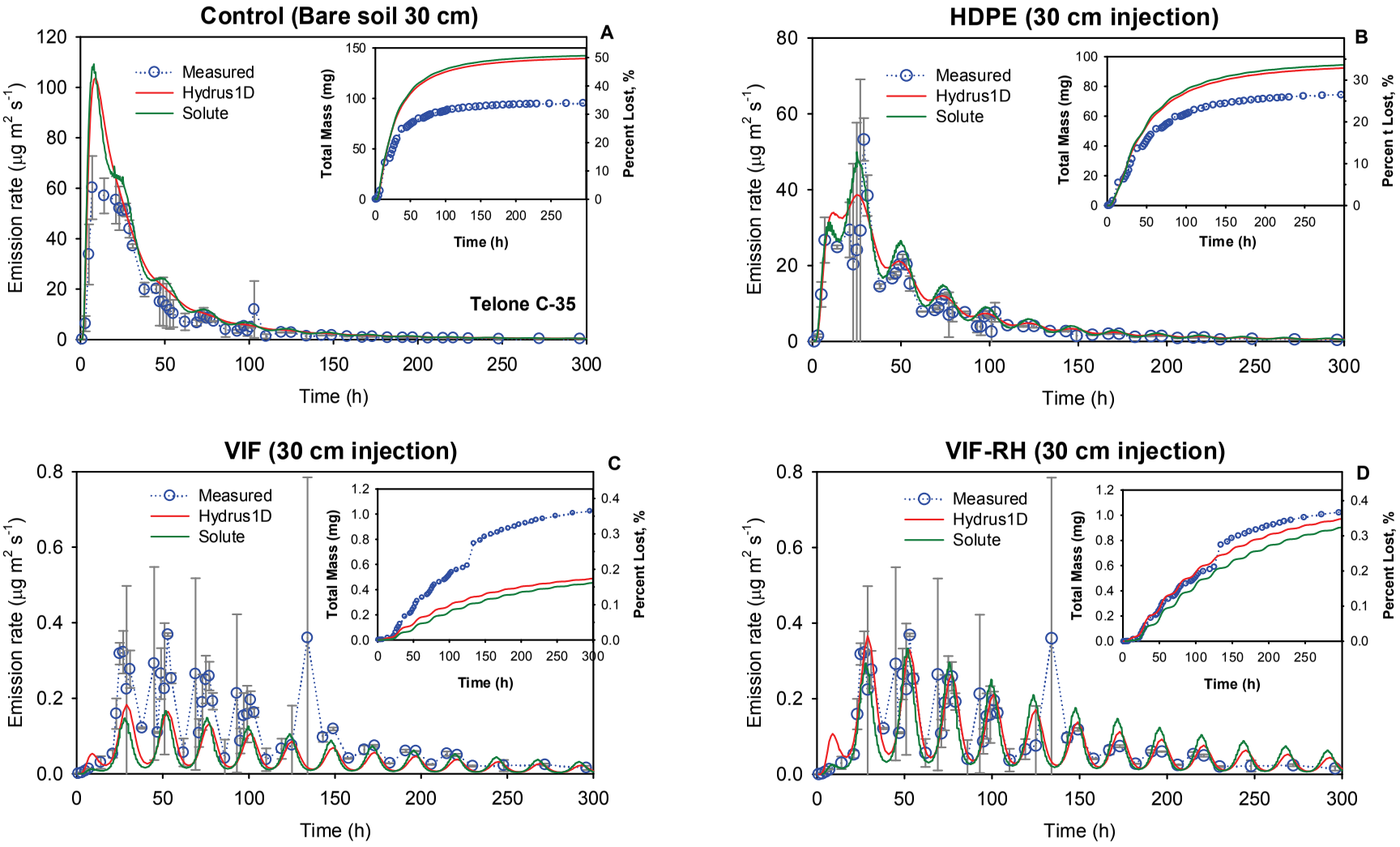

Figure 3.3. Comparison of simulated (Hydrus 1D and Solute 1D) and measured emission flux curves for Telone C-35 for control and a range of emission reduction strategies.

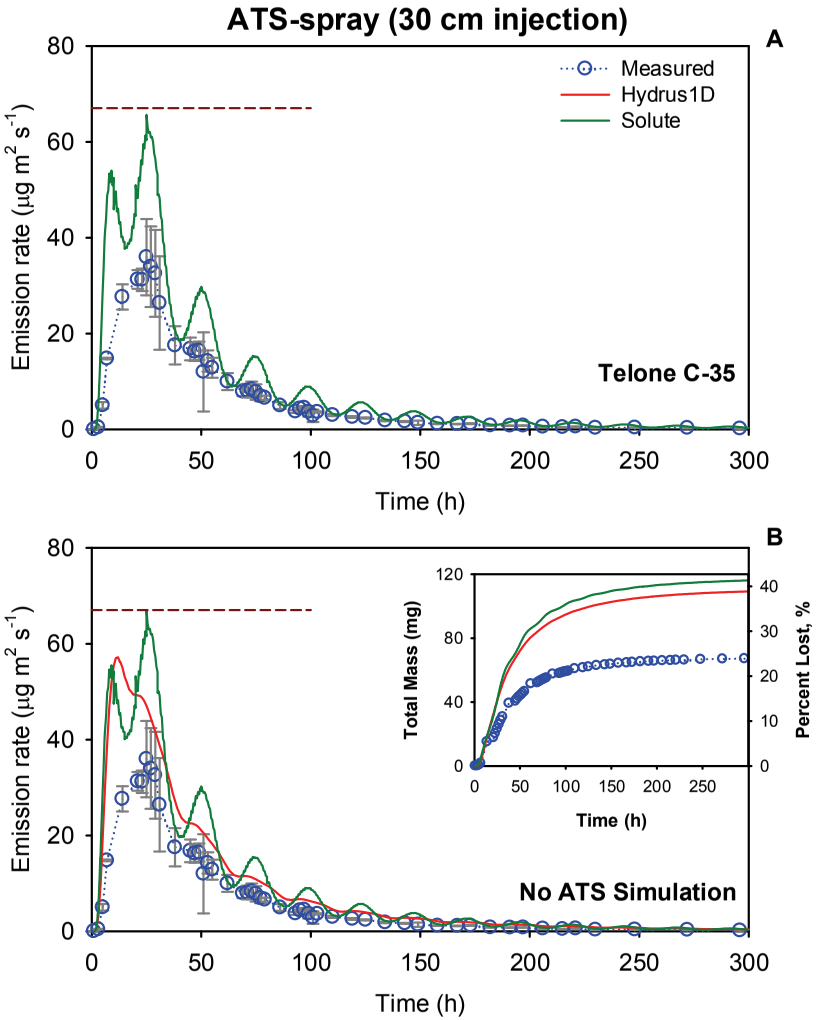

Figure 3.3.4. Comparison of simulated and measured Telone C-35 emissions after spray application with ATS. In (A), fumigant-ATS reaction is simulated. In (B), no fumigant-ATS reaction occurs.

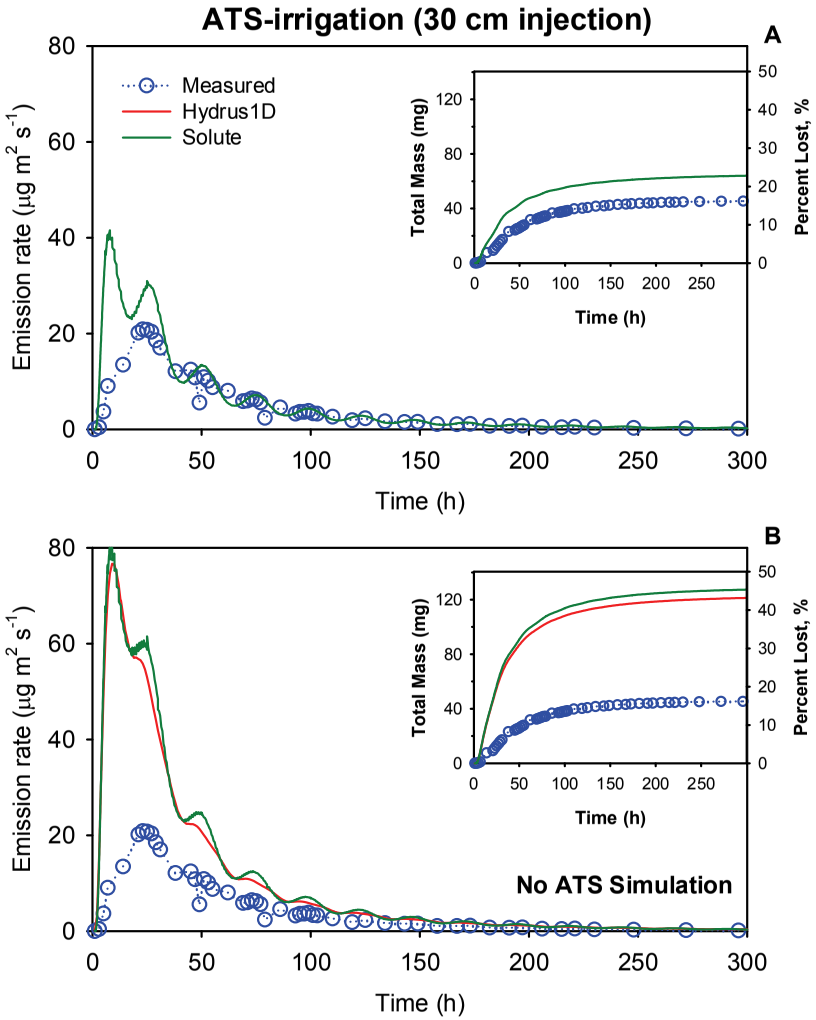

Figure 3.3.5. Comparison of simulated and measured Telone C-35 emissions after an irrigated application with ATS. In (A), fumigant-ATS reaction is simulated. In (B), no fumigant-ATS reaction occurs.

For the tarped treatments, the effect of the film on the soil surface was simulated by adjusting the film permeability to changes in temperature. For the VIF, the effect of relative humidity on film permeability (Papiernik et al., 2011) was also simulated. The simulations, in general, accurately predicted the measured emissions. For the HDPE treatment, the Hydrus 1D simulations tended to have less pronounced emission fluctuations due to changes in temperature compared to Solute 1D. Because of this, Solute 1D more accurately followed the measured emission rate. Both models underestimated the measured peak emission rate from 21–39%, but generally fell well within the experimental error bars. At other times during the simulation, the magnitude of the predicted emission fluxes follows the measurements with reasonable accuracy. The measured total emissions were about 27 % and the simulations were about 6 % higher.

The simulated emission rate for the VIF treatment under predicted the measured values but correctly predict the order of magnitude of the measured emissions. Although the underestimation appears significant, the emission fluxes were very low, with emission peaks between 0.2 and 0.4 $\mu g\ m^{-2}\ s^{-1}$, and the total error is < 1% of the applied fumigant material. Accurate simulation of such low emission levels proved difficult. The simulations successfully predict very low emissions when the soil surface is covered with a VIF. The measured total emissions were 0.36 % of applied Telone C-35 and the simulations were 0.16–0.17 %.

Papiernik et al. (2011) recently showed that the permeability of certain VIF films depends on the ambient relative humidity. In soil fumigant systems, the relative humidity in the air space between the soil and the film would normally be >50%, which could lead to increased film permeability. In an attempt to explore possible reasons for under-predicting the emission rate in Figure 3.3.3C, another simulation was conducted that decreased the permeability of the VIF due to an increased relative humidity on the soil-side of the film material (Papiernik et al., 2011). Since relatively few data are available to describe the behavior of film permeability due to changes in RH, the *b* values in Table 2.1.1 were reduced by 50%. Shown in Figure 3.3.3D is the predicted and measured emission rates and total emissions for a RH-affected VIF. It appears from this comparison that the effect of relative humidity on the VIF mass transfer coefficient provides a plausible explanation for the under prediction in Figure 3.3.3C, and provides evidence that the effective permeability of the VIF for the column experiment was about 50% less than the literature value. The simulated total emissions for this scenario were 0.32–0.35 % and much closer to the measured value of 0.36 %

In general, fluctuations in emission rates due to changes in the system temperature are effectively reproduced by both models. This suggests that both models describe the effects of fumigant diffusion and tarp permeability reasonable well. This is evident in both the HDPE and VIF treatment simulations.

A comparison between simulated and measured emissions after a spray application of ATS to the soil surface (i.e., < 0.04 cm) is shown in Figure 3.3.4A. In general, the simulations over-predicted the peak emission rates and total emissions, which could be a result of an incompatible second-order reaction coefficient. A value was obtained from literature data (Wang et al., 2000) based on reaction in the aqueous phase, but additional data are needed to reduce parameter uncertainty. This is an area that warrants further research activity.

Figure 3.3.4 shows the effect of simulating the second-order reaction between Telone C-35 and ATS (Figure 3.3.4A) as well as the case where the presence of ATS has no effect on Telone C-35 (i.e., no second-order reaction mechanism). The dashed line in both graphs shows the reduction in the peak emission rate when simulating a spray application of ATS. The measured and predicted peak and total emissions are reported in Table 3.3.3. Solute 1D over-predicted the peak Telone C-35 emissions by 83 % and the model predicts that the effect of the second-order reaction process would lead to a reduction in total emission of 1.2 %.

Since the second-order reaction only operates when both chemicals are in contact, a thin reactive zone would limit the amount of time available for degradation. Compared to a larger reaction depth (i.e., application with irrigation water), this would lead to reduced degradation and higher emissions. Based on the small difference between the simulated values in Figure 3.3.4A and Figure 3.3.4B it is clear that the model predicts that a spray application of ATS would be ineffective in reducing Telone C-35 emissions for these experimental conditions. This is contrary to the experimental results which show a 29 % reduction in total Telone C-35 emissions due to a spray application of ATS. This is also contrary to the results of Gan et al. (2000) who observed almost a 20 % reduction in total 1,3-D emissions in a laboratory experiment when the ATS was applied in 11 mL of water.

Figure 3.3.5 shows the effect of an ATS application in 1 cm of irrigation water. For this experiment, the soil depth of the ATS application was approximately 3 cm and is considerably deeper the surface spray scenario. These results also indicate that a combination of reducing the air-filled porosity and increasing the fumigant residence time in the reactive layer reduce both peak and total emissions. Comparing Figure 3.3.5A and Figure 3.3.5B shows that including a second-order reaction process in the simulation model can be important for obtaining accurate predictions. When the second-order reaction mechanism is turned off, both models predict peak emissions of 80 $\mu g\ m^{-2}\ s^{-1}$ and total emissions that are almost 3 times the measurements. Including this mechanism reduces peak emissions to 40 $\mu g\ m^{-2}\ s^{-1}$ and leads to predicted total emissions of 23 % vs. 16% for the measurements.

Overall, the total emission losses of Telone C-35 determined by measurement and model simulation were generally similar (Table 3.3.3). While there were differences between methodologies within a specific fumigant management treatment (see Figure 3.3.6), when viewed together, the overall behavior across treatments becomes clear. For example, in Figure 3.3.6, it is clear that the VIF and Deep injection treatments have significantly lower peak emissions than other treatments, and all methods show this result. The differences in total emissions also stand out when viewed across treatments (i.e. horizontal dashed lines representing average total emissions for group).

Using the average total emission values shown in Figure 3.3.6, the following order of reducing emission appears: Bare soil > ATS spray > HDPE > ATS irrigation > Deep injection > VIF. The average total emission percentages and standard deviation for this sequence, respectively, were 43.9±7.9 %, 34.3±9.1 %, 30.7±3.3 %, 19.5±4.7 %, 17.3±2.4 % and 0.28±0.12 %.

Table 3.3.3. Measured and simulated peak emission rate (μg m^{-2} s^{-1}) and total emissions (%) for 1,3-D, CP and Telone C-35 from laboratory (1D) soil columns. Total measured emission loss from each treatment are reported as a percentage of applied fumigant.

		Peak Emissions, μg m^2 s^{-1}			Total Emission Loss, %		
	k_{12} [§]	1,3-D	CP	C-35	1,3-D	CP	C-35
Measured							
Control	–	41.7	19.7	60.2	40.9	20.8	33.8
Deep	–	17.3	9.1	26.4	24.3	13.3	20.4
HDPE	–	51.8	1.4	53.2	40.2	1.1	26.4
VIF[*]	–	0.37	0.001	0.37	0.56	0.001	0.36
ATS spray	–	27.9	8.1	35.9	30.3	12.2	23.9
ATS irrigation	–	19.1	2.0	20.9	23.5	2.6	16.2
Simulated (Hydrus)							
Control	–	69.6	33.4	103.7	58.7	33.0	49.7
Deep	–	7.9	1.9	9.7	22.1	5.1	16.1
HDPE	–	31.7	8.8	49.9	44.4	11.8	32.9
VIF[‡]	–	0.17	0.009	0.18	0.26	0.01	0.17
VIF corrected[†]	–	0.35	0.018	0.37	0.52	0.021	0.35
ATS spray	No	45.3	12.6	57.2	50.1	18.3	38.9
ATS irrigation	No	58.9	18.5	76.7	54.4	22.6	43.2
Simulated (Solute)							
Control	–	74.3	34.9	109.3	60.0	33.5	50.7
Deep	–	7.6	1.7	9.2	20.5	4.3	14.8
HDPE	–	41.1	8.8	49.9	45.4	12.0	33.6
VIF[‡]	–	0.16	0.01	0.17	0.24	0.01	0.16
VIF corrected[†]	–	0.32	0.022	0.33	0.48	0.026	0.32
ATS spray	Yes	54.1	11.7	65.6	52.4	17.7	40.2
ATS spray	No	55.1	12.1	66.9	54.0	18.2	41.4
ATS irrigation	Yes	25.7	15.8	41.5	25.7	17.5	22.8
ATS irrigation	No	55.0	25.9	80.8	54.4	28.8	45.4
Simulated (Analytic)							
Control	–	61.6	29.5	91.0	47.9	27.7	41.2
Deep	–	12.3	4.0	16.1	23.2	7.7	18.0
HDPE	–	37.0	6.5	43.4	39.4	10.1	29.7
VIF[‡]	–	0.030	0.003	0.032	0.07	0.005	0.05
VIF corrected[†]	–	0.060	0.006	0.065	0.14	0.01	0.10

[§] – For yes: simulation included a 2nd order reaction process, for no: coefficient $k_{12} = 0$, and for '–' a 2nd order process doesn't apply.

[‡] – VIF mass transfer coefficient was obtained for 20–40% relative humidity on each side of film.

[†] – VIF mass transfer coefficient was obtained for 100% relative humidity on source side of film.

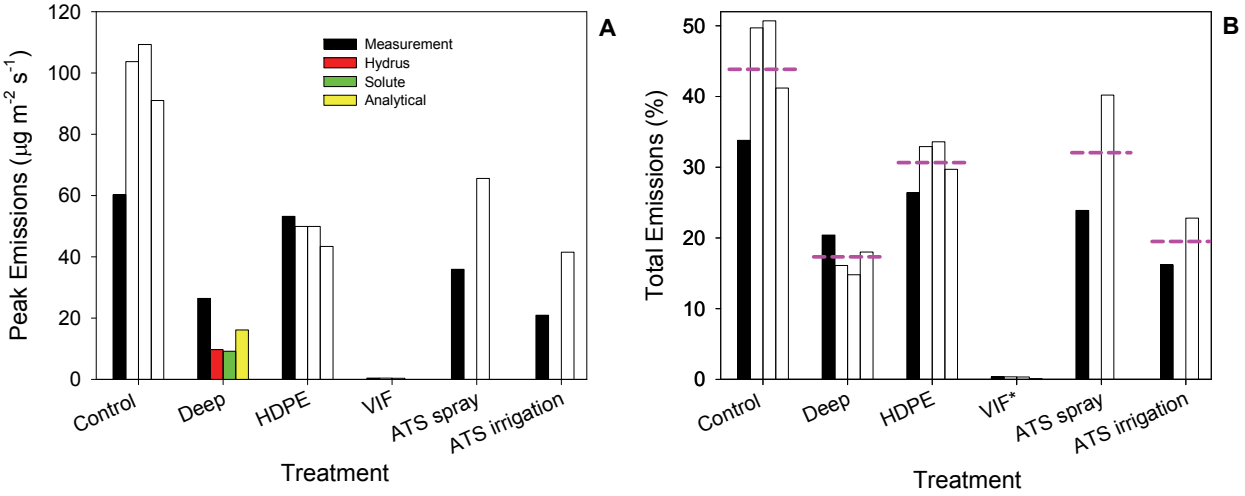

Figure 3.3.6. Comparison of different approaches to obtain peak and total emissions of Telone C-35 for several fumigation management treatments. In B, horizontal dashed lines indicate the mean total emissions calculated using the four bars (or two bars for ATS treatments) shown for each treatment.

3.4. Laboratory Shank Injection Studies: Extension to MeI fumigant.

3.4.1. Experimental Information

Duplicated laboratory soil column experiments with simulated shank injection of MeI were performed using the general description given in Section 2.2.1. The data have been reported previously (Ashworth et al., 2011). The experiments compared organic matter addition, irrigation and tarping with VIF to a control (bare soil). MeI application was made at 30 cm depth in each case. Effects of organic matter addition were assessed by using the HOM soil described in Section 2.1. For the tarped columns, VIF was applied over the soil surface and sealed between the soil column and the emissions chamber using epoxy resin so as to produce a leak-free covering. Irrigation was performed by inserting a pronged irrigation device into the volatilization chamber and evenly distributing 1 cm of water (113 mL) onto the soil surface. This was performed three hours after application of the MeI, and repeated daily for the first five days of the experiment. Model simulations of the column experiments were carried out using Hydrus 1D and Solute 1D (see Section 2.5.1 – 2.5.2).

3.4.2. Results and Discussion

Emission fluxes of MeI from the control, irrigated, HOM and VIF treatments are shown in Figure 3.4.1. If the increased flux rates observed in the VIF treatment following tarp ripping are excluded, the maximum peak in emissions from each treatment occurred very rapidly (in the 2–4 h sample period after fumigation). Indeed, this 2-h period accounted for 21, 28 and 31 % of the total MeI emissions, respectively, in the irrigated, HOM and control treatments. For the VIF treatment this interval accounted for only 8 % of the total emissions. Compared to other commonly used MeBr alternatives, MeI possesses relatively high Henry's constant and vapor pressure values (Table 3.4.1). This would explain the rapid gas-phase transport from 30-cm depth (the injection point) to the soil-headspace boundary. Compared to the control, which showed the highest maximum peak emission rate (570 μg m^{-2} s^{-1}), the maximum peak in the HOM treatment was reduced by 32 %, in the irrigated treatment by 33 %, and in the VIF treatment by 99.98 %. In a previous column study using MeI (Gan et al., 1997), tarping with VIF reduced the maximum emission peak by 82 % compared to bare soil. In the same study, potting mix with a high level of organic matter (9.60 %) exhibited a maximum emission peak 50 % lower than soils with 2.51-2.99 % organic matter. Compared to the other fumigants (1,3-D and CP) applied under similar conditions (see Section 3.3), the peak MeI flux rate measured here was very high. The peak emission flux of 1,3-D was around 14 times lower than for MeI (at the same application rate). Similarly, the peak CP emission flux was around 28 times lower than for MeI (at approximately half the application rate used here for MeI).

Following the initial emissions peak, the fluxes in each treatment generally decreased with time, characterized by extended tailing of the curve, to 338 h (for clarity the emission rates are shown only up to 120 h in Figure 3.4.1). Within this tailing, the observed fluctuations in emission fluxes over time were not strongly correlated with the diurnally varying soil temperatures when considered across the entire experiment. Nevertheless, when considered on a day-by-day basis, it was noted that emission fluxes were generally lowest during the night-time period (1900-0700 h) when soil temperatures were low, and highest during late morning and early afternoon periods

(1100-1300 and 1300-1500 h) when soil warming was evident (data for VIF-covered soil shown in Figure 3.4.2). This suggests that soil temperature was somewhat influential over MeI emissions, as would be expected given the positive relationship between temperature and MeI diffusion coefficient in soil. Moreover, for the VIF covered soil, this may have also been coupled with an increase in permeability of the film at higher temperatures.

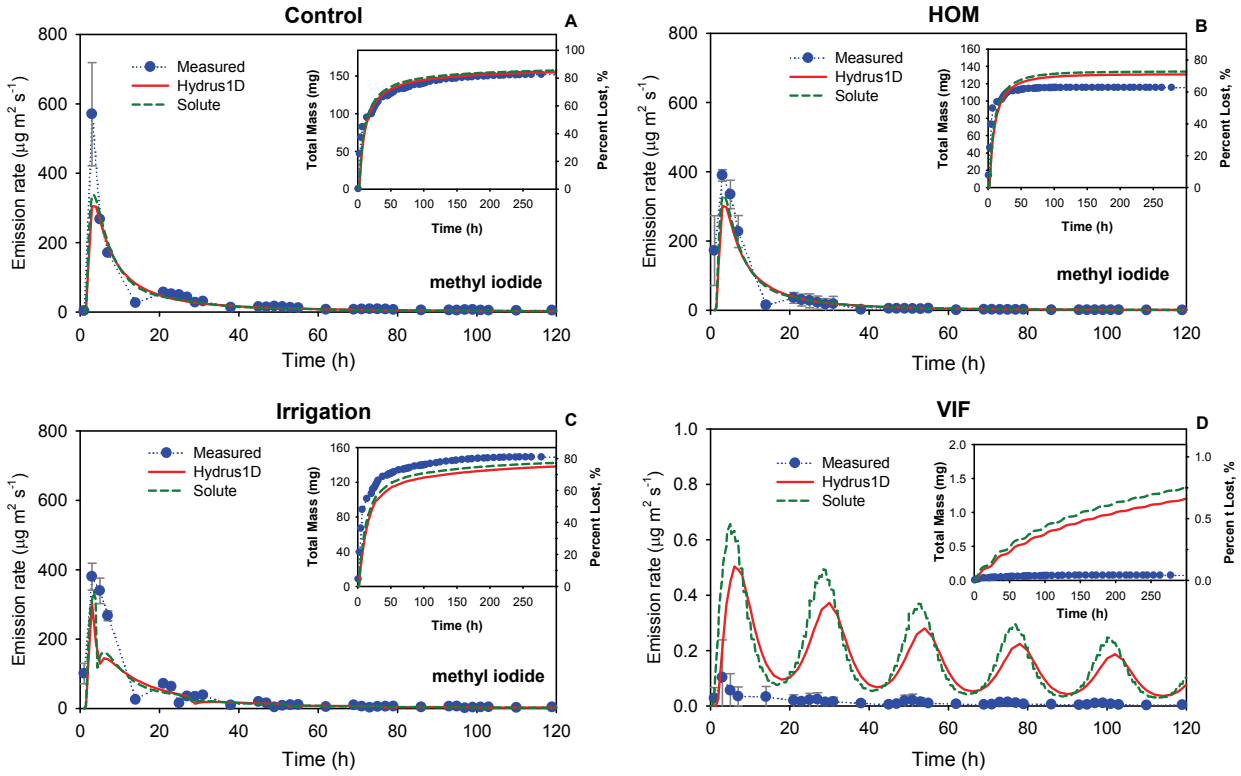

Figure 3.4.1. Measured and simulated MeI emission fluxes from the control, irrigated, HOM, and VIF treatments.

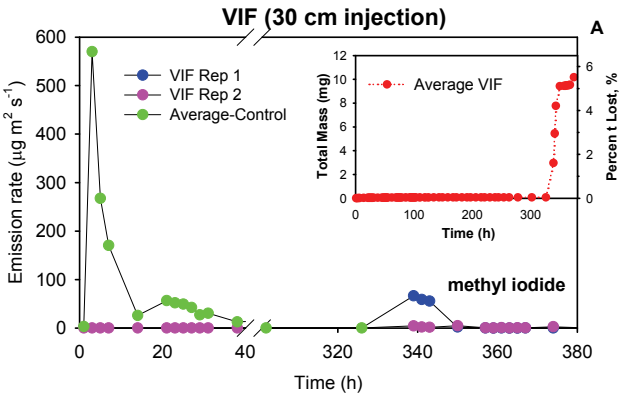

Figure 3.4.2. Comparison of measured MeI emission fluxes from the control and VIF treatments. The VIF was cut at 336 h producing an increase in measured emission flux.

Most effective in the reduction of MeI emission flux was the surface covering of VIF. However, one concern over the use of such coverings is the potential for fumigant release following tarp ripping, or removal, prior to crop planting. This is particularly an issue in situations where chemicals with relatively long half-lives (e.g. MeI) are being used. To quantify this potential for emissions, the VIF was ripped on Day 14 of the experiment (Figure 3.4.2). This produced a marked spike in average emissions from the two replicates from

0.0003 μg m^{-2} s^{-1} (at 338 h) to around 30 μg m^{-2} s^{-1} (at 340-344 h). As a result, emission fluxes from the VIF treatment at this time were greater than those in the other treatments at 338 h (when those treatments were ended). Nevertheless, this maximum peak in the VIF flux was small (almost 20 times lower) compared to the peak emission flux at 2-4 h for the control (bare soil) treatment.

Cumulative emissions of MeI, expressed as a percentage of the added mass, are also shown in Figure 3.4.1A (insets). Total loss from the control soil averaged 83 %. Despite reducing the maximum emission flux peak relative to the control, the irrigation treatment did not lead to a significant overall reduction in MeI emissions over the course of the experiment (average total loss 82 %). The addition of irrigation water was expected to lower emissions by blocking gas phase MeI transport in the water-filled pores close to the soil surface. Although 1 cm daily addition of irrigation water for 5 days can be considered a relatively large input, the rapidity of the emissions suggests that only the initial addition (30 min prior to fumigant application) would have had the potential to significantly influence emissions. The data may suggest, therefore, that the initial 1 cm addition was insufficient to effectively form a barrier of water-filled pore space. Moreover, it is considered that the relatively high Henry's constant and vapor pressure values of MeI likely resulted in a more efficient upwards gas transfer in the moist soil than might be demonstrated by, for example, 1,3-D and chloropicrin. In particular, the high Henry's constant is likely to have limited the transfer of MeI from the gas phase into the soil water. Overall, data from the irrigation treatment suggest that a single, large irrigation event immediately prior to fumigation may be most effective at reducing emissions. Subsequent events would likely have little impact.

The relationship between organic matter and MeI degradation is consistent with measured degradation rates in the present study. Applying the first-order decay model to the measured loss of MeI from soil over time, yielded rate constant (k) values of 0.00264 h^{-1} (r^2=0.99) and 0.00993 h^{-1} (r^2=0.97) for the control and HOM soil, respectively. Calculating half-lives yielded values of 10.9 d and 2.9 d, respectively. Therefore, the rate of degradation in the HOM soil was almost four times faster than the control soil. Interestingly, for the same two soils, we previously determined 1,3-D degradation half-lives of 5.3 d and 1.2 d, respectively (i.e. also around four times faster in the HOM soil) (see Section 3.2). The faster degradation in the HOM soil explains the reduction in MeI emissions; however, the alacrity of the emissions appeared to limit the extent to which a beneficial impact was attained. Previously, the same HOM soil was far more effective in reducing total emissions of 1,3-D; responsible for an almost six times reduction (total emissions of 5.7 % compared to 33.1 % in the control) (Section 3.2). This greater effectiveness may be attributable to the slower emissions of 1,3-D from the soil when compared to MeI. That is, the contact time between the 1,3-D and soil organic constituents may have been greater than that for MeI, due to the lower Henry's constant and vapor pressure values. Nevertheless, Luo et al (2010) found relatively low MeI emissions (29 % total loss) in soil with a high rate of MeI degradation (0.0779 h^{-1}, $t_{½}$ = 8.9 h) induced by soil amendment with citrus roots. Evidently, with such a short half-life, the potential to impact MeI emissions is greatly increased.

Total emission loss from the VIF treatment prior to tarp ripping at 338 h was 0.04 %. Two days after ripping, the total was 6 %. Even taking into account the fact that the emissions barrier offered by VIF was ultimately compromised, it would appear that a significant emissions

reduction benefit over the other treatments was obtained, both in terms of emission flux rates and total emissions. The reduction in MeI emissions induced by the Hytibar VIF covering was greater than that observed by Gan et al. (1997). These workers reported a series of column experiments to determine soil emissions of MeI under differing surface tarps. For a sandy loam soil, they measured 78, 72 and 52 % total emissions of MeI under control (bare soil), polyethylene-tarped and VIF-tarped (Hytibar) conditions, respectively. On the other hand, such a large reduction as was observed here for the Hytibar is consistent with the high MeI diffusion resistance value for this film (Section 2.1), and with the large reductions observed for other fumigants applied under this film. For example, Hytibar film has been shown to reduce emissions of the fumigant CP from 82 % in a control to just 4 % (24). Similarly, Hytibar-induced reductions in the emissions of both CP (from around 21 % to just 0.001 %), and 1,3-D (from around 41 % to 2.4 %) have been reported above (Section 3.3).

3.4.3. Comparison of Soil Column Experimental Data and Model Simulations

The parameters of the relevant experimental conditions and Hydrus 1D model simulations are given in Table 3.4.1 and a description of the finite element grid the simulations is provided in Section in 3.1.3.

Simulated emission fluxes of MeI, together with the measured values, are shown in Figure 3.4.1. The relatively simple trend in the emission flux for the Control, Irrigated and HOM treatments (i.e. large, very early, initial peak, followed by rapid decline in emissions and then tailing) was well reproduced by the model. However, it is clear that the magnitude of the initial peak was underestimated for the control and outside the experimental error bars. For the other treatments, the simulations either overestimated (VIF) or generally bracketed the measurements. The simulated peak values for the Control were around 41–46 % less than the measured value. For the irrigated treatment, the simulated peaks were from 11–20 % lower than the measured peak value. The simulated peaks values for the HOM treatment were from 15–23 % lower than the measured value. For the VIF treatment, the general pattern of higher emissions during daytime periods was reproduced by the model. Nevertheless, in contrast to the other treatments, the model markedly overestimated the measured emission fluxes. This could have been caused by using a value for the mass transfer coefficient that was too large for the piece of film actually used in the experiments. Even so, the model seemed to capture the order-of-magnitude effect of using the VIF, that is, a reduction in peak emissions from the range 100–1000 to 0.1–1.0 $\mu g\ m^{-2}\ s^{-1}$, or a reduction of 99.9 %.

Total emission losses (measured and simulated) are shown in Table 3.4.2. Considering the discrepancies between the measured and simulated peak emission fluxes, the total emission losses are relatively accurately simulated. Largest discrepancy was observed for the HOM treatment, presumably because the measured values did not differ from the control as would be expected. The simulated values seem reasonable based on the usual expectation of the effect of HOM on emissions of, for example, 1,3-D (see Sections 3.2 and 3.3).

Table 3.4.1. Parameters for Hydrus 1D simulations of Control, VIF, HOM, and Irrigation treatments for MeI. The surface area of the column was 113.1 cm^2 and the injection depth was 30 cm. Other parameters are in Table 2.1.1.

Treatment/ Data Type	Properties	Value	Units
Pesticide properties	Henry's law constant at 25°C [§]	0.23	
	Binary Gas diffusion coefficient at 20°C	370.5	$cm^2\ h^{-1}$
	Binary water diffusion coefficient at 20°C	0.115	$cm^2\ h^{-1}$
Activation energy for T-dependence	Binary Gas diffusion coefficient [†]	4403	$J\ mol^{-1}$
	Henry's law constant [¶]	26080	$J\ mol^{-1}$
	Degradation rate constant [¥]	58893	$J\ mol^{-1}$
Heat transport	Initial soil temperature with depth	25-22	°C
	Temperature range	19-32	°C
	Used default heating properties for sand		
Initial concentration	Initial mass, 150 µL of MeI	182.4	mg
	Initial water content:		
	0-15 cm deep,	10.5	$cm^3\ cm^{-3}$
	15-30 cm deep,	13.5	$cm^3\ cm^{-3}$
	30-45 cm deep,	18	$cm^3\ cm^{-3}$
	45-60cm deep,	21	$cm^3\ cm^{-3}$
	>60 cm deep,	24	$cm^3\ cm^{-3}$
All Treatments (unless other data provided)	Organic matter content	2.7	%
	Sorption coefficient	0	$cm^3\ g^{-1}$
	Degradation rate constant[‡]	0.0026	h^{-1}
HOM	Degradation rate constant	0.0100	h^{-1}
VIF	Film properties	See Table 2.1.1	
Irrigation	Irrigated 1 cm water each day at 10:30 am for 5 days (rate was 2 cm h^{-1})		

[§] Gan et al. (1996); [‡] Ashworth et al. (2011); [†] Reid et al.(1987); [¶] Yates et al.(2003) (the same as MeBr); [¥] Zheng et al. (2004); [£] Papiernik et al. (2011)

Table 3.4.2. Measured and simulated total emission losses of MeI from laboratory soil columns.

Total emissions (%)	Control	HOM	VIF*	Irrigated
Measured	83.3	63.2	0.04	81.6
Hydrus 1D	85.6	71.7	0.7	76.9
Solute 1D	87.0	73.5	0.8	79.1
Difference	2.3–3.7 %	8.5–10.3 %	0.7–0.8 %	2.2–4.7 %
Average	85.3	69.5	0.51	79.2
Standard Deviation	1.9	5.5	0.41	2.4

* - Emissions prior to removing VIF.

4. Drip Application Studies

4.1. Laboratory Drip Application with Telone C-35: Effects of HDPE and VIF tarps.

4.1.1. Experimental Information

Duplicated laboratory soil chamber experiments with simulated drip application of Telone C-35 were performed using the general description given in Section 2.2.2. A control (bare soil) experiment was performed, along with HDPE and VIF tarp covered treatments. Tarps covered only the bed surface and sidewall with the furrow left uncovered, and were sealed to the chamber top to prevent leakage. Model simulations were conducted using Hydrus 2D (Section 2.5.2 – 2.5.2).

4.1.2. Results and Discussion

Flux rates of the fumigants from the Bare soil, HDPE, and VIF treatments over the course of the experiment are shown in Figures 4.1.1 and 4.1.2 for 1,3-D and CP, respectively.

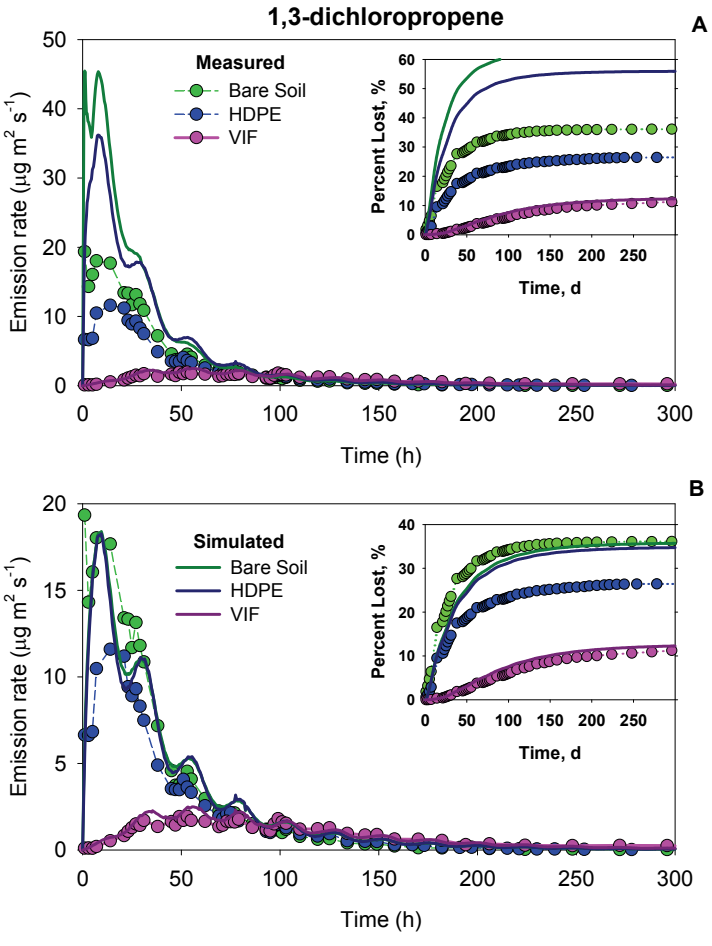

Figure 4.1.1. 1,3-D emissions from Bare soil, HDPE and VIF treatments (combined emissions from bed, sidewall and furrow).

Figures 4.1.1 and 4.1.2 show the total fluxes, which were obtained by combining the emissions from the bed, sidewall and furrow. In the Bare soil control, emissions of 1,3-D and CP were very similar in magnitude, although the CP peak was delayed compared to the 1,3-D. In the tarped treatments, greater flux rates occurred for 1,3-D than for CP. Emission fluxes of 1,3-D occurred over longer time periods than for CP. In general, CP emissions ceased after around 75 hours under HDPE and around 150 hours under VIF. Comparing the three treatments, it is evident that HDPE and, particularly, VIF reduced emissions of both fumigants relative to the control. Comparing the two tarps, it is noticeable that the HDPE led to a more rapid release of the fumigants causing an initial peak followed by extensive tailing over time. For the VIF treatment the lower fluxes were spread over a longer period and no obvious single emissions peak occurred.

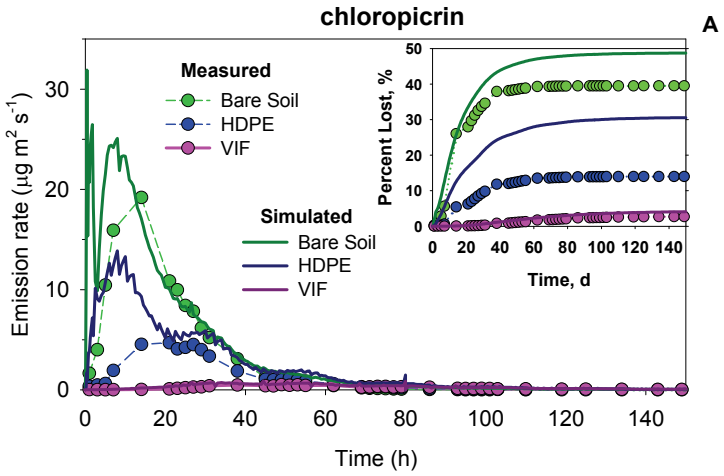

Figure 4.1.2. CP emissions from Bare soil, HDPE and VIF tarped soil chambers (combined emissions from bed, sidewall and furrow)

Compared to the VIF treatment, the higher emissions from the HDPE treatment were a result of the much greater permeability of this film to each fumigant. The lower CP mass transfer coefficients for both films are consistent with the lower emissions observed for this fumigant compared to 1,3-D. However, lower total emissions are also likely due to the difference in degradation rate, half-life, which was measured as 0.12 d for CP and 3.8 d for 1,3-D in this soil. Therefore, a more rapid degradation loss pathway for CP will have significantly reduced emission losses from the soil surface. In contrast, the relatively long degradation half-life and higher mass transfer coefficients for 1,3-D resulted in higher total emissions.

The influence of soil temperature is evidenced by the higher fluxes generally corresponding to afternoon and early evening times. Due to its influence over vapor pressure, the role of soil temperature in influencing the rate of 1,3-D (Ashworth et al., 2007; Basile et al., 1986) and CP (Ashworth et al., 2008) volatilization from bare soil, has been previously reported. In covered soils, the effect of temperature on the permeability of the plastic film must also be considered since increasing permeability of plastic film at higher temperatures has been reported (Wang et al., 1999; Papiernik et al., 2002), and differing films may exhibit differing temperature-dependent permeability. This is consistent with observations of increased emission fluxes during the warmer parts of the temperature cycle. Although both films appeared to exhibit this effect, the VIF seemed to be most strongly affected; exhibiting many fluctuations in emission flux over time.

The type of plastic film clearly had a marked impact on fumigant movement and release from the bed furrow system. With the higher permeability HDPE, the emission release of both 1,3-D and CP from the three headspace compartments followed the order bed > sidewall > furrow. This would be the expected pattern based on the positioning of the fumigant application and would also be the expected pattern for a non-tarped raised bed system. It has been reported (Ashworth et al., 2008; Van Wesenbeeck et al., 2007) that the vast majority of fumigant emissions occurred from the bed surface with bare soil or relatively permeable plastic covering (e.g. HDPE, LDPE, and semi-impermeable film). In contrast, the experimental data show that emissions from the VIF treatment were always greatest from the furrow. One can surmise that the very low film permeability, leads to a very low level of emissions directly above the application point (i.e. from the bed), and this leads to diffusive transport of the fumigant both downward and horizontally. Since both the bed and sidewall were covered with the VIF, the furrow base was the only region

from which emissions could readily occur. Consequently, a delay in emissions from the furrow was observed due to the time taken for gas diffusion to this region. Indeed, the broad nature of the flux rate curve from the VIF chamber is mostly due to this emissions delay.

When expressed as a percentage of the total amount of fumigant added to the system (Table 4.1.1) it is clear that CP emissions were lower than for 1,3-D for the HDPE and VIF treatments. The only exception was for the Bare soil treatment where the total CP emissions from the bed was greater than 1,3-D. Moreover, Table 4.1.1 highlights differences between the treatments. Although HDPE was relatively effective in reducing emissions of both 1,3-D and CP compared to the control, VIF dramatically reduced total emissions compared to the Bare soil and the HDPE. The distribution of emissions between the three compartments of the raised bed system is also shown in Table 4.1.1. With a bare soil and under HDPE the predominant emission loss for each fumigant was via the bed surface, i.e. close to the point of application. However, under VIF, emissions occurred primarily via the furrow, again due to the low permeability of the VIF tarp over the bed and sidewall compartments. A further emission reduction strategy within the furrow region (e.g. thiosulfate application) may offer further emission reduction benefit. However, in our previous work (reported by Ashworth et al., 2008), no emission reduction benefit was observed by using potassium thiosulfate solution in the furrows of HDPE and semi-impermeable film covered soils.

Table 4.1.1. Mean (n=2) and range of emissions (% of total applied) from each chamber compartment within each experimental treatment.

Treatment	Location	1,3-D	CP
Bare Soil	Bed	26.1 (±1.0)	35.6 (±2.8)
	Sidewall	7.9 (±0.5)	3.2 (±0.7)
	Furrow	2.1 (±1.7)	0.7 (±0.6)
	Total	**36**	**39**
HDPE	Bed	23.1 (±4.3)	13.6 (±1.1)
	Sidewall	2.8 (±0.8)	0.35 (±0.1)
	Furrow	0.07 (±0.03)	0.01 (±0)
	Total	**26**	**14**
VIF	Bed	0.5 (±0.2)	0.04(±0.02)
	Sidewall	0.3 (±0.2)	0.07(±0.03
	Furrow	9.6 (±1.0)	2.6 (±1.5)
	Total	**10**	**2.7**

4.1.3. Comparison with Model Simulations

The parameters of the relevant experimental conditions and Hydrus 2D model simulations are given in Table 4.1.2 and Table 2.1.1. A diagram of the finite element grid used in the Hydrus 2D simulations is shown in Figure 4.1.3.

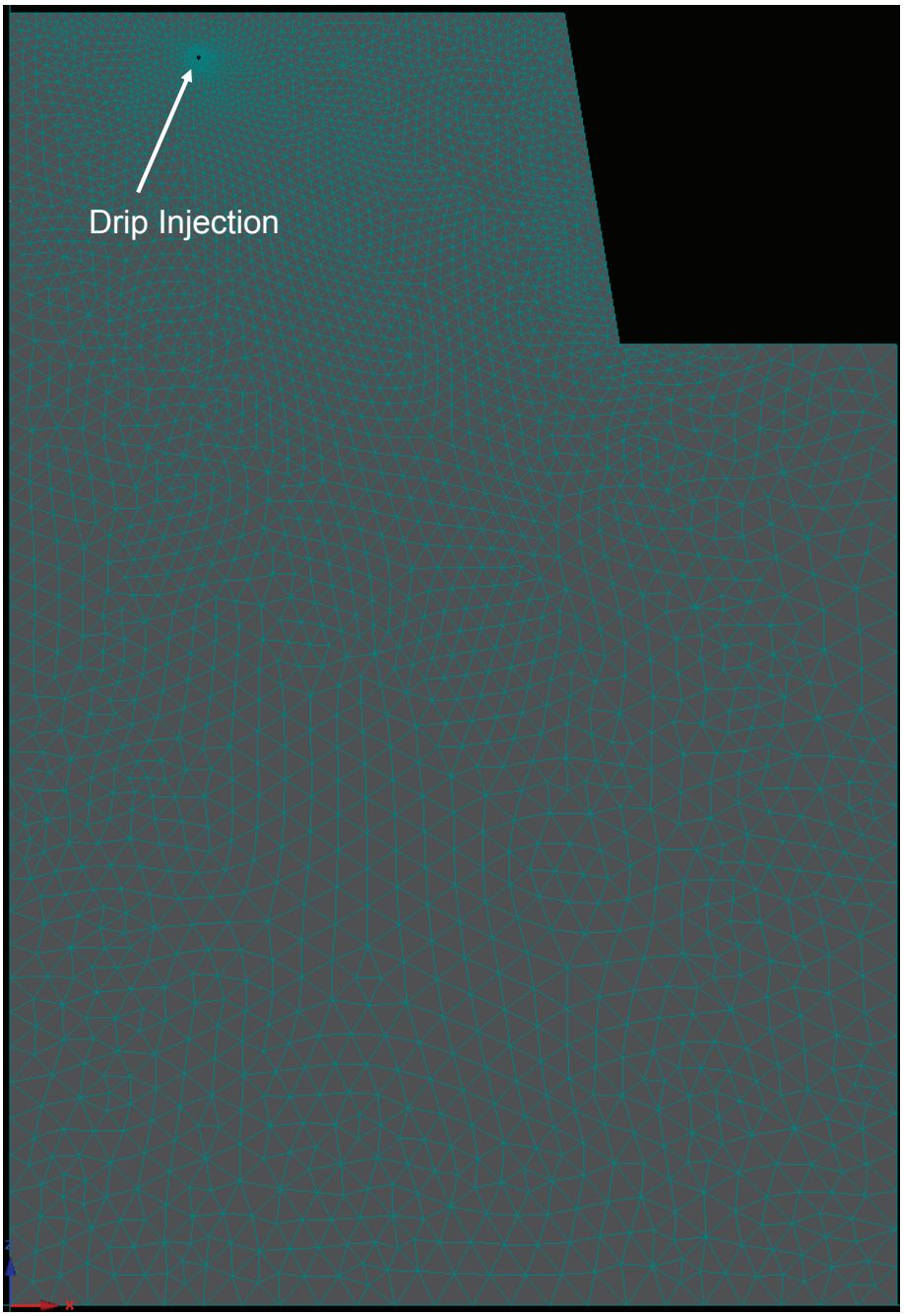

Figure 4.1.3. Finite element grid used for simulating 1,3-D and CP emissions from the 2B soil chambers.

Table 4.1.2. Parameters used for Hydrus 2D simulations of Control, HDPE and VIF treatments for Telone C-35.

Treatment/ Data Type	Properties	Value	Units
Initial Values	Mass 1,3-D applied	799	mg
	Mass chloropicrin applied	429	mg
	Water applied (rate 8 mL/min)	1	L
	Initial water content:		
	0-15 cm deep,	8.4	$cm^3\ cm^{-3}$
	15-30 cm deep,	11.0	$cm^3\ cm^{-3}$
	30-45 cm deep,	12.6	$cm^3\ cm^{-3}$
	45-60cm deep,	13.0	$cm^3\ cm^{-3}$
	>60 cm deep,	12.7	$cm^3\ cm^{-3}$
All Treatments (unless otherwise noted)	Degradation rate constant, 1,3-D	0.0077	h^{-1}
	Degradation rate constant, chloropicrin	0.0169	h^{-1}
	Stagnant boundary layer thickness	see Table 2.1.1	cm
VIF	Boundary layer thickness-1,3-D (cis) at 20°C	16,2485	cm
	Boundary layer thickness-1,3-D (trans) at 20°C	79,535	cm
	Boundary layer thickness-chloropicrin at 20°C	49,4030	cm
	Activation energy of b-VIF	see Table 2.1.1	$J\ mol^{-1}$

Figure 4.1.1 show the simulated and measured 1,3-D for the Bare soil, HDPE and VIF treatments. In Figure 4.1.1A, the simulation provides predicted emission rates based on the standard simulation procedures described above. The simulated emission rates significantly overestimate the measured values for the Bare soil and HDPE treatments. For the Bare soil scenario, the predicted peak emission rate was approximately 45 $\mu g\ m^{-2}\ s^{-1}$, which is 1.3 times greater than the peak measurement (19 $\mu g\ m^{-2}\ s^{-1}$). The model correctly predicts a very high emission rate during the drip injection process (i.e., < 2 h), which was also observed during the experiment. For the HDPE treatment the predicted peak emission rate was approximately 36 $\mu g\ m^{-2}\ s^{-1}$, which is 2 times greater than the peak measurement (12 $\mu g\ m^{-2}\ s^{-1}$).

For both the Bare soil and HDPE treatments, the measured total emissions were also overestimated. The Bare soil simulation predicted total emissions of 63 %, while the experimental value was 36 % (Table 4.1.3). A similar result occurred for the HDPE with predicted total emissions of 56 % and measurements of 26%.

Shown in Figure 4.1.2 are measured and predicted emissions of chloropicrin. The predicted chloropicrin emission rates are more similar compared to the results for 1,3-D. The measured peak emission rate for the Bare soil treatment was 19 $\mu g\ m^{-2}\ s^{-1}$ and total CP emissions were estimated to be 39%. The simulated peak emissions were 24 $\mu g\ m^{-2}\ s^{-1}$, if the large emission rate during the drip injection period (32 $\mu g\ m^{-2}\ s^{-1}$) is neglected. Unlike with 1,3-D, the measured chloropicrin emission rate didn't produce high values during drip application. The total CP

emission for the Bare soil treatment are also more similar compared to the 1,3-D; with measured and predicted value, respectively of 39 % and 49 % (Table 4.1.3).

Table 4.1.3. Measured and simulated total emission losses (%) for 1,3-D and CP for the Bare soil and HDPE treatments.

	1,3-D (%)		CP (%)	
Treatment	**Measured**	**Simulated**	**Measured**	**Simulated**
Bare Soil	36	63	39	49
HDPE	26	56	14	31
Difference	10	7	25	18

Compared to the Bare soil treatment in Figure 4.1.2, a larger difference occurred for the HDPE treatment, with measured and predicted peak CP emissions, respectively, of 4.6 $\mu g\ m^{-2}\ s^{-1}$ and 14 $\mu g\ m^{-2}\ s^{-1}$. Total emissions for the HDPE treatment were 14 % and 31 %, respectively, for the measurements and predictions.

For both 1,3-D and chloropicrin (Figure 4.1.2), the predicted peak and total emissions for the VIF treatment were very similar to the experimental values. The predicted peak 1,3-D emission rate was about 2.5 $\mu g\ m^{-2}\ s^{-1}$ and the measured peak rate was about 2.0 $\mu g\ m^{-2}\ s^{-1}$. The total emissions from the simulation and experiment, respectively, were 12.4 % and 11.9 %. For chloropicrin the predicted and measured total emissions, respectively, were 2.7 % and 4.2 % and the peak emission rate for both were less than 0.8 $\mu g\ m^{-2}\ s^{-1}$. The similarity between results for both 1,3-D and chloropicrin imply that appropriate soil and chemical properties were used for simulation. Since the VIF would limit emissions from the bed and sidewall, the modeling results would not be affected by surface boundary conditions.

Two potential explanations for the poor agreement for the Bare soil and HDPE treatments would be discrepancies between the physical system and the model in characterizing the injection process and/or the surface boundary condition. Either of these factors would have a lesser impact on the VIF treatment since emissions of fumigant require substantial transport distances toward the furrow surface.

For the Bare soil and HDPE treatments, the model predicts high emission rates which were not observed in the experiment and the fraction of emissions from the bed and sidewall are substantial. This is due to the close proximity of the soil surface to the drip injection point, a relatively high mass transfer between soil and the atmosphere. Therefore, rapid fumigant transport would occur during and shortly after injection. One explanation for this would be if, during injection, the fumigant moved along the soil-chamber boundary before entering the soil. This could lead to deeper movement in soil if, preferentially, the movement was in response to gravity (i.e., away from the surface). Since this would lead to a 3-dimensional process and require many unknown parameters, it is not practical to explore this scenario via simulation.

Another possible explanation for lower emission rates in the experiment would be if the boundary layer between soil and the atmosphere was more resistive to transport than assumed in Hydrus 2D, that is, that the stagnant boundary layer thickness, *b,* is greater than 0.5 cm for bare soil. Given the 2-D chamber configuration (see Figure 2.2.3) with three inlets/outlet separated by approximately 10 cm, the air exchange rate and the uniformity of the air velocity might not conform to a $b = 0.5$ cm; or boundary layer mass transfer coefficient of D_g^{air}/b.

An investigation of the potential effect of a larger "effective" boundary layer thickness is shown in Figure 4.1.1B for 1,3-D. For the Bare soil treatment, the boundary layer thickness was assigned a value of $b = 300$ cm, which is about three times larger than the value for HDPE treatment. This value was chosen by comparing the measured emission rate to the simulated rate and provides a much better representation of the measurements. For the HDPE treatment, the effective boundary layer thickness was obtained by adding bare soil value (i.e., $b = 300$ cm) to the b_{ref} value for HDPE (see Table 2.1.1). The results for the HDPE treatment are nearly the same as the Bare soil treatment. While there is improvement in the comparison between simulated and measured emission rates, it is unlikely that this provides a complete or satisfactory explanation. Problems that remain that are unanswered by this analysis (Figure 4.1.1B) include: (a) the simulated emission rates for Bare soil and HDPE treatment are nearly the same, but the experimental emission rates differ; (b) simulated values for chloropicrin are much closer in value using a $b = 0.5$ cm, implying that the model parameters are approximately correct based on this fumigant; and (c) the relative difference between the predicted total 1,3-D emissions for the Bare soil and HDPE treatments in Figure 4.1.1A is nearly the same as the relative difference between the measurements and implies that boundary layer thickness shown in Table 2.1.1 are consistent. Further research is needed to address this issue.

4.2. Laboratory and Field Study: University of California-Riverside, Field 2B (2009)

4.2.1. Experimental Information

Detailed description of the 2009 raised-bed field study carried out at Field 2B University of California – Riverside is given in Section 2.3. Briefly, Telone C-35 was drip applied at 10 cm depth to the center of raised beds at two application rates (equivalent to 100 and 70 % of typical field application rates). The 100 % rate was used for bare soil (control) and HDPE-covered beds, while the 70 % rate was used for HDPE-, VIF- and thermic film- covered beds. Emissions of 1,3-D and CP were determined using dynamic flux chambers placed on the bed surface. The proximity of the 2B field to the US Salinity Lab, together with the availability of agricultural equipment for the plowing, formation of beds etc, were major factors in deciding to use this site for the raised bed studies. However, the other studies in this project have all used the Buttonwillow soil and, although both the 2B and Buttonwillow soils are classified as sandy loam, it was considered important to compare the 2B soil and the Buttonwillow soil in terms of the behavior of 1,3-D and CP. Therefore, a 2D chamber experiment was performed (using the same method described in Section 2.2) using the Field 2B soil and a covering of HDPE, for comparison to the results of the HDPE chamber experiment using the Buttonwillow soil (Section 4.1). Results of this 'bridging' study are described first here, followed by those of the 2B field study itself.

4.2.2. Result from 2D Chamber Study using Field 2B Soil (Bridging Study)

Figure 4.2.1 shows the emission fluxes of 1,3-D and CP from the Field 2B soil chamber experiments (for HDPE cover). Comparing this to the emission fluxes for the Buttonwillow soil under the same conditions (Figure 4.1.1 and Figure 4.1.2; HDPE curve) It is evident that he overall trend in emission flux with time was similar for the two soils. In addition, the magnitude of the fluxes for CP were similar for the two soils, peaking at around 10–13 μg m^{-2} s^{-1}. However, despite both soils being classed as sandy loam, marked differences in the magnitude of 1,3-D emission fluxes between the two soils were observed. In the 2B soil, peak emission flux was around 42 μg m^{-2} $s^{-1,}$ whereas in the Buttonwillow soil it was only 25 μg m^{-2} s^{-1}; approximately a 40 % decrease. For both 1,3-D and CP, total emissions were greater for the 2B soil than for the Buttonwillow soil (Table 4.2.1). It is considered that the reason for the lower emissions from the Buttonwillow is a result of the faster degradation (shorter half-life) of the fumigants in this soil (Table 4.2.1). The extent of the increased emissions from the 2B soil must be borne in mind when comparing the results from the 2B raised-bed study (described below) with the various Buttonwillow experiments presented in this report.

Table 4.2.1. Percentage emission losses and half-lives of 1,3-D and CP in HDPE treatments of the Field 2B and Buttonwillow soils.

	1,3-D (%)	CP (%)	1,3-D (t½, h)	CP (t½, h)
Field 2B	40	15	154*	9.2*
Buttonwillow	26	8	90**	2.9**
Ratio	0.65	0.53		

*: data from Zheng et al. (2003); ** data from Ashworth et al. (2009).

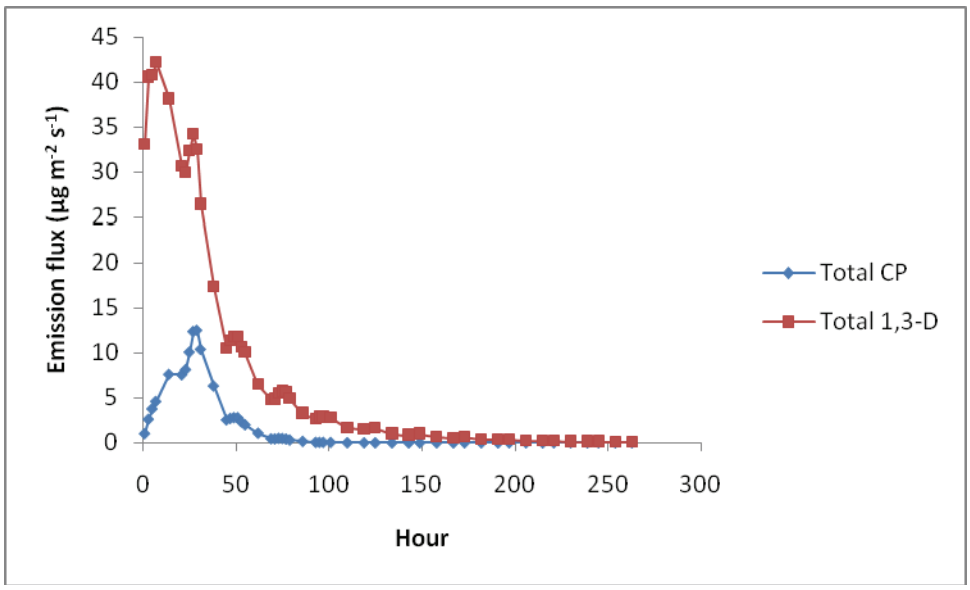

Figure 4.2.1. Emission fluxes of 1,3-D and CP from the 2B soil chambers covered with HDPE.

4.2.3. Results from Field 2B Raised-Bed Study

Total daily emissions from each treatment over the first five days of the experiment are shown in Figure 4.2.2 and Figure 4.2.3 for 1,3-D and CP, respectively. In all cases except 1,3-D in the VIF treatment, emissions decreased over time. This would be the expected behavior since the fumigants were applied relatively close to the soil surface and would have rapidly converted to the gaseous form due to high summer soil temperatures soon after application. Temperatures measured within the soil at 4 cm depth for the Bare, Thermic and HDPE plots are shown in Figure 4.2.4 (temperatures of the VIF plots were not measured but are assumed to have been similar to the HDPE plot). It is evident that even in the Bare soil plot, temperatures reached in excess of 40 °C during the hottest part of the day (late afternoon). Such high temperatures would have facilitated the rapid conversion of liquid fumigants to a gaseous form and led to high emissions on the first day.

On each day, total mass loss (Figure 4.2.2 and Figure 4.2.3) and percentage loss (Figure 4.2.5) from the bare soil (100 % rate) was markedly greater for both 1,3-D and CP compared to the HDPE treatment (100 % application rate). The percentage losses of both chemicals appear to be in line with previously reported data for field and laboratory fumigant emission studies for 1,3-D and CP (e.g. data presented in this report; typically between 20 and 40 %). Evidently, the HDPE provided an efficient barrier to the soil-air transfer of both chemicals, with the mass loss of 1,3-D reduced by 60 % and the mass loss of CP reduced by 80 % due to HDPE cover. For the HDPE treatment, reducing the application rate to 70 % of the typical level, led to reductions in mass loss of 1,3-D of between 73 and 84 % for the first two days of the experiment. Thereafter, no benefit, in terms of reduced emission loss, was observed. Moreover, for CP, greater emission losses were actually observed for the 70 % application rate when compared to the 100 % rate.

Nevertheless, for each chemical, the total percentage losses from these two treatments (Figure 4.2.5) were not markedly different.

Comparing the three tarps at an application rate of 70 %, it is evident that the VIF offers a significant benefit in reducing emissions compared to the HDPE and Thermic tarps. Although the Thermic tarp is manufactured to enhance soil heating for the purposes of solarization, it is possible that such a tarp may also cover fumigated fields (e.g. where solarization and fumigation are used in conjunction). These results suggest that as a barrier to fumigant transport to the atmosphere, the Thermic tarp is less effective than HDPE, but likely offers some benefit over a bare soil. Total mass losses from the HDPE treatment were 57 and 51 % of those from the Thermic treatment for 1,3-D and CP, respectively. Total mass losses from the VIF treatment were 49 and 22 % of those from the HDPE treatment for 1,3-D and CP, respectively. These findings can be related to the permeability of the tarps, as described by their respective R-values (Section 2.1).

Based on the comparison given in Section 4.2.2, the results from the 2B raised-bed field study are likely to overestimate the results had the experiment been carried out at the Buttonwillow site, or with Buttonwillow soil. According to Table 4.2.1, total 1,3-D emission loss from the Buttonwillow soil chambers was a 0.65 fraction of that from the 2B soil chambers. For CP, the fraction was 0.53. If these values are assumed to be applicable to the field study data, and consistent across treatments, potential percentage emission losses for the Buttonwillow soil can be estimated (Figure 4.2.6).

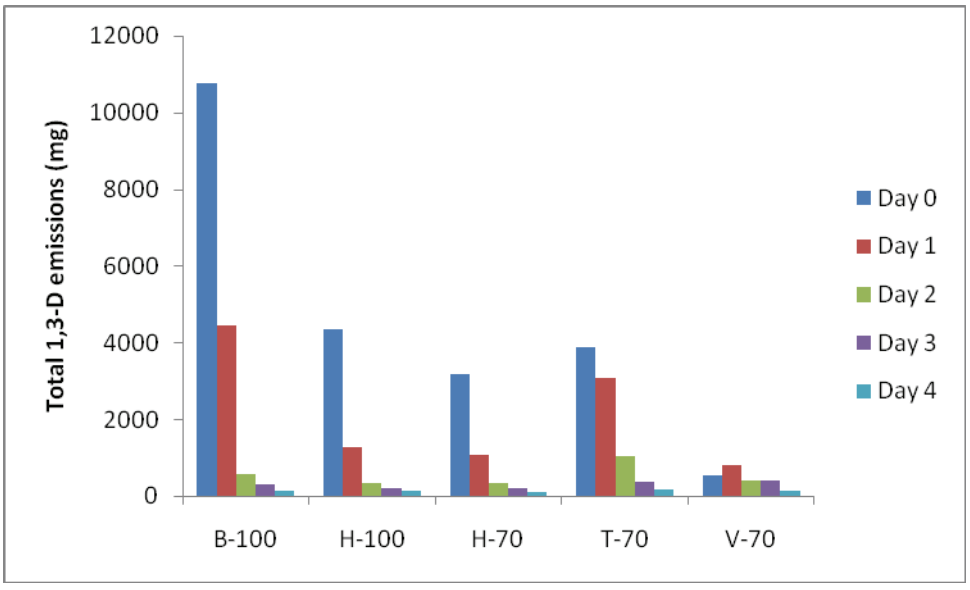

Figure 4.2.2. Daily 1,3-D emission losses from each treatment of the Field 2B raised-bed study.

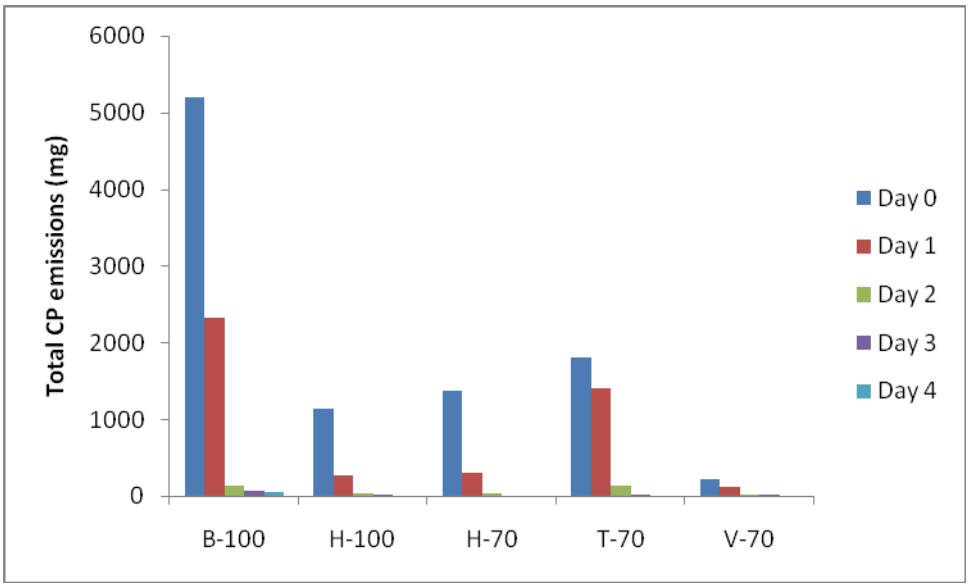

Figure 4.2.3. Daily CP emission losses from each treatment of the Field 2B raised-bed study.

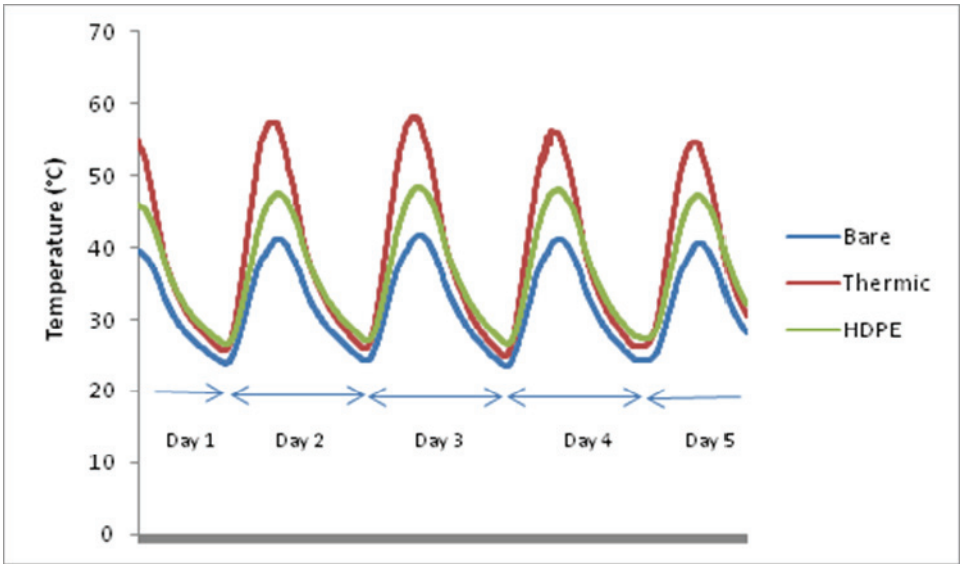

Figure 4.2.4. Diurnal temperature fluctuations measured at 4 cm depth in the center of each raised-bed plot.

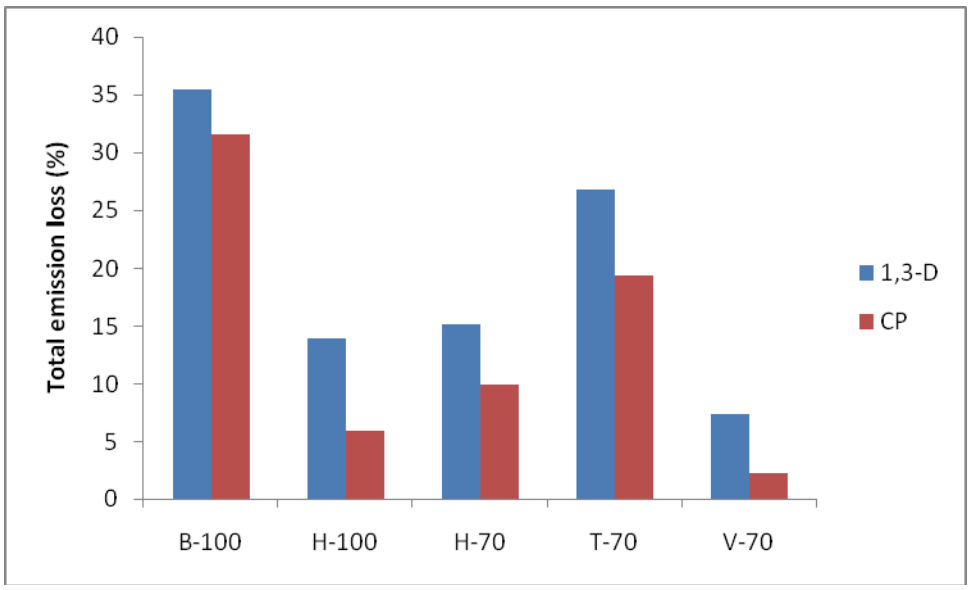

Figure 4.2.5. Total percentage emission loss of 1,3-D and CP from each treatment

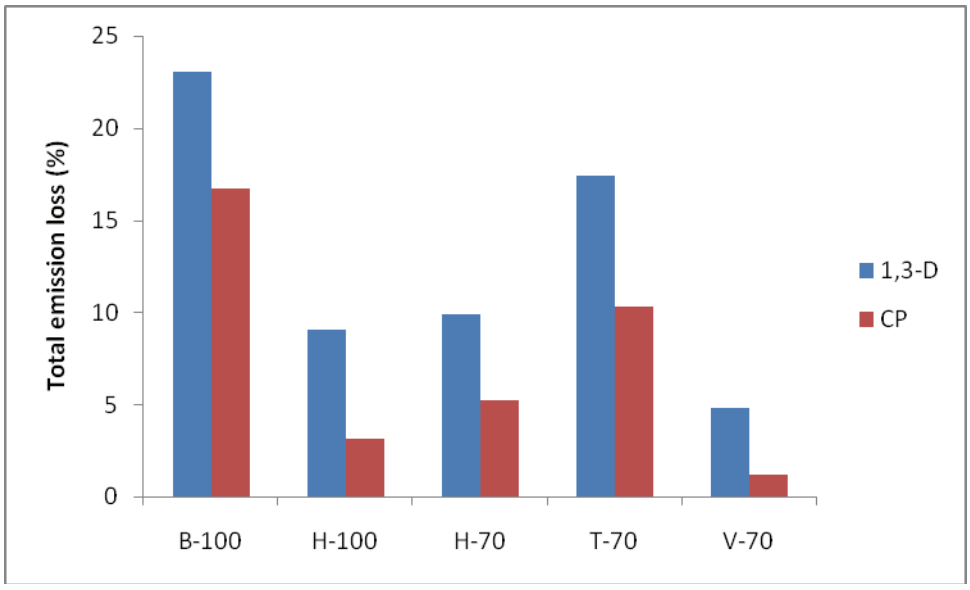

Figure 4.2.6. Estimated (i.e., potential) emission losses of 1,3-D and CP from the Buttonwillow soil. Estimates were based on data in Figure 4.2.5 for 2B soil and data in Table 4.2.1 which shows 1,3-D emission from Buttonwillow soil to be a 0.65 fraction of those from 2B soil and CP emissions from Buttonwillow soil to be a 0.53 fraction of those from 2B soil.

5. Summary and Conclusions

All the approaches used in this research project to manage soil fumigations reduced emissions of 1,3-D and chloropicrin compared to standard fumigation practices. Emissions were reduced the most by using virtually impermeable films, followed by high organic matter soils, repeated irrigations and deep injection. Applying composted municipal green waste to the upper 15 cm of the soil reduced 1,3-D emissions by approximately 80%; but further research is needed to determine the practicality of this method and the potential for plant pest control to be compromised by a reduction in fumigant concentrations at the soil surface.

Surface Water Seals. Repeated surface irrigation appears to be a simple, relatively low cost, and effective method to reduce fumigant emissions (approximately 50% emission reduction). The current research shows that by 4–5 days, most of the 1,3-D had either been emitted or degraded, suggesting that further application of water would not offer any greater benefit to emission reduction. Incorporating this emission-reduction strategy into existing production systems should relatively easy and straightforward. Recent laboratory and field research has also demonstrated similar results providing additional support for this methodology.

Fertilizer Amendments. Application of fertilizer amendments as a low water-volume spray reduced emissions by approximately 20–30% across a range of large-scale field measurements and laboratory measurements. However, simulated emissions for a low-water spray of ATS showed only modest reduction in emissions (i.e., < 2 %). If the experimental results hold for typical agronomic conditions, this methodology would represents a relatively simple approach to reduce emissions and could be readily incorporated into typical production systems. Further research is needed to determine why the simulation did not provide the same reduction in total emissions as the experiments.

Both experiments and simulations demonstrate that additional reductions in emissions are possible if the fertilizer amendment ATS is applied with 1 cm or more of irrigation water. However, research is needed to quantify the relationship between amounts of water added relative to applied thiosulfate. Previous research has shown that increasing the total applied water also increases the effectiveness of this emission reduction strategy.

Virtually Impermeable Films. Simulated emission rate for VIF treatments (i.e., 1,3-D, chloropicrin and MeI) correctly predicted the order of magnitude of the measured emission rates and improved accuracy was obtained when the VIF permeability was adjusted for the effects of relative humidity. Due to a scarcity of data, additional research is warranted to better describe the relationship between film permeability and relative humidity. For all experiments and simulations, emission flux rates and total emission percentages were very low.

Drip Applied Fumigants. For drip-applied 1,3-D and chloropicrin in a bed-furrow system with the bed and sidewall covered with VIF, the predicted peak and total emissions for the VIF treatment were very similar to the experimental values. The predicted peak 1,3-D emission rate was about 2.5 $\mu g\ m^{-2}\ s^{-1}$ and the measured peak rate was about 2.0 $\mu g\ m^{-2}\ s^{-1}$. The total emissions from the simulation and experiment, respectively, were 12.4 % and 11.9 %. For chloropicrin the predicted and measured total emissions, respectively, were 2.7 % and 4.2 % and

the peak emission rate for both were less than 0.8 μg m^{-2} s^{-1}. The similarity between results implies that the mathematical model is suitable for predicting fumigant fate and transport when travel distances to through soil are relatively large (i.e., from drip application site to furrow surface). For this scenario, the VIF would limit emissions from the bed and sidewall so the modeling results would not be affected by bed or sidewall surface boundary conditions.

The model proved less accurate in predicting fumigant emissions for bare and HDPE covered soil. It is unclear why the model fails to accurately predict fumigant behavior over the relatively short transport distances from the injection point to the bed surface and additional research is needed to address this discrepancy.

Predicting Field Scale Emissions. Overall, mathematical simulation predicted the large scale field emission experiments with reasonable accuracy. While, the differences between period emission rates may deviate, the different methodologies for determining total emissions were generally within about 5 % and within the range of field scale emission estimates (i.e., ADM and Calpuff). For the 2007 field experiment, comparing ADM, Calpuff, Hydrus and Solute simulations gave percent mass loss estimates for the Control, Deep injection and ATS spray treatments, respectively, of 28.9±4.6, 22.3±5.1, and 25.5±1.1 % (see Table 3.1.4). Based on the increased accuracy of the 1-D modeling approach, it appears that the fumigations can be predicted sufficiently well and that incorporating the additional complexity of a shank fracture may be unwarranted.

For the 2005 Buttonwillow field experiment, comparing ADM, Calpuff, Hydrus and Solute simulations for the Irrigation and HOM treatments, respectively, gives 12.2±2.3 and 4.6 ± 2.4 % total emissions. The deviation between methods for estimating total emissions (i.e., 5 %) is well within the uncertainty associated with various field measurement methods (20–50 %, see Executive Summary).

Using the average total emission values for Telone C-35 shown in Figure 1.1.1, the following order of total emission becomes evident: Bare soil > ATS spray > HDPE > ATS irrigation > Deep injection > VIF. This data leads to average total emission percentages and standard deviation for this sequence of fumigation practices, respectively, of 43.9±7.9 %, 34.3±9.1 %, 30.7±3.3 %, 19.5±4.7 %, 17.3±2.4 % and 0.28±0.12 %. With the exception of the Bare soil and ATS spray treatments, the deviation between estimation approaches is below 5 %.

6. References

Ashworth, D.J., and Yates, S.R., Surface irrigation reduces the emission of volatile 1,3-D from agricultural soils, Environ. Sci. Techn. 41:2231-2236. 2007.

Ashworth D.J., Ernst, F.F. and Yates, S.R. Soil chamber method for determination of drip-applied fumigant behavior in bed-furrow agriculture: Application to chloropicrin. Environ. Sci. Techn. 42:4434-4439. 2008.

Ashworth, D. J., Ernst, F., Xuan, R. and Yates, S. R. Laboratory assessment of emission reduction strategies for the agricultural fumigants 1,3-dichloropropene and chloropicrin. Environ. Sci. Techn. 43:5073-5078. 2009.

Ashworth, D. J. and Yates, S.R. Methyl Iodide. In: Krieger, R. (Ed) 3rd Edition of the Hayes' Handbook of Pesticide Toxicology. Academic Press, San Diego. 2010.

Ashworth, D.J., Luo, L., Xuan, R. and Yates, S.R. Irrigation, organic matter addition, and tarping as methods of reducing emissions of methyl iodide from agricultural soil. Environ. Sci. Techn. 45:1384-1390. 2011.

Basile, M., Senesi, N., Lamberti, F. A study of some factors affecting volatilization losses of 1,3-dichloropropene (1,3-D) from soil. Agric. Ecosyst.. Environ. 17:269-279. 1986.

Businger, J.A. Evaluation of the accuracy with which dry deposition can be measured with current micrometeorological techniques. J. Clim. Appl. Meteorol. 25:1100-1124. 1986.

Dungan, R., Gan, J. and Yates, S.R. Effect of temperature, organic amendment rate, and moisture content on the degradation of 1,3-dichloropropene in soil. Pest. Manag. Sci. 57:1107-1113. 2001.

Dungan, R.S., Papiernik, S.K. and Yates, S.R. Use of composted animal manures to reduce 1,3-dichloropropene emissions Environ. Sci. Health Part B-Pestic. Food Contam. Agric. Wastes. 40:355-362. 2005.

Gan, J. and Yates, S.R. Degradation and phase-partitioning of methyl iodide in soil. J. Agric. Food Chem. 44:4001-4008. 1996.

Gan, J., Yates, S.R., Ohr, H. and Sims, J. Volatilization and distribution methyl iodide and methyl bromide after subsoil application. J. Environ.Qual. 26:1107-1115. 1997.

Gan, J., Yates, S.R., Becker, J.O. and Wang, D. Surface amendment of fertilizer ammonium thiosulfate to reduce methyl bromide emission from soil. Environ. Sci. Techn. 32:2438-2441. 1998.

Gan, J., Yates, S.R., Crowley D. and Becker, O.J. Acceleration of 1,3-D degradation by organic amendments and potential application for emission reduction. J. Environ.Qual. 27: 408-414. 1998b.

Gan, J.Y., Becker, J.O., Ernst, F.F., Hutchinson, C. and Yates, S.R. Surface application of ammonium thiosulfate fertilizer to reduce volatilization of 1,3-dichloropropene from soil. Pest. Manag. Sci.56:264-270. 2000.

Gan, J., Yates, S.R., Ernst, F.F. and Jury, W.A. Degradation and volatilization of the fumigant chloropicrin after soil treatment. J. Environ.Qual. 29:1391-1397. 2000b.

Gao, S. and Trout, T.J. Using surface water application to reduce 1,3-dichloropropene emission from soil fumigation . J. Environ. Qual. 36:110-119. 2006.

Gao, S., Trout, T.J. and Schneider, S. Evaluation of fumigation and surface seal methods on fumigant emissions in an orchard replant field. J. Environ. Qual. 37:369–377. 2008.

Jury, W.A., Spencer, W.F. and Farmer, W.J. Behavior assessment model for trace organics in the soil. I. Model description. J. Environ. Qual. 12:558-564. 1983.

Leistra, M. Distribution of 1,3-dichloropropene over the phases in soil. J. Agr. Food Chem. 18:1124-1126 (as cited in Yang, 1986). 1970.

Liu, H. and Foken, T. A modified Bowen ratio method to determine sensible and latent 340 heat fluxes. Meteorologische Zeitschrift 10:71-80. 2001.

Luo, L., Ashworth, D.J., Dungan, R.S., Xuan, R., Yates, S.R. Transport and Fate of Methyl Iodide and Its Pest Control in Soils. Environ. Sci. Techn. 44:6275-6280. 2010.

Majewski, M.S. Error evaluation of methyl bromide aerodynamic flux measurements. p. 135–153. *In* J.N. Seiber, et al. (eds). Fumigants: Environmental fate, exposure, and analysis. ACS Symposium Series 652. American Chemical Society, Washington, DC. 1997.

McDonald, J., Gao, S., Qin, R., Trout, T. and Hanson, B. Thiosulfate and manure amendment with water application and tarp on 1,3-dichloropropene emission reductions. Environ. Sci. Technol. 42:398-402. 2008.

Papiernik, S.K. and Yates, S.R. Effect of environmental conditions on the permeability of high density polyethylene film to fumigant vapors. Environ. Sci. Techn. 36:1833-1838. 2002.

Papiernik, S.K., Dungan, R.S., Zheng, W., Guo, M., Lesch, S.M. and Yates, S.R.. Effect of application variables on emissions and distribution of fumigants applied via subsurface drip irrigation. Environ. Sci. Techn. 38:5489-5496. 2004.

Papiernik, S.K., Yates, S.R. and Chellemi, D.O. A Standardized Approach for Estimating the Permeability of Plastic Films to Soil Fumigants under Various Field and Environmental Conditions. J. Environ.Qual. doi:10.2134/jeq2010.0118. 2011.

Reid, R.C., Prausnitz, J.M. and Polling, B.E. The Properties of Gases and Liquids. (4th ed.), McGraw-Hill, New York. 1987.

Šimunek, J. and van Genuchten, M.Th. The CHAIN_2D code for simulating two-dimensional movement of water flow, heat, and multiple solutes in variably-saturated porous media, Version 1.1. United States Salinity Laboratory Research Report #136. United States Salinity Laboratory, Riverside, CA. 1994.

Šimunek, J., van Genuchten, M.Th. and Šejna, M. Development and applications of the HYDRUS and STANMOD software packages, and related codes. Vadose Zone J. 7:587-600. 2008.

Van Wesenbeeck, I.J., Knuteson, J.A., Barnekow, D.E., Philips, A.M. Measuring flux of soil fumigants using the aerodynamic and dynamic flux chamber methods. J. Environ. Qual. 36: 613-620. 2007.

Wang, D., Yates, S.R., Gan, J. and Knuteson, J.A. Atmospheric volatilization of methyl bromide, 1,3-dichloropropene, and propargyl bromide through two plastic films, transfer coefficient and temperature effect, Atmos. Environ. 33:401-407. 1999.

Wang, Q., Gan, J., Papiernik, S.K. and Yates, S.R. Transformation and detoxification of halogenated fumigants by ammonium thiosulfate. Environ. Sci. Techn. 34: 3717-3721. 2000.

Wauchope, R.D., Butler, T.M., Hornsby, A.G., Augustijn-Beckers, P.W.M, and Burt, J.P. The SCS/ARS/CES Pesticide properties database for environmental decision-making. Rev. Environ. Contamin. Toxic. Springer-Verlag. 123:1–155. 1992.

Wilhelm, S.N., Shepler, K., Lawrence, L.J. and Lee, H. Environmental fate of chloropicrin. In "Fumigants: Environmental Fate, Exposure, and Analysis", ACS Symposium Series 652, pp. 79-93. 1996.

Wilson, J.D. and Shum, W.K.N. A re-examination of the integrated horizontal flux method for estimating volatilisation from circular plots. Agric. For. Meteorol. 57:281-295. 1992.

Yates, S.R. Simulating herbicide volatilization from bare soil affected by limited solubility in water. Environ. Sci. Techn. 40:6963-6968. 2006.

- Simulating herbicide volatilization from bare soil affected by limited solubility in water: Supporting Details. 3 pgs. 2006. http://pubs.acs.org/subscribe/journals/esthag/suppinfo/es061303h/es061303hsi.pdf

Yates, S.R. Analytical Solution Describing Pesticide Volatilization From Soil Affected by a Change in Surface Condition. J. Environ.Qual. 38: 259-267. 2009.

Yates, S.R., Gan, J., Wang, D. and Ernst, F.F. Methyl bromide emissions from agricultural fields. Bare-soil, deep injection. Environ. Sci. Techn. 31:1136-1143. 1997.

Yates, S.R, Gan, J. and Papiernik, S.K. Environmental fate of methyl bromide as a soil fumigant. Rev. Environ. Contam. Toxicol. 177:45-122. 2003.

Yates, S.R. and Gan, J. . Reducing Emissions of Volatile Organic Compounds (VOCs) From Agricultural Soil Fumigation. Final Report Contract No. 05-351, California Air Resources Board, Sacramento, CA. 91 pg. 2010.

Yates, S.R. and Enfield, C.G. Decay of dissolved substances by second-order reaction. Problem description and batch-reactor solutions. Environ. Sci. Health, Part A. Environ. Sci.Eng. A23:59-84. 1988.

Zheng, W., Papiernik, S.K., Guo, M. and Yates, S.R. Competitive degradation between fumigants chloropicrin and 1,3-dichloropropene in unamended and amended soils, J. Environ.Qual. 32:1735-1742. 2003.

Zheng, W., Papiernik, S.K., Guo, M. and Yates, S.R. Remediation of methyl iodide in aqueous solution and amended soils with thiourea. Environ. Sci. Techn. 38:1188-1194. 2004.

Zheng, W., Yates, S.R., Papiernik, S.K. and Wang, Q.Q. Reducing 1,3-dichloropropene emissions from soil columns amended with thiourea. Environ. Sci. Techn. 40:2402-2407. 2006.